REAL-TIME MATERIAL STATE ASSESSMENT OF COMPOSITES USING ARTIFICIAL INTELLIGENCE AND ITS CHALLENGES

by

MUTHU RAM PRABHU ELENCHEZHIAN

Presented to the Faculty of the Graduate School of

The University of Texas at Arlington in Partial Fulfillment

of the Requirements

for the Degree of

DOCTOR OF PHILOSOPHY IN AEROSPACE ENGINEERING

THE UNIVERSITY OF TEXAS AT ARLINGTON

May 2021

Supervising Committee:

Kenneth Reifsnider, Advisor

Rassel Raihan, Co-Advisor

Endel Iarve

Ashfaq Adnan

Ye Cao

Eric Reifsnider

Acknowledgements

I would like to express my sincere thanks to Dr. Kenneth Reifsnider, my supervising professor, for his guidance, kindness, patience, motivation and support towards this dissertation work. I learnt a lot of knowledge, skills and personal behavior. I have been surprised several times on his knowledge of composites and artificial intelligence topics, and amazed by his keen interest towards new findings and research topics. I am proud to be his doctoral student.

Next I would like to thank Dr. Rassel Raihan and Dr. Vamsee Vadlamudi, my supervisors and mentors at Institute for Predictive Performance Methodologies (IPPM) at UTA Research Institute (UTARI) who have guided me through my academic and professional path. Without their motivation I could not have done multiple research work. This dissertation would not have been done without their support and constant push.

I would like express my gratitude to Dr. Endel Iarve, Dr. Ashfaq Adnan, Dr. Wen Shen, Dr. Ye Cao and Dr. Eric Reifsnider for their time and effort to serve on my committee. Their valuable inputs during comprehensive exam, and over the research has been of significant contribution to this dissertation.

I would like to thank all my colleagues at IPPM from 2016 to 2021, who have been more supportive and helping me with all my experiments. A special thanks to Sai Sri Nidhi Munaganuru and Sabarinathan Pushparaj Subramaniyam for being helpful with all my troubles. I would also like to thank Ron Laposa, Adam Kaulsky, Jared Beaty, David Manivanh, Andy Houck from MTS and all other UTARI staff for all their assistance during my research. They have been life savers at most of the occasions.

Finally, I would like to express my sincere thanks to my parents Elenchezhian.R and Jegadheeswari.E, who believed in me and have supported me to pursue my dreams, and my beloved support systems Sunitha Ravichandran, Nirmal Kumar Umapathy, CoCo and all my beloved friends at UTA from 2015 to 2021.

April 29, 2021

Dedicated to

In Memory of Late Professor Dr. Wen S Chan

Abstract

REAL-TIME MATERIAL STATE ASSESSMENT OF COMPOSITES USING ARTIFICIAL INTELLIGENCE AND ITS CHALLENGES

Muthu Ram Prabhu Elenchezhian

Supervising Professor: Kenneth Reifsnider

Over several decades of careful experimental investigation and exhaustive development of discrete damage analysis methods including integrated computational mechanics methods, our community knows a great deal about how discrete defects such as matrix cracks and defect growth (e.g. delamination) can be predicted in structural composites. For many practical situations controlled by laminated multiaxial composite structures, the loss of performance and "sudden death" end of life is controlled by defect coupling which becomes a precursor to fracture plane development. These interaction sequences are highly dependent on local details of manufacture, design configurations, and loading for a given application material and influenced by small variations in loading history and other applied conditions.

Therefore, it is difficult to create a general analysis approach which relates real time measurements of a material variable which can be directly related to remaining strength and life. The solution to this puzzle requires a two-step advance in the reliability analysis and active control of in-service structural composites. First, a material state variable has to be identified that is easily measured and directly, precisely, and uniquely related to the coupling process that defines remaining strength and life. And second, a methodology

must be defined to use that variable to calculate remaining strength and life in real time, for arbitrary loading types and histories.

The present research work addresses both of these challenges by identifying dielectric response as a material state variable that is easily measured on composite structures in real time and uniquely related to the defect coupling process that marks “the beginning of the end”, and then by proposing an Artificial Intelligence (AI) method of using a continuous real-time record of that variable to predict residual strength and life, and further achieve real time control and system reliability. This is achieved by using the Broadband Dielectric Spectroscopy method and Fiber Optic distributed Sensors to measure the dielectric property and strain respectively. These state variables are used to establish a method to identify damage in the composite material, predict the characteristic damage state (CDS) and residual strength, life of material with uncertainty estimates. Interpretable machine learning methods are utilized to identify the contributing features to model and explain the predictions.

Table of Contents

List of Illustrations

List of Tables

Chapter 1

INTRODUCTION

1.1 Problem Statement

The Term "Composite" means "made up of two or more different parts." A composite material contains two or more elements which are combined in a macroscopic scale. The material formed can have the performance and properties superior to those of the constituent material acting independently. Composite materials typically have the most superior properties such as light weight, excellent corrosion, and high strength to weight ratio, fatigue resistance and ease of manufacturing compared to the traditional materials. Advanced Composites are widely used as an alternative to metallic structures.

The characteristics of composites such as high specific strength, low density, and high specific stiffness make composites highly desirable in primary and secondary structures of both civilian and military aircraft. The strongest sign of acceptance of composites in civil aviation is its extensive use in the world’s largest airliner, Airbus A380 and also used in the Boeing 787. Approximately, Composite materials account for 50% of the weight of the Boeing 787, including most of the fuselage and wings.

Over several decades of careful experimental investigation and exhaustive development of discrete damage analysis methods including integrated computational mechanics methods, our community knows a great deal about how discrete defects such as matrix cracks and defect growth (e.g. delamination) can be predicted in structural composites. For many practical situations controlled by laminated multiaxial composite structures, the loss of performance and “sudden death” end of life is controlled by defect coupling which becomes a precursor to fracture plane development. These interaction sequences are highly dependent on local details of manufacture, design configurations, and loading for a given application material and influenced by small variations in loading history and other applied conditions.

Therefore, it is difficult to create a general analysis approach which relates real time measurements of a material variable which can be directly related to remaining strength and life. The solution to this puzzle requires a two-step advance in the reliability analysis and active control of in service structural composites. First, a material state variable has to be identified that is easily measured and directly, precisely, and uniquely related to the coupling process that defines remaining strength and life. And second, a methodology must be defined to use that variable to calculate remaining strength and life in real time, for arbitrary loading types and histories. The present research work addresses both of these challenges by identifying a material state variable that is easily measured on composite structures in real time and uniquely related to the defect coupling process that marks "the beginning of the end", and then by proposing an Artificial Intelligence (AI) method of using that variable to predict remaining strength and life, and further achieve real time control and system reliability.

1.2 Motivation and Background

Predictive Maintenance, also called Condition Based Monitoring (CBM) of aircraft and spacecraft structural components is a well-developed field with foundations in non-destructive testing (NDT) and Structural Health Monitoring (SHM) methods that were adopted by the industry in the early 1990s. Several excellent review articles document the extensive work in this field and the breadth and scope of the results. This prior work includes computational analysis, a variety of physical methods of condition monitoring, and some work on data analysis and interpretation including some artificial intelligence and pattern recognition. This is a strong foundation for can be said to be an excellent record of safety and reliability of, for example, commercial aircraft produced and maintained by the leading OEMs in several countries.

What it does not provide (as evidenced by recent in-flight failures) is an in-flight system or reliable methodology for assessing structural integrity and expected performance that can predict the risk of continued operation of aging equipment of this type. That is the objective of the present work.

Under various applied field conditions, heterogeneous materials i.e. composites degrade progressively. To evaluate such changes in material state, Broadband Dielectric Spectroscopy (BbDS) is a unique robust tools which extracts the material-level information, including the morphology changes caused by micro-defect generation and the orientation and connectivity of those defects. A literature review on BbDS has shown that under the application of a vector electric field, with varying material state the dielectric properties of the material system also change. The uniqueness of this technique is that it is capable of interacting with the local details of the material system and can project the intensity of damage.

Also, Understanding how engineering structures respond to loads and their environment is of paramount importance for their successful design and reliable operation. Analyzing the strains, stresses, temperatures, and deflections in a bridge during rush hour, a composite aircraft's wing spar during a storm, or a high end bicycle during the Tour de France is what allows engineers to predict a structure's lifetime, increase its safety, and optimize its performance. Armed with a complete picture of these quantities from the early design stages to the end of a product's lifecycle, designers would undoubtedly create safer, stronger, and more efficient engineering structures. A fiber optic sensing instrument is capable of providing this information in real time. This distributed sensing technology enables monitoring of strains, temperatures, stresses, out of plane deflections, and three dimensional shape using a small and lightweight package.

Both the Broadband Dielectric Spectroscopy method and Fiber Optic Sensing system, have proved to be excellent CBM and SHM techniques. Hence, coupling these methods properly with artificial intelligence, we would be able to achieve our goal of real-time inflight monitoring systems

The currency of these AI methods is the data that are generated by a physical system. Unfortunately, if we are uncertain about the physics of the system, we also do not know the level of uncertainty in the data that we use to represent it. In this research, the nature of the physical data retrieved and recorded is also critical. What physical dielectric observables best represent the 'state of material' in the specimen, and at regions of the material. However, based on our research, these data are direct estimates of material strength, not analogues that then require analytical interpretations. Also in future, this research AI model is applied to a history of loading after we have "trained" it. That history might include, for example, a series of high amplitude fatigue loading followed by a series of low amplitude fatigue cycles, compared to a reversed sequence (low to high); we know from prior experimental experience that the remaining strength of such specimens is very different. Constructing this 'validation' for more general loading histories is a challenge. Hence, proper Uncertainty Quantification methods are also to be established, for us to understand the predictions made by the artificial intelligence models.

1.3 Objective of the Dissertation

The primary objective of this research is to use reliable state of the art sensor technologies which includes dielectric sensor and fiber optics, for integrated SHM/ CBM to collect data defining the material state and hence predict the damage mode, remaining strength and life of the material. The goals are listed as follows:

- Use real-time measurements of dielectric parameters through the thickness of the laminate that are directly related to the material state, measured by BbDS and strain, and temperature collected point wise along their length measured by fiber optic sensors to directly predict responses such as the strength and life from its material state being assessed via Machine learning models and Recurrent Neural Network interpretations, for a composite laminate aeronautical structure under service loading that varies in time
- Introduce changes in loading history and other variations in applied conditions to sort out the effect of "real life" load history effects, i.e., to support "tail number" (individual vehicle, structure, or specimen) prediction of strength or life in real time at any instance during its life, and provide a real time risk assessment.
- Using progressive defect analysis (PDA) we will identify the defining features of such data, especially the changes that predict accelerating damage and impending structural failure.
- Evaluate and establish the feasibility of the proposed approach as the first step in a sequence of Feasibility, Development, and Implementation, which can be further integrated via transfer of our learning to an Industrial Internet of Things (IIOT)

The global objective of this research to develop a Cure on the Fly – Intelligent Prognostic Health Management System (COTF-IPHMS) for Composite materials. The COTF-IPHMS aims to continuously monitor the composite structure by SHM techniques to collect the MS in real-time and use AI to predict the material properties, remaining strength and life based on its current and previous MS, as well as provide control measures and decisions for the safe operation of the structure.

1.4 Outline of the Dissertation

This dissertation is outlined as follows:

Chapter 1 describes the problem statement, brief motivation and background and gives the objective of this dissertation.

Chapter 2 deals with the in-depth literature review of composites and its complexities ; diagnostics and prognostics methods in composites which includes the review on the electrochemical impedance methods and fiber optic sensor systems ; use of artificial intelligence methods in these diagnostics and prognostics ; uncertainty quantification methods in aircraft structural prediction systems, use of interpretable machine learning methods and finally identifies the gaps in the literature, proposing the contribution work.

Chapter 3 describes the various technologies used in this dissertation in detail, which includes the composites manufacturing processes, broad band dielectric spectroscopy, fiber optic sensing system, artificial intelligence algorithms, and interpretable machine learning process.

Chapter 4 presents the research work done on dielectric assessment of the damage states in composites, which are caused by introducing foreign object defects during manufacturing process. It also describes the prediction of these defects using machine learning algorithms, and helps us identify which dielectric parameters are contributing towards the prediction by using interpretable machine learning processes.

Chapter 5 presents the research work on using artificial intelligence methods for identifying the damage precursors in composites, under quasi-static loading conditions using the dielectric spectroscopy data.

Chapter 6 presents the research work done on the residual strength and life prediction in composites using the dielectric and strain data collected from the sensors, and development of the artificial intelligence models for these predictions. It also describes the uncertainty quantification processes using the interpretable machine learning models.

Chapter 7 provides the conclusion of all the results obtained through this research work and further provides the direction for future work in the field of diagnostics and prognostics of composites using artificial intelligence.

Chapter 2

LITERATURE REVIEW

The outline of this chapter is as follows: Section 2.1 describes the basics of composites, various composite configurations, types of damage modes and the entire variations that make each material and its property unique. Section 2.2 introduces AI (Artificial Intelligence) and its methods. Section 2.3 describes the current SHM and CBM – diagnostics and prognostics methods used in the composite structures, and the sub-sections of 2.3 also identifies the major literatures where AI, data-driven methods are used in composites SHM, NDT, prognostics. As per the focus of this dissertation, the in-depth literature for Fiber Optic Sensing systems and the Broadband Dielectric Spectroscopy (BbDS) are provided in the sub-sections 2.3.1.3 and 2.3.1.4 Section 2.4 indicates the uncertainty and reliability associated with these methods. Section 2.5 briefly outlines the public datasets available for data researchers, scientists working in composites. Section 2.6 describes the proposed application of Cure On The Fly – Integrated Prognostics Health Management System (COTF-IPHMS) with the Industrial Internet of Things (IIoT) that concludes our review with the future work and recommended measures for researchers developing such methodologies for real-time prognosis in composite materials.

It is to be mentioned that parts of this chapter are published in a review article [1].

2.1 Composites and its Complexity

Composite materials, are essentially made up of two or more constituents, primarily consisting of a fiber and matrix in the present discussion. However, each polymer composite could be manufactured with so many variations as shown in the Figure 2.1.

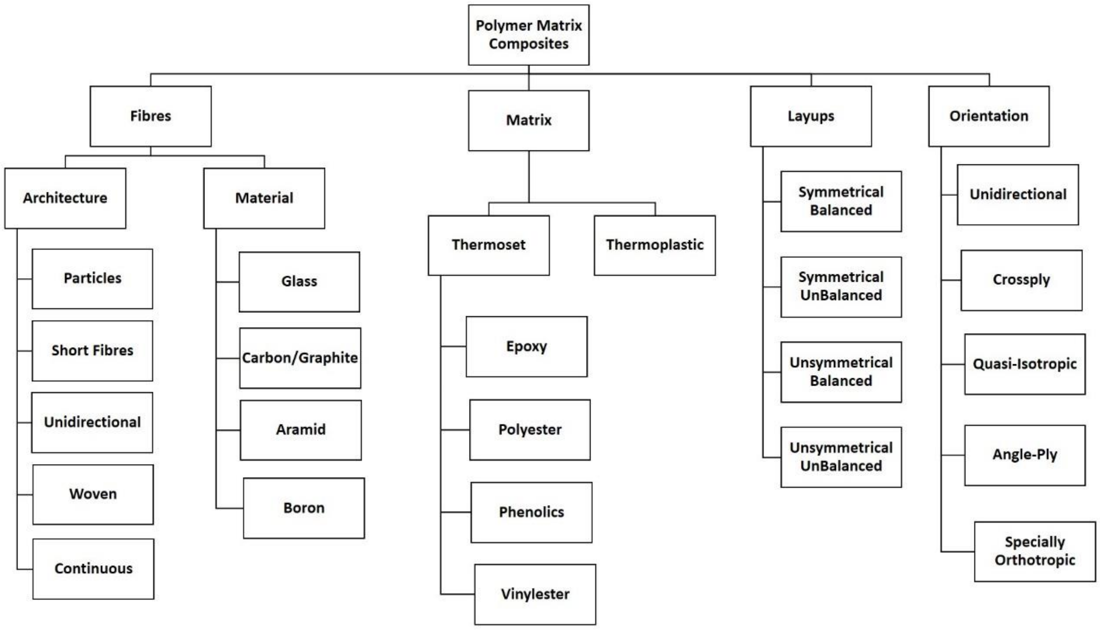

Figure 2.1: Composite materials and their variations

For example, 5 architectures, 4 material types, 4 resin systems, 4 orientation laminate types, make a combination of 320 varieties of composites. Considering the layup alone, a 16 ply laminate could have 7 angles (0,15,30,45,60,75,90) in each layer and hence could make a 112 combinations. The most amazing fact about composite materials is that each small variation could influence the property of the material, and hence it is complex in nature to predict the strength and life of the material. Another important parameter to consider is that these predictions are also influenced by the environmental, operating conditions that are unexpected. The behavior of these complex material systems is dependent on the interaction of constituents in the micro (local) scale and interaction of the laminae at large on the global scale. Unlike metals, composites are designed to develop distributed damage and so that the initiation of a single microscopic crack does not individually affect the strength/life of these materials. Therefore, the primary interest is not in single local events but in the process of interaction of multiple events that have a collective global effect on the material behavior. The interaction of these local events are interpreted using 'state' of the material by the means of 'state' variables e.g. strength, stiffness etc. and the evolution of these state variables with life was used as the measure of durability.

A vast amount of literature is available on different damage modes, and their progression; damage could initiate because of defects during processing or could develop during service as shown below [2–4].

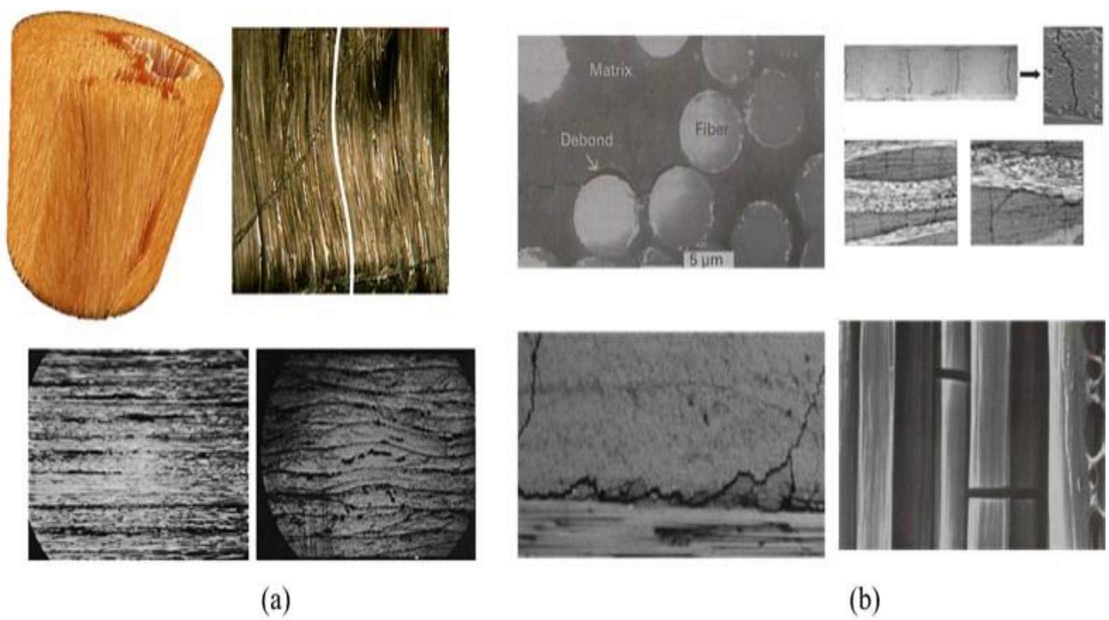

Figure 2.2: Defect types typically observed in structural composite materials[5].

Reifsnider et al observed that the evolution is more of a sudden death phenomenon as shown in Figure 2.3a. The damage development shown in Figure 2.3a depicts the progression of damage in unidirectional composites during fatigue [6]. As observed, the initiation of damage starts with matrix micro cracking followed by debonding between fiber-matrix or debonding between fiber-matrix leading to micro cracking [3]. These matrix cracks initiate at different sites along the length of the specimen until a saturation state referred to as the characteristic damage state (CDS) is obtained [6]. CDS is most often referred to a state where in the crack spacing reaches a saturation value after which no more individual cracks are developed in the current ply. At this state, there is generally a significant drop in stiffness but not in the strength as shown in the Figure 2.3b. This is then followed by creation of secondary cracks that are transverse to the primary cracks in the neighboring plies, followed by coupling of these primary and secondary cracks at the free edge of the sample to initiate edge delaminations. These secondary cracks are created at various sites along the width of the specimen and initiate local interior delaminations which differ from edge delaminations. In the final state of damage development, these secondary cracks interact and grow at a rapid ‘rate’ such that the locally failed regions find a path which then (aided by fiber fractures) lead to sudden drop in the strength and to final failure.

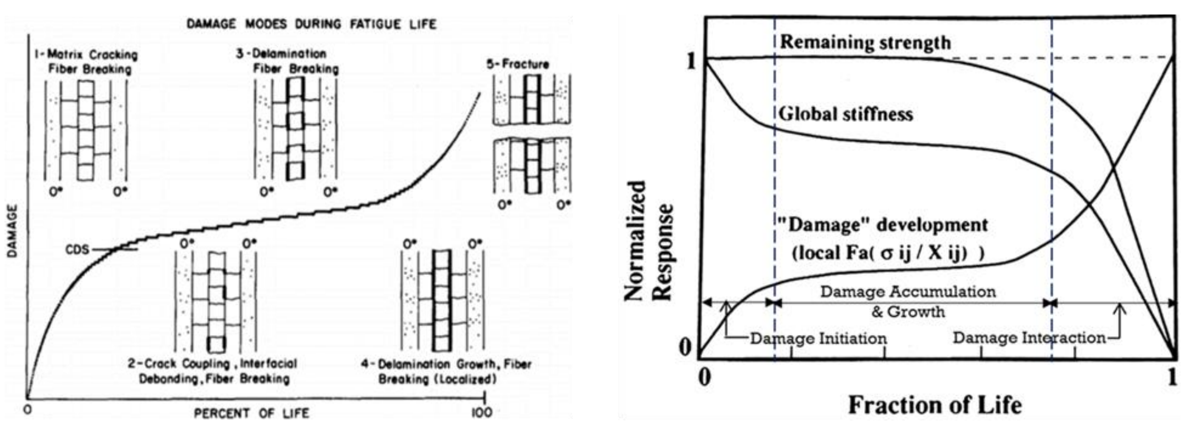

a b

Figure 2.3: (a) Typical damage development stages in a multiaxial composite laminate during tensile loading (b) Changes in global strength and stiffness during damage development

As discussed above, the evolution of damage can be classified in to three stages: Damage Initiation, Damage Accumulation & Growth and Damage Interaction as shown above in Figure

2.3. It can be observed that even though the damage development is progressive, the evolution of remaining strength isn't proportionately progressive and is more typically a sudden death phenomenon.

The modes of damage in woven composites are different then what is observed in uni-directional composites. The response to loading in the fiber directions can often be approximated as linear. However, the response to off-axis loading orientations is highly complex and significantly non-linear with typically very high strain to failure. Figure 2.4 shows the typical response of a [+/-45°] tension specimen [7]. The response can be described in four zones based on applied strain; a different type of behavior is observed in each zone. As loading begins, an initial elastic (mostly) response is observed (zone 1) up to approximately 0.5% strain. At this point, matrix cracks begin to occur (zone 2) and on continuous loading, the density of these matrix cracks keeps increasing, and the response becomes non-linear. Around 4% strain (zone 3), the density of matrix cracks saturates and very few new single cracks are formed (CDS). Once a state of crack saturation is attained, the non-linearity resulting from matrix cracking is no longer prevalent. In this zone, the behavior is dominated by the fibers which have a tendency to reorient towards the loading direction. This behavior is referred to as trellising wherein the angle between reinforcement directions changes from 90°. The result of this is a stiffening response as observed in zone 3. Fiber trellising continues until about 13% strain, where the fibers eventually begin to fail (zone 4). The final non-linearity is the likely result of statistically based fiber failure over a range of axial strain

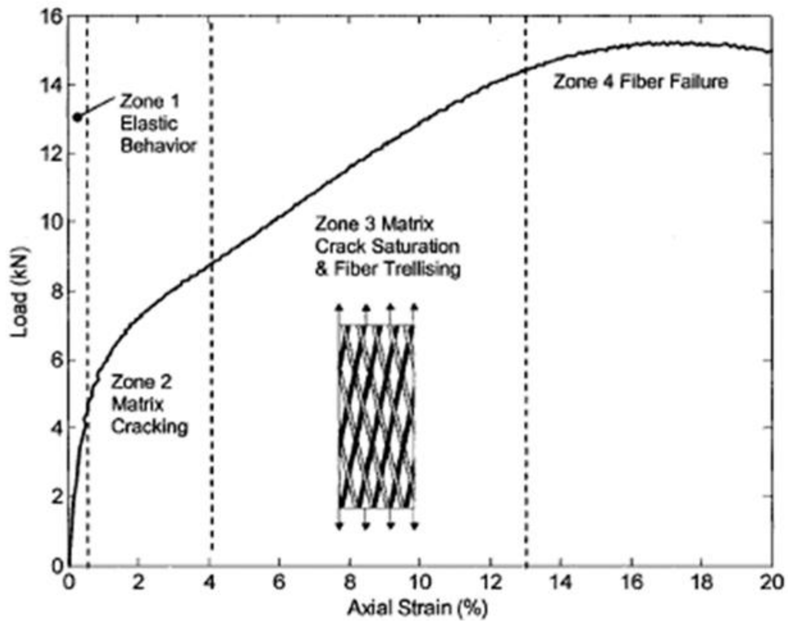

Figure 2.4: Constitutive response of an off-axis woven composite [7]

From literature, it is evident that the evolution of the material state is not uniformly progressive in nature even though the damage progression is progressive. Given the complexity of damage modes; the location of the damage is mostly internal. Using advanced non-destructive evaluation (NDE) techniques one can accurately determine the location and nature of damage; however by the time that information is obtained the structure would have already lost its load bearing capability as shown in Figure 2.5. Hence as an engineer, it is important to predict the state of the material to avoid catastrophic failures. Different research groups have used various SHM and condition-based monitoring techniques coupled with AI to identify and predict the material state and will be discussed in the coming sections.

Throughout this dissertation, the term “damage modes” refer to one or multiple of the damage modes mentioned in Fig 4a, the term “damage state” refers to manually created levels of damage by various researchers, based on load levels, or sensor readings and the term “damage type” refers to other types of damage such in indentations, bond failure, surface cracks and impact damage.

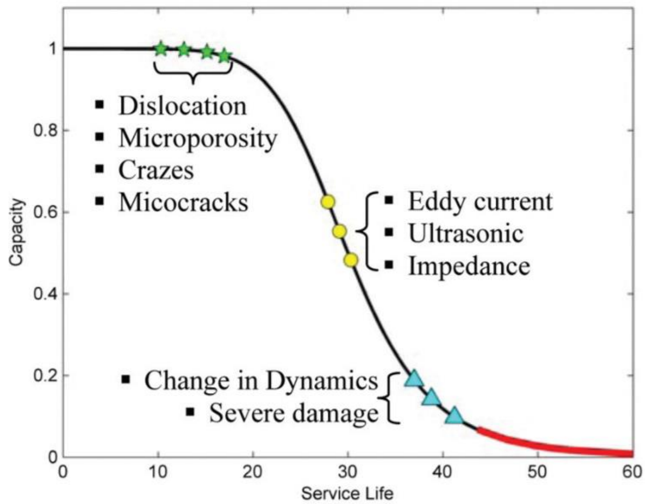

Figure 2.5: Capabilities of current SHM techniques to capture damage in composites during service life[8]

2.2 Artificial Intelligence

The concept of "data driven" grew out of the general subject of data analytics, especially in the business world. The classical sequence shown below in Figure 2.6 illustrates the general contents of the concept.

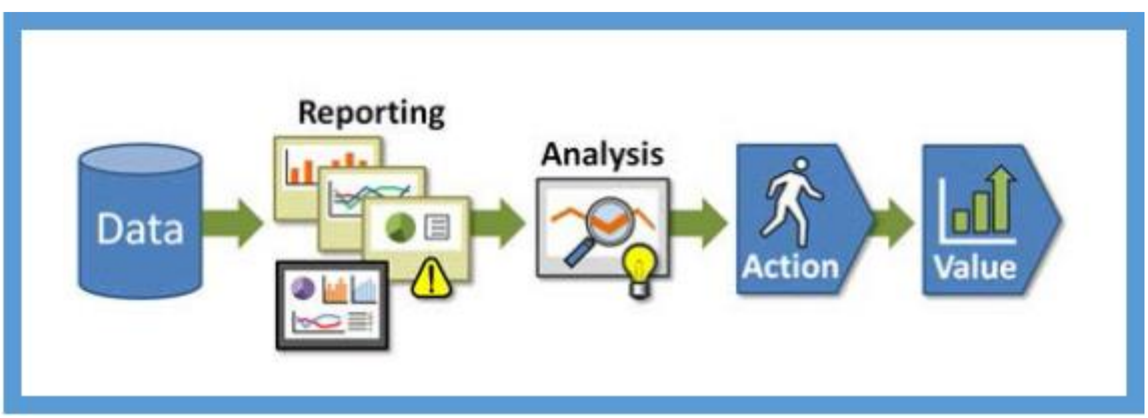

Figure 2.6: Data Driven Methodology

AI is the new “electricity,” which powers millions of digital systems. AI can be defined by 3 different kinds:

1. When the training data generated for optimal decision making are of geometry only, i.e., AI with no physics involved, such as to train a machine to play chess.
2. When the training data are of geometry and known physics, such as Newton’s law, such as GPS applications, tracking the trajectories of rockets, satellites.
3. When the training sets do not have enough physics and depend on the past and current data to fit a model to predict results, such as driver-less cars, autopilot planes, SHM of structures.

AI methods are deterministic and non-deterministic. Common AI tools can be classified by type of approach such as machine learning, evolutionary computation methods, and probabilistic methods - Statistical AI. Machine learning is the most non-deterministic AI in application. The commonly used methods of machine learning are

- Supervised learning – both input and prediction data are provided
- Unsupervised learning – only input data is provided. No explicit output labels are provided, and hence the algorithm finds relationships among the input data
- Deep learning – a machine learning algorithm, supervised or unsupervised or reinforcement learning based with several layer of NNs, to obtain higher level features from input data
- Reinforcement learning – The process to train algorithms to make sequence of decisions, where the agent learns the methods to achieve a goal in an uncertain

complex environment. This agent is allowed to learn the behavior to achieve such goals by trial and error.

A few of the most commonly used types of AI models with composites are shown in Figure 2.7.

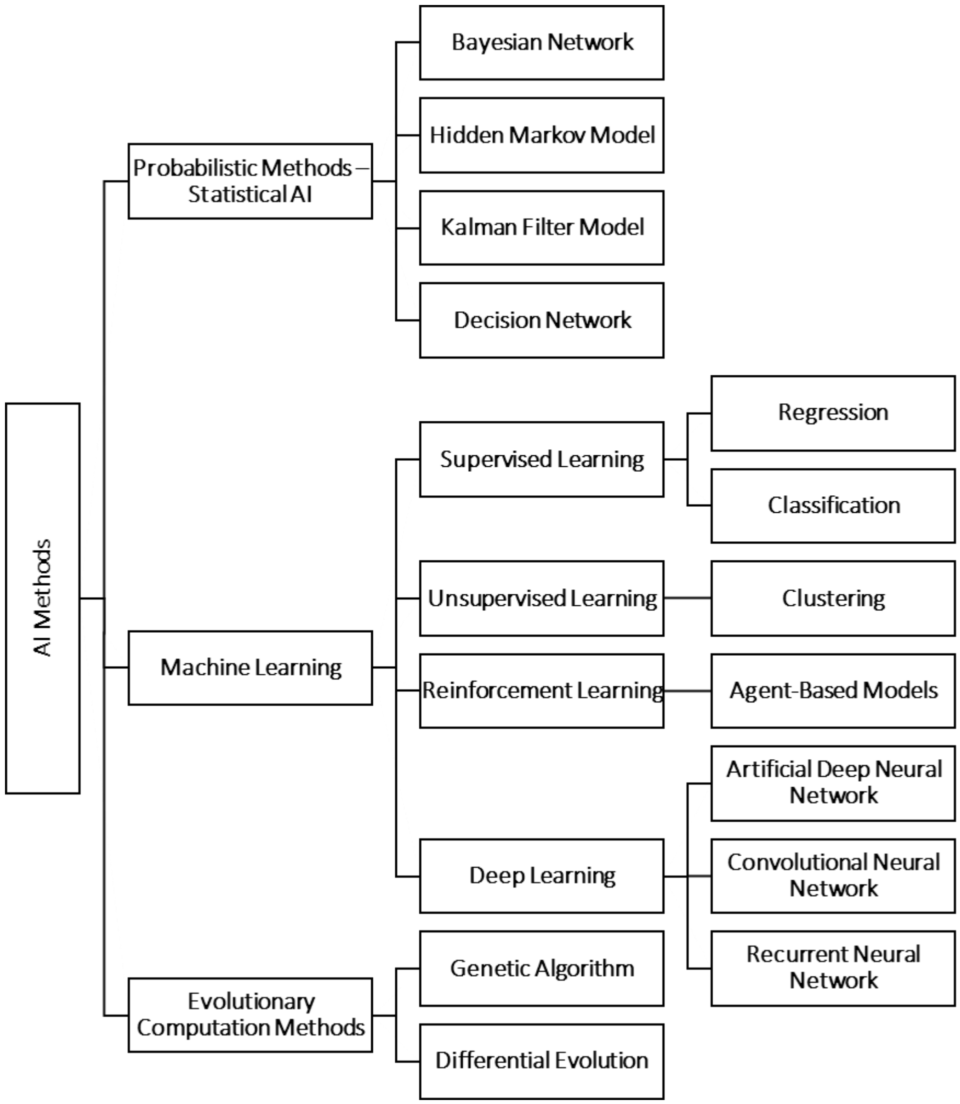

Figure 2.7: Classification of Artificial Intelligence techniques

Recent developments in these AI methods, have established several intelligent systems for aerospace applications. In addition, the advancements in sensor technologies and data acquisition methods allow complex structures to be equipped with several sensors, which can analyze quantities such as structural responses, like deformation and environmental behavior such as temperature and humidity. Regardless of this development of the sensing methods, interpretation of this big-data of measurements to obtain useful information on structural conditions remains a challenge. This leads to a massive need for developing a good data-driven AI system by applying the proper methods to learn and understand such data to make proper decisions.

In the context of machine learning, the most important elements of the method are the prediction algorithms, which give the predictions of the defining probabilities based on the trained data. As general regression modeling deals with the linear equations, using models such as ANNs, and polynomial input features, gives the ability to derive complex non-linear equations, particularly useful to model the composite.

2.3 Diagnostics and Prognostics in Composites

AI has first been implemented in composites for material design[9–16]. Early in 1991, an expert system called EXCOCOM was developed by Torbaghan et al.,[9] which is an adequate tool for composite materials design and optimization. To design and manufacture the composites, proper components of fiber, resin system and other parameters need to be selected, from which the desired mechanical properties can be obtained, which is done by the EXCOCOM. Precise explanations on the manual process in designing of composite materials and the need for the expert system in composite material such as fiber expert and resin expert, and the manufacturing expert have been proposed and this routine design of composites was replaced by developing AI techniques [10]. AI has also been developed for obtaining the elastic modulus without the need to perform depth sensing indentation as NDT[11]. Yang et al., [12] used CNN to predict material properties such as stiffness, strength and toughness, which are obtained by the FEM models, and used as a demonstration of deep learning (DL) to accelerate the composite design optimization.

The researchers compared CNN with LR and RFR and attempted to open the Black Box of DL, visualizing the features. A detailed review on design of composites by using machine learning techniques has also been summarized[13].

AI methods are also used a lot in the manufacturing, optimization and inspection of composites [17–26].Hong et al.,[17] built a time dependent RNN with the experimental and computational data for evaluating and predicting the degree of cure in the composite material. Hsiao et al.,[18] implemented a Streamlined Intelligent RTM, which consists of two parts – the design software VIMDS-LCM and the automation control system Auto-RTM. The VIMDS-LCM contains AI, Simulation Engine, and its own database. It designs the Intelligent RTM by planning the sensing and control strategies to counteract the disturbances in RTM. Tsao et al.,[19] proposed an approach integrating ANN with Taguchi method to predict and evaluate thrust force and surface roughness in drilling of composites. It was observed that the thrust force was influenced by the feed rate and drill diameter whereas surface roughness estimates were influenced by the specimen feed rate and spindle speed. Recently, Oromiehie [20] used ANN to predict the inter-laminar shear strength, elastic modulus, flexural stress and strain, based on the input of layup speed, hot gas troch heat source and consolidation force. The complex relationships between the input and the output were established. Sacco [21,22] used a ML algorithm - CNN to locate and characterize the defects from profilometry scans. This proposed technique can accelerate the process while keeping and informing the human inspector to be integrated and in control, and increases the speed of inspection, and robustness of the human checking to be missed or misclassified. They deployed the models by developing a User Interface for the end user. Finally, as a summary of all manufacturing and inspection methods in AI, Scott Blake [23] presented the elements and mechanisms for applying AI to composites fabrication. It is also mentioned that AI can not only be implemented in inspection, but also for prognostic methods too. A CNN has been used in inspection to detect Foreign Object Defects (FOD) in aircraft structures. The CNN was trained using a small dataset, by using transfer-learning method. Blake has represented the closed loop manufacturing process as the model shown in Figure 2.8.

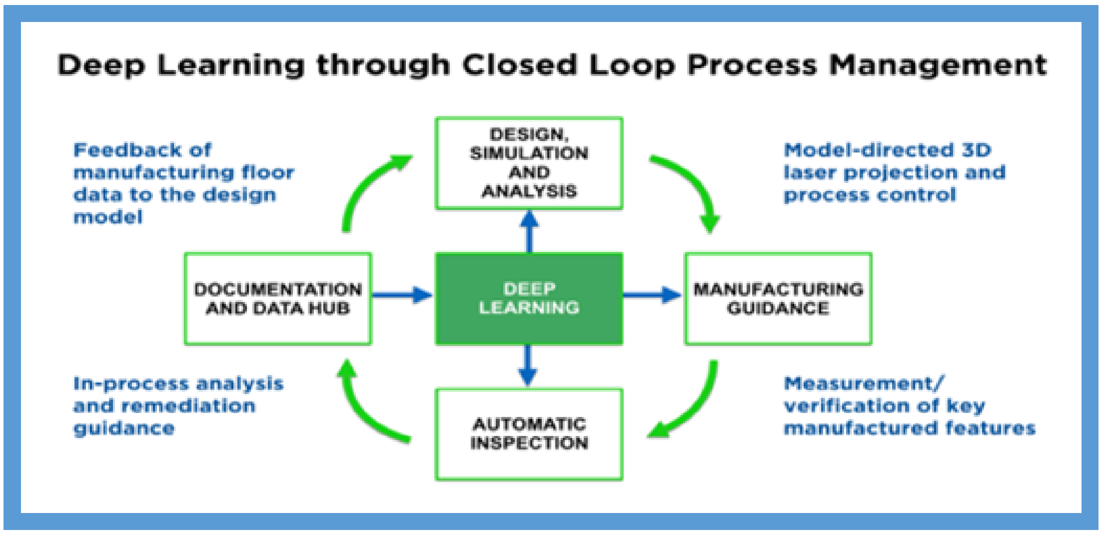

Figure 2.8: Closed loop manufacturing process[23].

2.3.1 Diagnostics Paradigm

Traditional methods of diagnosing damage involves interpreting the data acquired from sensors to obtain meaningful information about the type of damage. However, in many cases these are human biased, and becomes more complex, as the human cannot validate the source of damage, or accurately identify it. Hence, integration of AI with the sensor data, will reduce the human error, and will be purely based on the current and past data. These integrating algorithms work by identifying the deviations, which are associated with damage.

In this section, the literature articles are categorized as per the sensors used by the SHM and NDT methods. Figure 2.9a represents the number of papers published on the SHM and prognostics of composites using the AI methods. It is clearly visible that the development of “intelligent smart structures” and “intelligent health monitoring systems” started early in 1990s. However, it was only recently in the last decade that the application of AI in composites has been blooming with development of high performance computing machines. Also, it should also be noted that, the field of prognostics is not paid as much attention as SHM.

The figures are based only on the publications considered in the literature review. A few of the publications do have multiple sensor systems, hence they were counted once for each category. In addition, a few publications are from same team of researchers, and have the same datasets, hence they were counted only once for accurate estimates.

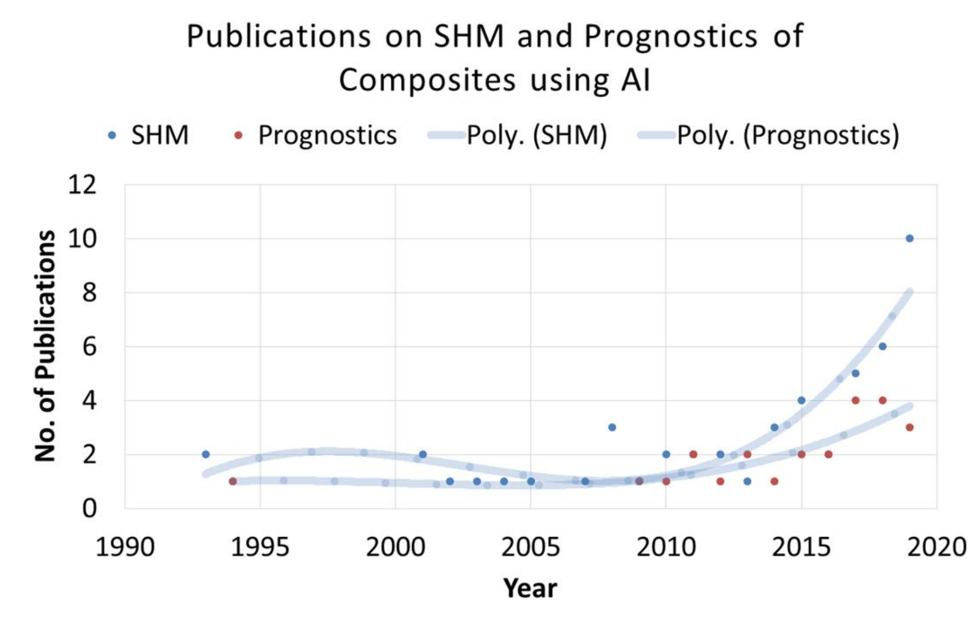

a)

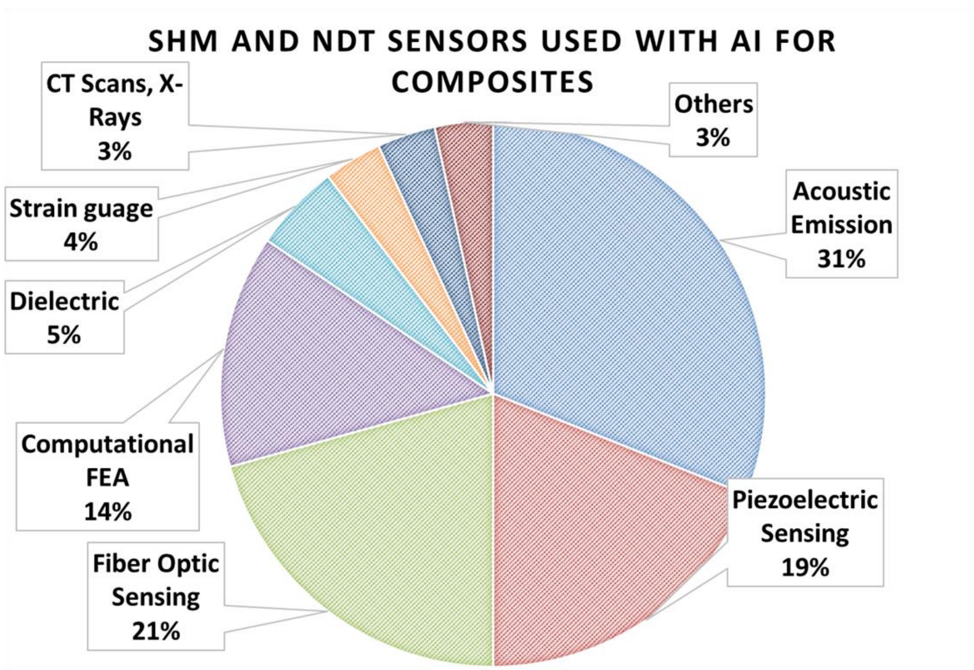

b)

Figure 2.9: (a) Number of publications on SHM and Prognostics of composites using AI and (b) Pie-Chart on SHM and NDT Sensor systems used along with AI in Composites.

2.3.1.1 Acoustic Emission (AE)

Wirtz carried out fatigue and bending tests on carbon/epoxy samples, while integrating with AE based SHM and classified the damage mechanisms using SVM. However it was stated that such approaches of SHM are more complex as the relations among methods, test conditions, sensors were more scattered and a direct relationship could not be established[27]. Argus proposes using AE techniques on omega profile composite structures, and uses the PZT sensors time-wave data in an ANN system to detect the location of the damage. Their proposed technique uses a low-cost hardware system, for capturing the data, and training the model using Raspberry Pi devices. These kind of systems are well suitable platforms for experiments which can be used with different ANN configurations and sensing methods [28]. Another intelligent SHM system was proposed by Staszewski to use ANN using the Acousto-ultrasonic wavelet data and Optical fiber strain data to identify the damage in composite laminates. Proper procedures on implementation of the system are proposed. [29]. Also, a new type of AE sensor made from fiber optics, was developed as Fiber Optic Acoustic Emission Sensor (FOAES), and ANN was used to identify the AE source localizations in CFRP composite materials. [30]. Alternatively, Voth et al., have used a mathematical approach of Short Term Fourier Transform (STFT) to identify the damage mechanisms based on AE signals. They claim that this method isolates the frequencies of wave modes, hence can provide specific characteristics of sources and damage mechanisms that initiate acoustic events. Also this physical relationship has a benefit of AE analysis that cannot be achieved through complex ANN and clustering techniques [31]. Banerjee et al., used the Kalman filter and particle filter – conventional data driven methods to identify the delamination region from PZT wafers data of AE guide waves on fatigues tests. These delamination regions were validated by the optical transmission scans and the future damage areas were accurately predicted with 95% confidence intervals [32].

Unlike supervised learning, most of the researchers have used the un-supervised learning methods using the AE-SHM techniques. The failure modes and growth of crack was predicted by Kohonen-SOM, MLP - hybrid AI algorithms using the AE signals data collected during fatigue tests of tensile and notched carbon epoxy specimens. Surprisingly the variations in type of load, orientation, layup did not have a huge influence on their damage mode estimates from AE signals [33]. Dia has used hybrid composite materials made with aluminum and glass fibers, and performed quasi-static and fatigue tests on the tensile coupons. They have used 8 different input parameters to identify and predict the damage, using PCA, K-means and CART algorithms. To categorize the damage mechanisms, the most relevant AE parameters were identified as amplitude, frequency, duration and counts to peak [34]. Fracture toughness tests were carried out by Oskouei et al., on double cantilever beam specimens and the damage classes were classified by the fuzzy c-means algorithm based on the energy, amplitude, the rise time, the counts, the peak frequency and the duration of the signals obtained from AE with PZT. The values of their AE data, were correlated with the values obtained from the literature to obtain the respective damage mechanism [35]. Doan et al., carried out fatigue testing on composite split disks, and collected the AE data. These data were used by clustering algorithms after noise reduction and fast feature extraction techniques, to identify AE clusters. A mahalanobis distance based noise modeling approach was used. They identified the loading and unloading phases during the mechanical tests. However, the AE clusters were not validated against damage modes, and other complementary NDT and future experiments need to be performed to understand these clusters [36,37]. Crivelli et al., and Jumaili et al., performed fatigue tests on composite panels to predict the fatigue damage mechanisms -

matrix cracking and delamination damage mechanisms using unsupervised neural networks, clustering, Delta T mapping, and parameter correction techniques. These damage mechanisms were identified by ultrasonic C-scans [38,39]. Boussetta et al., used the K-means and Kohonen Self Organizing Map (SOM) to identify the damage behavior using the AE signals in glass-polyester filament wound composite [40]. Ramasso et al., used the consensus clustering unsupervised learning algorithm to predict the early signs of failure, based on the AE time series data obtained from tensile tests of ring shaped composite split disk specimens. The damage states were predicted with good accuracies even in these complex configured structures and high emissivity [41]. Also several other unsupervised learning models such as k-means, hierarchal, fuzzy c-means, Gaussian methods, incremental clustering were all performed using the AE features obtained to predict the damage mechanisms on tensile and bending tests [42,43]. The real-time structures such as wind turbine blades were exposed to fatigue testing for 21 days and the AE data, from PZT sensors were collected by Tang et al., These data were used to develop hybrid models of unsupervised and supervised learning. The unsupervised clusters created were correlated with fracture mechanisms by detailed analysis. This method helps to generate the dataset for supervised pattern recognition method, and new data were classified accurately [44]. Nair et al., used the K-means, PCA, MLP and SVM methods to identify the damage mechanisms in GFRP coupons and CFRP- RC beams using the AE features data. The data were first classified using the unsupervised learning and correlated to damage mechanisms , and then trained into supervised learning for making predictions [45,46].

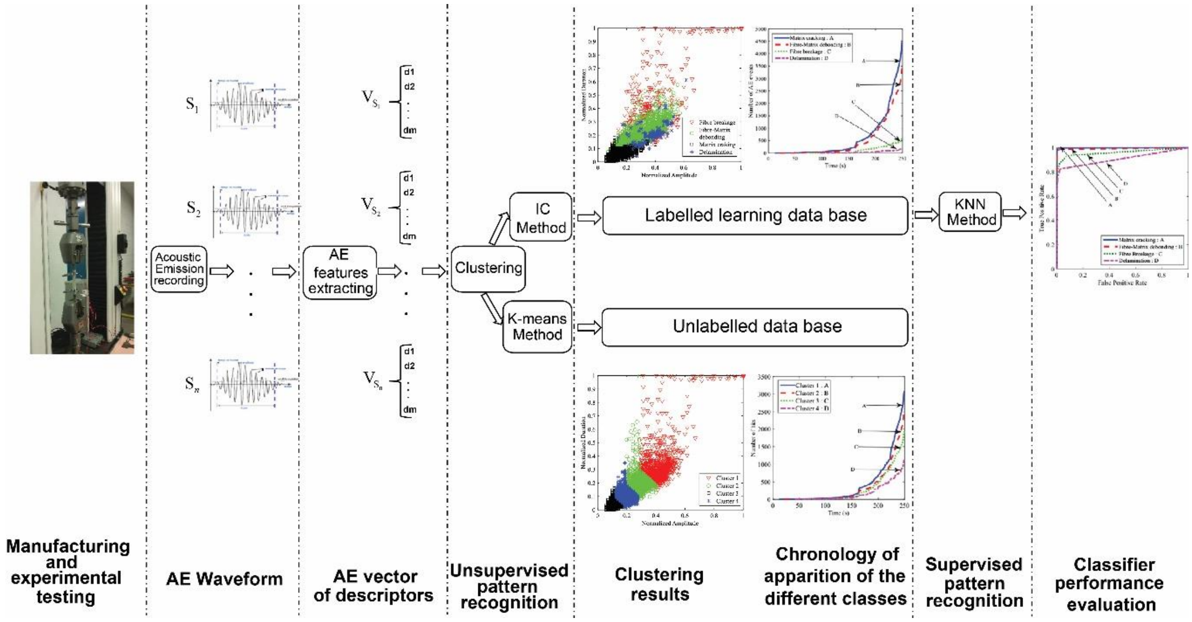

Figure 2.10 Method of Using Unsupervised along with Supervised Learning[43]

2.3.1.2 Piezoelectric Guided Wave Sensing

The guided wave sensing method can be used for identify defects like foreign bodies, and also for identifying the damage in the material. But the characterization of the damage mechanism using the Piezoelectric Transducer (PZT) sensors is very difficult, which builds the path for AI to play a role.

Schillemans et al., used pattern recognition algorithms such as K-nearest, potential function classifier, linear classifier, F-machine and modified K-nearest in identifying the defects of foreign bodies like aluminum and Teflon in carbon epoxy panels using the time domain PZT signals. Classifying error is lower order than classifying in random, hence the pattern recognition reduces the manual human work and has great potential [47].

Many researchers have used the ANN to identify the damage type using the ultrasonic system with PZT sensors [48–51]. Su et al., used ANN with the data generated by FEA and PZT to predict the position, geometric identity, and orientation of the damage and Kral used the ANN combined with SOM, to identify the initial onset of damage by placing piezoelectric wafers in Carbon/Epoxy laminate panels [48,50]. A hybrid learning approach of ANN with Neuro-Fuzzy technology was implemented to detect and locate the impact damage in the carbon epoxy laminates embedded with PZT. The phase, frequency and magnitude data were used. This adaptive system has a significantly short training procedure [49]. Another hybrid algorithm called Radial Basis Function Neural Network (RBFNN) was applied to identify the impact damage in CFRP tensile coupons using the piezoelectric signals[51].

Decision tree algorithms were used by Talaie et al., on the PZT data, along with dielectric, optical fiber data to monitor the curing of glass fiber laminate, and hence identify its physical and mechanical properties [52]. The PZT time wave data was used to detect the induced damage modes of vibration tests on carbon epoxy coupons by using the SVM and K-Nearest Means algorithm by Das et al.,. They also classified the anomalies based on the unusual patterns [53]. SVM was also used to predict the location of the load based on the PZT signals on a carbon epoxy panel, subjected to surface to response excitation analysis[54].

In a study by Manson et.al, the damage in composite panels subjected to environmental changes such as humidity and temperature were obtained by using PZT lamb waves. By performing PCA and outlier analysis, it was observed that damage-sensitive features are more sensitive to temperature in comparison to humidity, hence data normalization techniques are required to cover all normal operations of a damage-free structure[55]. Tibaduiza et al., developed hierarchical nonlinear PCA, fine and weighted K-nearest neighbors algorithms for damage prediction in carbon epoxy plates and sandwich structures[56].

CNN has been used on the ultrasonic wave images obtained from carbon epoxy laminates to identify the impact location and classify it by Tabian et al., The impact energies were classified into different categories as safe, alert and danger. The model had excellent accuracies of 98.3% demonstrating it as a reliable method. However, thresholds of the risk categories must be established from experiments, or from material properties [57].

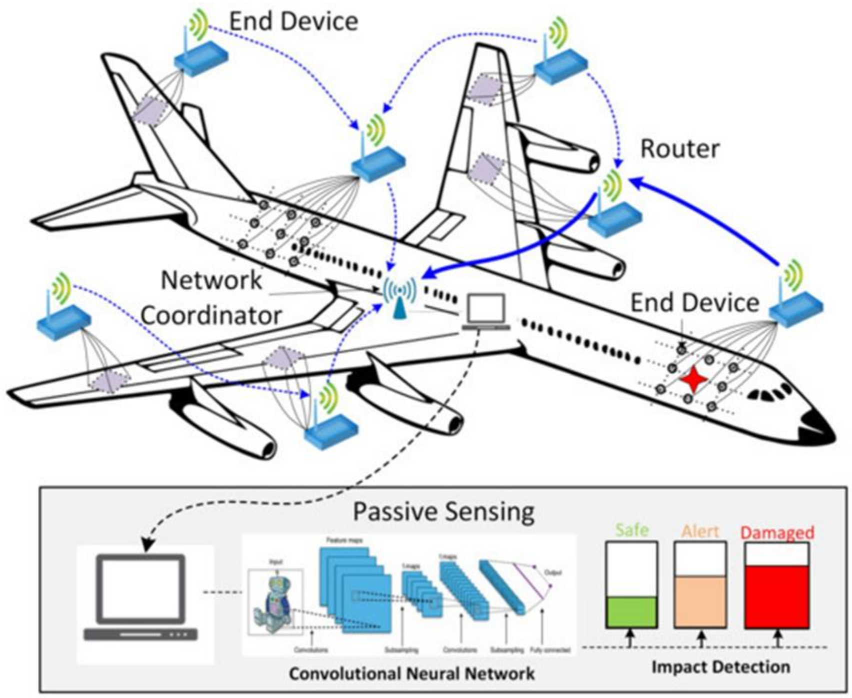

Figure 2.11: Passive sensing with embedded wireless sensor networks mounted on a aircraft and CNN for impact detection[57].

2.3.1.3 Fiber Optic Sensing

Fiber Optic Sensors (FOS) are widely used in SHM due to its various advantages due to its immune nature to electromagnetic interference, corrosion resistance, collecting multiple material states and easier installation compared to the traditional strain gauges.

Miller et al., installed the FOS on a straight tapered composite wing at NASA, to calculate the distributed vertical shear, bending moment and torque loads along the wingspan. The results were compared with the conventional foil strain gauges and demonstrated the advantages in using

FOS for providing distributed wing load information, reducing instrumentation weight and reducing load test calibration complexity [58].

As a combined manufacturing and SHM process, Talaie et al., have used optical fibers along with dielectric and PZT sensors, simultaneously embedded in composites for cure monitoring and hence therefore predicting the class of laminate and its physical and mechanical properties, by monitoring the strain and temperature and developing a decision tree based AI algorithm [52]. Oliviera et al., have used the ANN and SOM algorithms using the strain data to detect the damage – matrix cracking, delamination and fiber breakage on glass-polyester laminate panels subjected to tensile loading. They have used the optical fibers with FBG's and interferometer, and also AE based sensing for validation [59]. Another AI application of damage detection using embedded FBG's was implemented on glass epoxy tensile coupons subjected to mode I tension compression testing, and static tests. An SVM algorithm was developed using the FBG wavelets [60]. Datta et al., used least square support vector regression to predict the impact of damage and estimate the energy using the strain data obtained in carbon epoxy laminates subjected to drop test[61].

Panopoulou et al., and Loutas et al., have developed ANN and SVM algorithms respectively[62,63] using the fiber optic data obtained by varying vibration analyses on carbon epoxy thin panels, and honeycomb sandwich panel – stiffened panels. The inputs were strain data in frequency and time domains. The structural damage types were predicted. Lu et al., used the FBG wavelength data to identify the damage in carbon epoxy plates using Fourier transform, PCA,SVM,C-SVC[64].

Perez et al., Montoya et al., [65–67] have used the fiber optic sensors in the real-time UAV wing sections. They have performed bending tests, real-time flight tests under various flight conditions and have collected the strain data. These strain data have been used by different algorithms such as PCA, SOM, and unsupervised algorithms such as Fuzzy C-Means and Gustafson Kessel to accurately predict the damage in the composite wing structure with high accuracies. The UAV wing structures are made up of carbon-epoxy material, and with balsa as a hybrid structure. Guemes and Perez conducted impact drop tests on CFRP composite panels, Isogrid structures and real-size wind turbine blades, with embedded fiber optic sensors to collect the strain data. A PCA algorithm was used to predict the damage index in the structure. Ultrasonic C-scans were used to validate the damage in the composite panel[68]. The researchers have proposed the use of unsupervised learning followed by supervised learning. As it is possible to have data from all the different operational conditions for a composite structure and, therefore, construct a model (e.g. statistical) from these data. Such developed models may be too general and some data from damage conditions may fit into the model and, subsequently, be classified as a normal condition. One successfully-proved approach is to use unsupervised-learning, density-based classification to create clusters according to the operational condition and, then, build models for each specific cluster.

2.3.1.4 Computational Finite Element Analysis (FEA) models and its validations

Early in 1994, Ramu et al., developed an AI algorithm by integrating fuzzy logic with ANN to identify, categorize and assess the extent of damage on composite materials. They used the displacement data, obtained by FEA models using vibration analysis and experimental data from literature to validate their model. However they concluded that obtaining a huge number of data to include in the training is cumbersome. Also, developing a trained network is a heuristic and laborious process with no knowledge of theoretical foundation and convergence takes a huge amount of time with the available computational resources [69]. Anderson et al., developed an electric potential based damage detection technique using an ANN to detect the size and location of damage. A MATLAB based boundary element method tool was developed and validated against ANSYS FEM code results. The damage was defined by the reduction in electrical conductivity[70]. Another ANN model was developed using the input as Lamb wave's data obtained using 3D FEA modelling. The model was validated using PZT Lamb waves and the position, geometric identity and orientation of the defects were identified [48]. Kesavan et al., developed FE models of composite beam and composite T-joints made up of E-Glass fabric materials, to the strain data along the bond line during delamination. These FEA models were validated with the experimental models. More data points were obtained from FEA models, and an ANN was constructed to assess the presence of damage, the size and location of delamination's with an acceptable level of accuracy[71]. Other ANN models with FEA data were developed by Nasiri et al., where they have used the frequency response and modal analysis data obtained during vibration analysis of glass epoxy laminates to detect and localize the delamination [72]. Agosto et al., used FEA models to obtain curvature and thermal data to develop a neural network model for a sandwich composite beam. These models were validated with experimental data obtained by vibrometer and IR sensors [73]. Gomes et al., identified and predicted the structural delamination by conducting an inverse optimization problem using GA and ANN. It was performed on the vibration testing data of CFRP plates through FEA analysis [74].

An interesting case study on composite airfoil was carried out to assess the robustness of the ANN SHM system, when the ANN was exposed to a noisy input. This study investigates the manufacturing uncertainty in SHM. The predictions were increased to above 90% with signal to noise (SN) weighting data and the noise in the data accounts for the thickness uncertainties. The FE model was developed in Abaqus and validated against the experimental data for a hybrid laminate of Glass, PVC foam and carbon epoxy. In the performed case study by Teimouri et al., a suitable SN ratio was determined for noisy damage data for each input neuron [75].

An SVM approach to predict the damage class, life, and as a foundation to take prognostics measures on helicopter rotor blades was developed by using a physics-based model and FEA aero elastic analysis. The vibratory hub loads were utilized as the input to the model. The SVM based blade damage detection approach maintains a substantial stand in the online damage detection system owing to its capability to provide optimal performance with a limited training data [76]. Khatkhate et al., used FEA methods to obtain the strain values for a composite box constructed with stiffeners, and the FEA model was validated with experimental data, using FBG sensors. A study on the sensor failure detection was carried out [77]. A more complete survey for identification and optimization in composites using FEA computational techniques, identifying the inverse problem are given by Gomes et al.,[78]. However, all of these computational methods may be used as a support to implement the SHM on composites, on finding optimization location points for sensors, but they will need another sensor-based system to validate the techniques.

2.3.1.5 Electrochemical Impedance Spectroscopy Methods

Using electrical methods to monitor structural integrity of composites has been around since 1970's. Several dielectric damage indicators have been derived from the electrical resistance, impedance, conductivity and permittivity values. Robinson studied the change in resistivity of carbon fiber reinforced composites (CFRP) (on-axis) loaded in tension and compression and correlated the increase in resistance to damage in fibers and discussed the possibility of insitu measurements of resistance during flight to warn the pilot of impending failure; but emphasized the importance of uncertainty and reliability in measurements with a confidence interval [79]. Schulte et al. performed similar measurements of resistance change in on-axis CFRP during fatigue loading to continuously monitor the condition of structure [80]. Irving et al. performed insitu electrical resistance measurements during fatigue and concluded that significant resistance changes observed during initial cycles corresponded to lower fatigue life and may be used as a basis for life estimation for in-plane fatigue [81,82]. Schueler et al. used electrical conductivity mapping by developing electrical impedance tomography (EIT) methods for orthotropic materials to detect damage in CFRP using a series of network resistors to determine the change in resistance along a damage region [83]. Todoroki et al. identified delamination using variation of resistance measurements taken from multiple co-cured electrodes on the surface of a composite [84]. Wang et al. observed that during fatigue the resistance increased suddenly when delamination was initiated as it decreases the chance that fibers in adjacent layers touch each other. Under continued fatigue, another sudden increase was observed followed by noisy response due to the percent increase in area of delamination [85,86]. Several other research groups have used the electrical resistance measurement methods to monitor structural integrity [87,88]. Abry et al. examined the dielectric properties of $[+45;-45_{]8s}$ laminates and found non-linearity in the complex impedance response[89,90]. However, a key point to consider is that the electrical resistance measurements depend on the change in resistivity of the material system due to damage and hence works well with CFRP. However, for glass fiber reinforced composites (FRP) the use of carbon black fillers in matrix or embedded carbon nano tubes (CNT) have been implemented to obtain these measurements..

Historically, EIS has been used to monitor moisture absorption and induced damage in composites. Glass et al. used EIS to monitor damage in CFRP due to moisture absorption. They observed that with increase in moisture absorption the capacitance increases because of the opening of matrix cracks due to swelling and with time the capacitance started to decrease due to loss of active surface area. However, they observed that with increase in uptake of moisture the shear strength decreased as well and during ex-situ measurement the capacitance also decreased because of broken fibers that isolated the areas of composite exposed to moisture [91]. Bekas et al. used EIS to monitor damage in nano-enhanced composites and found direct correlation of change in impedance to damage events [92]. Fazzino et al. used EIS with woven composites and showed that the micro cracking due to fatigue changed the impedance measurements dramatically and definitively. They induced surface-initiated damage using end-loaded bending. The samples were soaked in 5M NaCl solution and this ionic solution filled the micro cracks and penetrated through the surface to the interior of the sample leading to conductive regions leading to a decrease in impedance. During continuous fatigue, these micro cracks coupled through the thickness and created a path (fracture plane) filled with this ionic solution resulting in a significant decrease in impedance measurements [93].

Using BbDS, Raihan et al. studied insitu dielectric response of off axis woven composites during tensile loading and observed that the dielectric permittivity rapidly increased in the beginning owing to matrix micro cracking resulting in creation of new surfaces (interfacial polarization), followed by saturation of permittivity due to crack saturation, gradual decrease due to coupling and fiber trellising, and final decrease with increased slope during the initiation of fiber fracture [94]. They categorized the response into various damages. They postulated that the decrease in permittivity during coupling is because of transition from surface to volume effects.

Further, Reifsnider et al. calculated the second variation of strain energy and the second variation of the measured capacitance with strain; normalizing both of those plots by the initial value, it was observed that the two variations were remarkably similar. They concluded that the physics of damage initiation (micro-crack formation) events drives corresponding changes in strain energy and dielectric response measured in the laboratory, i.e., that those observables are dual responses to the process of damage development . Several other researchers have used the BbDS technique for damage monitoring in composites and observed variation in the dielectric properties during damage development [95–98].

Seo et al., used ANN to predict the stiffness degradation and hence the fatigue life, based on the change in electrical resistance observed by dielectric sensors. Simple instruments could obtain this electrical resistance change. The ANN model overcomes the limitation of electrical resistance damage models which showed better results for predicting the stiffness degradation.[99] Eumetric 100A dielectric sensors were used in a composite laminate manufacturing process for monitoring the cure of the glass fiber epoxy laminates, obtaining its permittivity values. These permittivity values, along with strain and dielectric loss value, are used in a decision tree pattern recognition techniques to predict the class of the laminate, its mechanical and physical properties[52].

2.3.1.6 Strain Measurements

Early in 1993, Grady et al., used strain gauges to obtain strain data for carbon epoxy composite materials subjected to vibration testing. These strain data were used by pattern recognition techniques to identify the damage modes and delamination of the material. These researchers from NASA presented a framework of the monitoring technology using feature extraction and learning, and requirements for the data base needed to build such methodologies [100]. This article serves as one of the very first research efforts as per the author’s knowledge for an AI based structural health monitoring system. Kesavan et al., has used the strain gauges on the experimental testing to obtain strain values and to validate with FEA models. These data were used by ANN to predict the damage size and location of composite beams and T-joint structures [71].

2.3.1.7 CT Scans, X-Rays

Delelegn used the CT scans to detect, identify and characterize the cracks and delaminations in carbon fiber composite laminate panels subjected to static and monotonic indentation tests. CNN has been used as the AI algorithm with digital image processing methods to make the predictions. This method will allow researchers to utilize volumetric models for a sound understanding of the propagation of damage in materials, which result in design optimizations that avert catastrophic failures. The researcher also suggests that the future work should include optimizing the algorithms for fast predictions, developing improved and automated contrast enhancement algorithms, identifying and labeling the different types of anomalies detected within an image, and expanding the training data sets to include more types of damage, porosity, wrinkles [101]. X-ray images of the composite materials have been used by a wide range of researchers, mainly as a validation tool, to validate the other sensor data. Few researchers have used the images in CNN based AI algorithms to make predictions. However, CT scans and X-Rays can be used as a research tool with AI, but cannot be implemented to make real time predictions during the in-service flight of the aircraft. Such AI research tools can be used by NDT inspectors to inspect the aircraft during regular maintenance intervals, and will reduce the human error.

2.3.1.8 Other SHM methods with AI

In one study, a hybrid carbon epoxy beam with urethane was subjected to vibration and thermal analysis by experimental and FEA methods. Laser Doppler Vibrometer and IR camera sensors were used in the experimental analysis. ANN was developed to predict the damage. When both sensor data were used together with a Bayesian probabilistic neural network, curvature and thermal base analysis complemented each other to augment the damage detection capabilities [73]. Marani et al., used thermography NDT inspection on glass epoxy composite panels to identify the defects, holes using the unsupervised H-Clustering algorithm. The heat maps of laminates were input to the model. Results have been compared with other well-known techniques and clearly prove the capability of the proposed method to detect defects underneath the specimen surface, also lowering the number of false positives [102].

Another new technology called the mechanoluminescence, which is the phenomenon of light emission from organic / inorganic materials due to the mechanical stimuli, was used as an SHM method. This method has difficulty in mapping the physical characteristics of the structure with relevant sensor data using mathematical models or physics based approaches. The elastic modulus of a structure was predicted based on the input parameters such as stress and measured output light, using a multivariate regression model [103]. Farhangdoust et al., developed an ANN to predict the bond damage location using the heterodyne effect for bonds based on the amplitude response obtained. The defects in bonds creates new frequencies[104].

2.3.2 Prognostics Paradigm

There have been several researchers around the world, who have worked on improving the SHM methods to the next advanced level - prognostics, and implementing real-time prognostics measures. Since these involve continuing research work and improvements on the diagnostics and prognostic approaches, these sections are classified based on the research group and their contributions in this field.

2.3.2.1 Fatigue Life Modelling

The fatigue life modelling of composites is not a structural health monitoring or prognostics application, as the input data are not from a sensing system, but as they predict the fatigue life based on the material property and load conditions, these models could help reduce the experimental testing cost and time by implementing them to model various composite material behavior and their fatigue life. It will also serve as guidelines to choose AI models wisely to predict the remaining life.

A team of researchers from UAE led by H. El Kadi has performed a series of experiments, and have contributed a lot to the field of data driven analysis in prognostics of fatigue life. The experiments consisted of the tension-tension and tension compression fatigue testing of glass fiber/epoxy composites. Specimens were fabricated at five different orientation angles (0, 19, 45, 71 and 90). The input to the ML/AI models where the fiber orientation angle, maximum stress and stress ratio (R = 0.5, 0.-1) of fatigue testing and the output was the number of cycles to failure. Several AI models, which included ANN, Adaptive Neuro-Fuzzy model, Feed Forward Neural Network, Modular Neural Network (MNN), Polynomial classifiers (PC), Radial basis function networks, Recurrent Neural Network, Self-Organizing Feature Maps (SOFM), Principal Component Analysis networks were developed. Kadi et al., also used strain energy alone as the input to predict the fatigue failure using the ANN and MNN models. They also studied different composite materials and their fatigue life data from literature, and predicted the fatigue life by using a PC algorithm.

As per these researchers, AI is not recommended to determine the relationship of input and output since it represents linguistic and subjective descriptions. When a large number of data are available, using techniques like SOFM for clustering the input data with neighboring preserving predicts accurate fatigue life. Also huge amount of data is required to obtain good predictions. Using PC produces repeatable results with less computational requirements. The scatter in fatigue life data negatively influences the estimates from ANN or PC. The researchers aim to predict the fatigue failure of multidirectional laminate from the data of unidirectional lamina using ANN. The authors recommend reading the review paper by Kadi for more detailed insights [105–112].

The number of cycles to failure of composite coupons were predicted by using various AI algorithms such as ANN, ANFIS, GP, RNN, RBFNN, FFNN, and GRNN. The inputs to these models were the fiber orientation angle, maximum stress, applied stress, stress ratio, thickness of the plies [113–115]. Vassilopoulos et al., demonstrated that using 50% of the experimental data was enough to model the fatigue life, and build constant life diagrams for multiple material systems using ANN. These data were obtained from constant amplitude fatigue loading of multidirectional laminates [113]. Mini et al., carried out the fatigue analysis using FEA to predict the fatigue life using ANN [114]. For a more extensive literature on modelling the fatigue life, authors recommend the book chapter on computational intelligence methods by Vassilopoulos et al., [116]

2.3.2.2 Remaining Useful Life (RUL) Predictions

2.3.2.2.1 NASA Prognostics Dataset

The researchers from Prognostic Center of Excellence (PCoE) of NASA Ames Research Center along with Stanford Structures and Composites Laboratory (SACL) carried out run-to-failure experiments on CFRP panels with periodic measurements to capture internal damage growth under tension-tension fatigue. Monitoring data consists of lamb wave signals from a network of 16 piezoelectric (PZT) sensors and multiple tri-axial strain gages. Additionally, periodic x-rays were taken to characterize internal damage as ground truth information. Three different layups were tested. Based on this dataset, both physics-based and data-driven AI based algorithms have been developed.

Saxena et al., initiated the accelerated aging experiments for composites materials and extracted the damage growth Condition Indicators (CI) as Change in Power Spectral Density (PSD), Scatter Energy, and Time of Flight (TOF). They also proposed to use the Bayesian Filtering Gaussian Process regression algorithm. These CI's characterized the damage growth with their monotonically increasing. Later a key contribution was made by Peng et al., as the inclusion of micro-scale damage evolution models acting as a state transition equation that are hierarchically connected to a macro-scale stiffness reduction model into a Bayesian filtering algorithm that sequentially updates both damage states and model parameters as time evolves. Through stochastic embedding, these deterministic models are converted to probabilistic models by introducing a modeling error term. This modeling error term is controlled by a probability density function whose parameters are sequentially estimated in addition to the rest of model parameters. Larossa et al., used 9 features - TOF, Amplitude (A), Energy (E), PSD peak, PSD rate, PSD change (PSDchange), TOF/PSDchange, PSDchange/TOF, A/TOF, in a Gaussian Discriminant analysis that was based ML algorithms on the same experiments. Their results had an error rate of 21%, high precision and recall values and it was sensitive to layup configuration. Another framework predicting the balance of release strain energies from competing damage modes to establish a reference threshold for prognostics was also introduced. Later again, the Bayesian framework was extended to support multiple damage mechanisms and it estimated the damage growth and fatigue life [117–123].

However these models consider a number of hypotheses and assumptions. The framework assumes that the damage data were given in form of matrix micro cracks, which is considered to be the dominant damage mode and hence other possible damage modes like delaminations and fiber-breakage among others, were not explicitly modeled. Also the model completely relied on normalized effective load and stiffness measurements which defines the energy release rate.

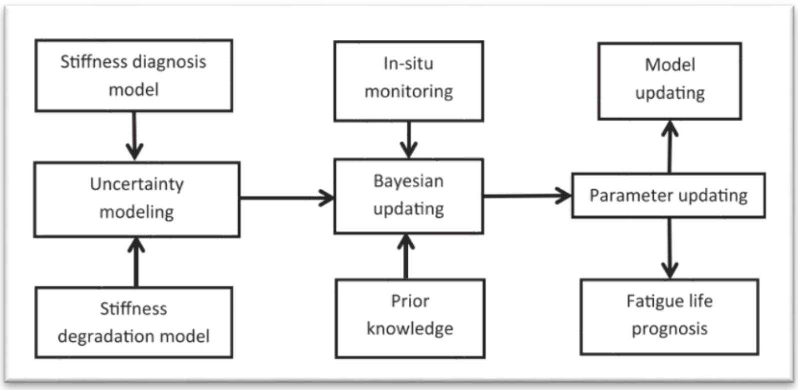

Figure 2.12:In-Situ Fatigue Life Prognosis model [121]

Apart from the team from NASA, since NASA Prognostic center published it as an Open access dataset, it was available to other researchers to develop data-driven models. Lahmadi et al., used the load, cycles and degradation data to predict the RUL using RNN. Liu et al., developed Linear, SVM, Random Forests, Adaboost, Gradient Boosting, extra trees, Ensemble Learning models using the time of flight (TOF), power spectral density (PSD), interrogation frequency, path number and usage cycle from the dataset to predict the delamination crack growth. These AI models had learning capabilities but not excellent prediction accuracies [124–126]. The researchers consider that the global damage effect on the lamb wave propagation, lack of complete experimental data causes the high error rate.

In summary, both physics based and AI based models have been developed to this dataset for RUL of composites; however, there was no research combining, forming hybrid models. Also, the parameters of those physics based models depend on the shape, orientation, failure type, applied loads and hence it limits the applicability of these models.

2.3.2.2.2 Prognosis of Composites based on SHM - ReMAP – European Project

A team of researchers from Europe – TU Delft and University of Patras – Loutas, Zarouchas and Eleftheroglou along with a team have worked on in-situ prognosis of composites using data-driven AI methods. This team is currently working on a project called ReMAP (https://h2020-remap.eu/) for certification of Condition Based Maintenance of Aircraft structures. They propose to use four different SHM technologies, which are dynamic strain measurements (vibrations) with FBGs; AE measurements; static strain measurements with FBGs and distributed sensing; Acousto-ultrasonic measurements with PZT sensor networks.

The initial experiments consisted of constant amplitude fatigue tests of open-hole carbon-epoxy composite coupons. AE data was recorded using PZT sensors during in-situ fatigue testing. The damage model was developed based on non- homogeneous hidden semi Markov (NHHSMM) approach using the input data. Also an ANN model was developed. The predictions were made with the confidence intervals. NHHSMM provides much less volatile predictions its confidence intervals shorten as more data come into play. Also recently data fusion methodology was proposed combing the AE and Digital Image Correlation (DIC) data. They have also established new prognostic performance metrics called the Modified Mann-Kendal (MMK) monotonicity metric and Confidence Intervals Distance Convergence (CIDC) metric**.**

Based on their initial experiments they observed a large scatter of the experimental data and a strong stochastic behavior of fatigue damage. These prognostic models are dynamic and utilize all data points from beginning of fatigue loading and make real-time predictions. Also, there is a need to consider the autogenously heating effect during the fatigue tests and how it will affect the RUL of the coupons with increase in stresses or strains. However this heating effect does not affect the performance of the model. The temperature rise may indeed decrease the actual RUL by accelerating the damage initiation and propagation in the material, but this is expected to be captured by the AE measurements, and thus, it is indirectly reflected in the predictions. Hence, this gives a flavor of in-service conditions where temperature changes are anticipated.

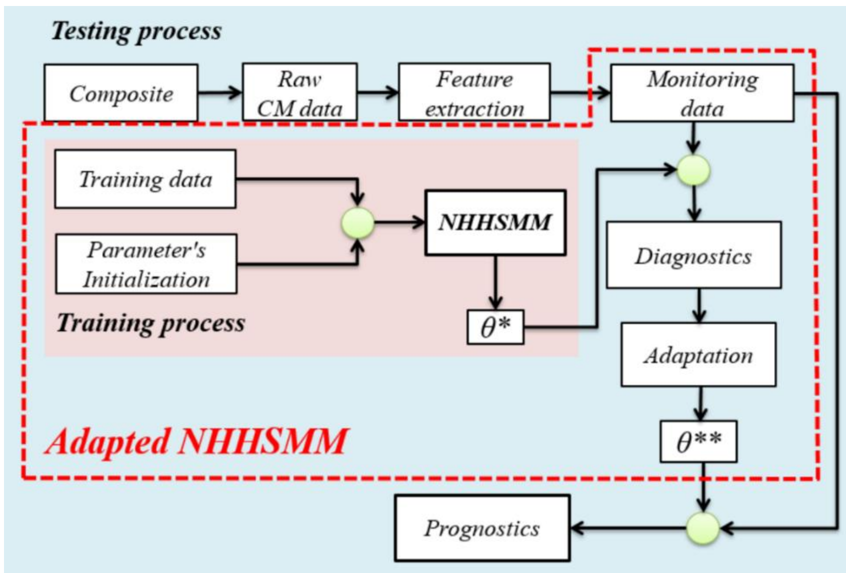

Figure 2.13: Adaptive Prognostics Methodology

The results from their recent experiments concludes that the DIC RUL estimations scored better in all prognostic performance metrics. Consequently, when compared with the AE and fusion data, DIC data was the optimum prognostic performance data. However, the authors have not discussed the limitations on using DIC as real-time sensors as it could be used as a correlation method only. More recently, an extension to NHHSMM, called the Adaptive NHHSMM or ANHHSMM has been proposed. This ANHHSMM, was tested on unseen events, and has proven to adapt to unexpected events and make prognostics of RUL. Also it has the capability to learn and update its weights in real-time. It is also recommended to consult the book chapter by Zarouchas and Eleftheroglou for more reading into their work [127–132].

2.3.2.2.3 Other Prognostics of Remaining Strength and Life

Teti et al., have predicted the residual strength of glass epoxy notched coupons using the AE and load data in Neural Networks. Their results obtained emphasize the usefulness of neural network processing in materials technology problems where analytic solutions are not available [133]. Choi et al., developed an ANN model to predict the longitudinal split growth under tension dominated fatigue testing of carbon-epoxy notched specimens. Their ANN model is found to work better than the power law model as a predictive tool for split growth [134]. Another ANN model with a Levenberg-Marquardt learning algorithm was developed to predict the stress on the CFRP and GFRP composite coupons belonging to the same resin system, based on the strain and the material properties[135]. A research effort for predicting the fatigue crack growth was attempted by deploying the two sided cumulative sum model on fatigue testing of notched coupons. The load and crack size were considered as the input parameters. This data is time step based data as the prediction depends on the previous state and serves as a model-based prognosis method[136]. Also damage precursors were identified based on the AE signals, temperature data and the dissipated energy using dynamic Bayesian network, combined with particle filtering and SVM on glass/epoxy samples in fatigue bending tests. However the non-homogeneity of data was not taken into account [137]. .

Liu et al., have predicted the damage state and RUL of carbon epoxy coupons subjected to uniaxial and biaxial fatigue loading. They used the time series data of PZT and AE sensors on PCA and Gaussian process based systems. The prognosis algorithm initiates after a certain damage level to collect sufficient previous damage state information. On-line damage state prediction and remaining useful life estimation showed good correlation with experimental data at later stages of fatigue life. They predicted future damage states with 95% confidence intervals and RUL information. It was also proved that the accuracy of future damage state prediction improves as more and more experimental information (such as strain measurements and the corresponding estimated damage states) was available. By comparing the on-line prediction from PZT and acoustic emission features it was observed that piezoelectric features provided better prediction accuracy than AE counts. This could be due to the fact that the model was not familiar with the signal processing and filtering aspects of the AE system and therefore it is difficult to use these kinds of features or improve on it [138,139]. Another approach to predict the RUL was carried out by Joint Extended Kalman Filter (JEKF) algorithm using the PZT ultrasonic wave's data of glass epoxy coupons subjected to tensile loading. This combination of sensors and JEKF algorithm, teach that the real-time calculation of the remaining useful life is possible and it could be sufficiently effective to be study in a real-time situation [140].

2.4 Uncertainty Quantification

Uncertainty Quantification(UQ) is an important engineering factor, because the engineer's judgment in design, manufacture, operation and maintenance – including decision making for structural prognostics, needs the prediction estimates with credible uncertainty bounds for safe operation and failure prevention. In composites, due to the complex damage mechanisms, the models lack confidence in real world applications. The uncertainty in this system may come from the sensing systems by means of inaccurate data transmitted from sensors or imprecise database developed during the damage analysis, manufacturing errors, environmental errors, loading perturbations, model errors. Potential sources of uncertainty are shown in Figure 2.14

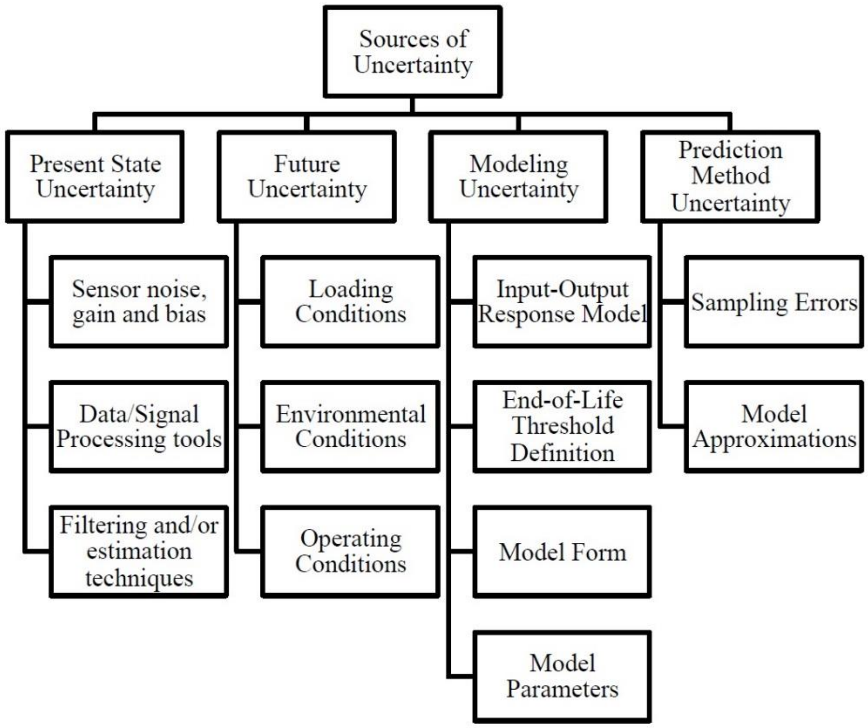

Figure 2.14: Sources of Uncertainty[141]

One of the main concerns in implementing AI techniques in real-world aerospace applications is the scarcity of data, containing all possible conditions subjected to the structure during flight. These data are to be collected from sensors in real-time for training the AI models. Since majority of the AI models developed are in laboratory scales, these are not exposed to the operational conditions and hence will lead to false positive estimates. In addition, by using a large dataset with high statistical variations will decrease the accuracy in predictions. Hence, a proper methodology to handle these uncertainties associated with abrupt changes to load and environmental conditions need to be developed.

For example, in case of an aging aircraft in service, as shown in Figure 2.15 below, the complex flow of knowledge- both quantitatively and qualitatively from the databases 1,2,3,4 and M are required for reliable predictions. This UQ model depicted in the Figure 2.15, needs the specific input from the 5 databases which are 1. Damage failure mechanism database, 2. Current SHM, inspection reports database, 3. Material property database, 4. Loading/Constraints Database and 5. Physics based/AI based Model's learned knowledge database-M in order to effectively predict the remaining fatigue life estimates of the aging aircraft structure. The figure 13 also represents the uncertainty error in each event and databases, which are associated with all sorts of uncertainties and errors due to data collection, data mining, analysis and modeling the data driven model. Researchers from NIST have worked on solutions for similar problems uncertainty quantification in aging bridges, pipelines by integrating statistical design of experiments, AI and developing intelligent python codes [142].

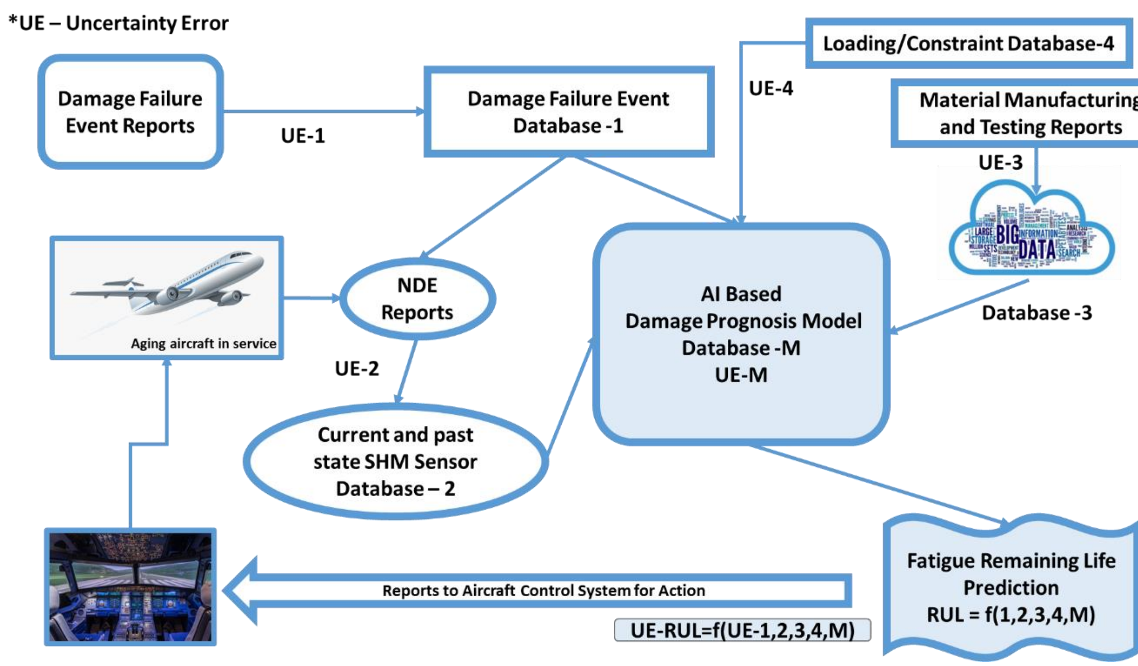

Figure 2.15: Conceptual approach of Uncertainties involved in RUL estimates

As per the above figure if we consider the model M as a black box – AI model, and if we know that the governing equations, physics of the model are not fully understood and the list of parameters that define model M contains some unknown, unidentified uncertainties, it is incumbent upon us to introduce another important uncertainty source, Uncertainty Error (UE) for model M, UE-M, that is intrinsic to model M which together represents all additional uncertainties inside the black box. Researches have shown that data driven AI models are capable to handle such uncertainties to an extent, and hence then UE-M becomes UE-RUL. AI tools with a human partnership are, therefore, more reliable and cost-effective in managing an aging structure. Hence, the UQ is to be addressed on two fields – 1. Using AI models to determine and handle the uncertainty on ISHM and IPHM systems; and 2. Uncertainty Quantification of the prediction of AI models.

2.4.1 Using AI models to determine and handle the Uncertainty on ISHM and IPHM systems

This section discusses on the physics based and data driven AI models that incorporated the capacities to handle the uncertainties involved from various sources.

Ramu et al., integrated fuzzy logic with ANN to handle the uncertainties of making damage assessments. The fuzzy logic representation has been found to be a most efficient means of treating uncertainties [69]. The failure of optical fiber sensors, in SHM is a serious concern and detection and isolation of such events are extremely critical. Khatkhate et al., have proposed methods combining FEA and ANN to isolate the failure of sensors based on static strain patterns. However, their proposed methodology considers only sensor failure at a particular grid location on the structure, and not the entire failure of the optical fiber sensor, by debonding issues[77].

One alternate possible solution is to include the uncertainty scenarios in the training set, but this approach would involve developing a vast damage database which often requires considerable time and budget for industries. Another approach would be weighing the conventional neural network by signal-to-noise coefficients. In a performed case study for composite airfoil, the noisy damage signature data were analyzed for each input neuron to calculate an appropriate SN ratio. The approach dramatically increased the efficiency of the ANN- based SHM, even though it was only trained with the original damage scenarios and predicted the noisy damage data. By using signal to noise (SN) ratio methods on the input layer of an ANN model, the uncertainty to noisy input data was reduced and damage location, size predictions was increased to 90%. It is critical to ensure that a given damage signature database contains a sufficient number of damage scenarios to accurately represent the reality. For a sufficiently large damage database, and with uncertainty propagated throughout the structure, caution must be taken not to pre-define/prefer limited sensor locations to be used for training proposes. Such models provide robust SHM development. A practical problem with this approach, however, is the reliable estimation of SN weights. This estimation may come from past experience, expert knowledge or by developing a sub-set of initial DSD encompassing uncertainty cases. [75]. Model, measurement and future loading uncertainty are handled by using a joint parameter state estimation with a particle filter, in prognostics of fatigue crack growth [136].

Montoya et al., suggest the use of data preprocessing methods such as kernel density estimation and hampel identifier through which, Probability Density Function (PDF) can be obtained for the measured sensor data. Low PDF values are treated as a greater degree of outlierness and the associated data are discarded as they lie outside of the defined confidence intervals (i.e. 95%, 99% and 99.5%). Spikes and measurement errors are also removed by this process. Through some variations to the pattern recognition techniques developed, it was shown that with this methodology in a composite wing structure under flight testing with a suitable performance, the damage can be estimated with an accuracy of 0.981 and an F1 score of 0.978 where KDE with a confidence interval of 95% was used as a preprocessing technique[66].

In another approach, Elenchezhian et al., built ANN and Random Forest Regression models, on an artificially created data set based on the average stress criterion to predict the notched strength of a composite coupon. They also obtained the feature importance of the input features used in the AI model, and the feature importance's related to the physical relationship. It is incorporated that models based on a physics based law were able to produce excellent results since they follow a pattern, and suggests that the hybrid models with both physics based and data based data should be constructed for more fidelity[143] .

Lopez et al., has presented a review paper on the uncertainty methods for structural health monitoring, but it specifically does not focuses on composites. However, the methods suggested may be applied to the data driven models built with composites. Fuzzy logic, Dempster-Shafer theory, Bayesian framework with relevance vector machines combined with particle filters are few suggested techniques [144].

Saxena et al., proposed using the Bayesian filtering methods like particle filters which have the capability to manage the uncertainty in the prediction process through importance sampling, thereby refining the current estimates of multiple damage growth model predictions using the evidence from measurement data. Guassian Process Regression provides variance around its mean predictions to describe associated uncertainty in the predictions, which will be extremely useful in incorporating the effect of various uncertainties for RUL prognostics. Chicachio et al., and Ruano et al., predicted the evolution of damage in composites under fatigue loading, with the associated uncertainty estimates using Bayesian methods. According to them the ability to deal with uncertainties from models and data can be the biggest advantage of Bayesian methods since the existence of uncertainty in composite materials is an undeniable fact. Peng et al., used an uncertainty parameter to account for the noise in the physics based model. Corbetta et al., proposed a particle filter using an AD or KS sub-algorithm to filter the uncertainty linked to the model parameters. However it does not include the uncertainty from future loading conditions [117,119,121,123,145].

2.4.2 Uncertainty Quantification of the prediction of AI models

The "$a_{90|95}$ value," which is determined from the probability of detection curves, is used as a performance measure indicating the minimum damage size that is detected with a probability of 90% and 95% confidence. Long-term strength and life prediction of critical aerospace, military composite structures entails large-grain uncertainty that must be represented and managed effectively, i.e. as more and more data becomes available, "means" must be devised to narrow or "shrink" the uncertainty bounds. Khawaja et al (2005) introduced a novel confidence prediction neural network that employs confidence distribution nodes based on Parzen estimates to represent uncertainty and a reinforcement learning algorithm which is implemented as a lazy or Q-learning routine that improves uncertainty of online prognostics estimates over time. It is the time correlation between measurements that allows to characterize the evolution of a fault [146].

Kral has performed design of experiments, statistical analysis on the data and predicted the outputs of the AI models with 95% confidence intervals. It was shown that, damage could be predicted to within 1 in., and damage size of 0.375 in. in diameter with 95% confidence [50]. Two common statistical metrics that, used along with PCA are the Q index (or squared prediction error index) and the T2 index (or D index). These quantitative indices are intended to consider whether the results of different experiments or studies are homogeneous or not, provide information about the magnitude of the effect of the relationships studied together with a confidence interval and statistical significance and whether there is heterogeneity between different experiments or studies, and identify variables or characteristics that may affect the results. This PCA model is used for damage detection in UAV wings using FBGs [65,66].

Consensus clustering with bootstrap ensembles allows the estimation of uncertainty envelopes of each cluster, and provides an interval of cumulated loading thresholds to activate a particular damage. The uncertainty of the assignment of clusters applied to pattern discovery in AE signals was investigated by using a supervised method based on a ground truth supplied by the end user. The proposed clustering consensus method makes it possible to represent the uncertainty on clusters in an unsupervised manner. This approach was implemented to predict the robust damage from AE time series data in composites [41,147].

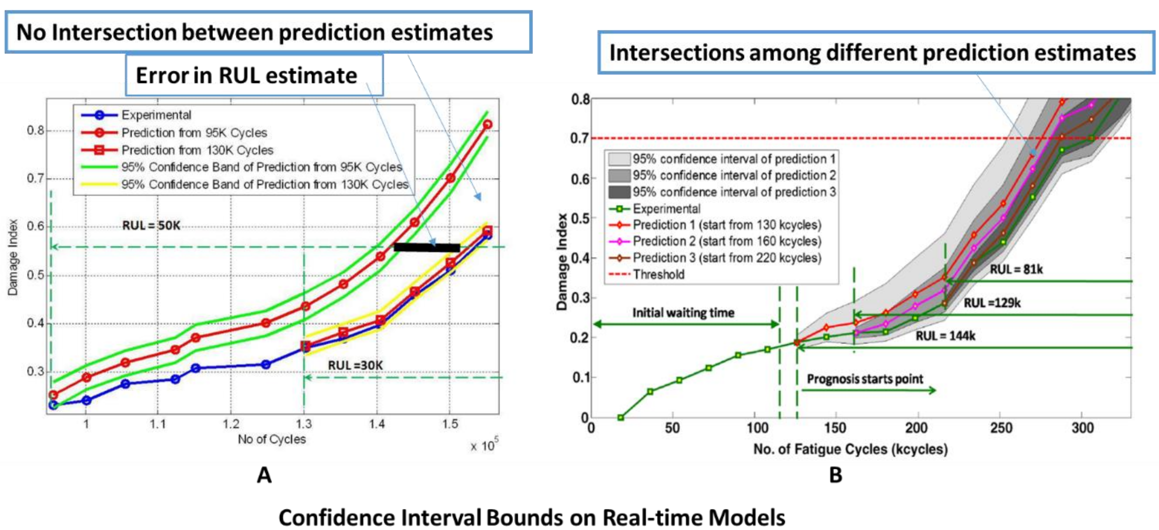

Figure 2.16: Need for Real-Time In-situ predictions.

Liu et al., predicted the damage index and remaining useful life, with 95% confidence intervals from the data driven models developed. From Fig. 14, in model A, it is observed that the prediction estimates from 95K cycles, were different from the prediction estimates from 130K cycles. However, the estimates were accurate to the experimental readings as more data was involved in the model. In another model B, we can observe that the prediction 2, and prediction 3 are within the confidence interval levels of prediction 1, and hence the accuracy of future damage prediction has improved as more material state values are available to assess the damage states [138,139].

Eleftheroglou et al., have used the NHHSMM technique, and used the confidence interval for the mean RUL values based on the cumulative distributive function. Also they introduced a new metric for prognostics accuracy called the Modified Mann–Kendal (MMK) and Confidence Intervals Distance Convergence (CIDC), which is based on the fact that that as the amount of data increases during the fatigue life, the confidence intervals distance should converge. [127–129,131].

2.4.3 Interpretable Machine Learning / Explainable Artificial Intelligence

A major disadvantage of using Machine learning AI models is the insights about data, and the functioning of model is hidden in increasing complex models like deep-neural networks. The term "Interpretability" is defined as the degree to which a human can understand the cause of a decision.[148] It is also the degree to which a human can consistently predict the model's result[149]. Hence, when the Interpretability of the AI model is higher, it is easier to comprehend on why that particular decision was made. The ensemble models which are a blend of several data driven models, result in best performance metrics but cannot be interpreted, even if a single model among them would. As result, when these AI models focus on performance, it becomes more opaque. The goal of science is to gain knowledge and understanding, but many problems are solved with big datasets and black box machine learning models. The model itself becomes the source of knowledge instead of the data. Interpretability makes it possible to extract this additional knowledge captured by the model [150] Hence Interpretable AI models need to be developed for critical applications such as aviation, defense, and anything that involves lives. These models can be either intrinsically interpretable models or model-agnostic methods. Model-agnostic methods which are employed on the black-box AI models work by varying the input of the model and measuring the variations in the estimates predicted. These methods can be differentiated based on their capability to explain local and/or global prediction.

2.4.4 Summary on UQ

The ability of these data-driven AI methods for prognosis under measurement and modeling uncertainty has been proven through numerical examples. However, they have assumed known values of current and future loading, which is not the case in real-life scenarios. In order to address the issue of uncertainty, contextual information, knowledge, and experience must be well incorporated. To reduce uncertainty in the diagnosis and prognosis processes, knowledge must be maximized via integration of various information sources.

As Sankaraman et al., have mentioned it is not possible to analytically calculate the uncertainty in the remaining useful life prediction even for certain simple problems involving Gaussian random variables and linear state-prediction models. Therefore, it is necessary to resort to computational methodologies for such uncertainty quantification and to compute the probability distribution of remaining useful life prediction.[141]

Any prognostic method should be able to process stochasticity and provide probability estimation and a confidence band around predictions. Figure 2.16 also leads to the idea of uncertainty, where the predictions of different IPHM models, AI based and physics based, or two AI based models can be combined together and the interaction regions of the predictions and their confidence regions could be used for decision making. Such that multiple models can be fused, hybrid models can be created to get more accurate prediction estimates with tighter uncertainty bounds

Physics-based models can only be used up to a certain accuracy, as they are not able to predict all possible phenomena. Similarly, AI models have limitations. Hence, a single methodology cannot be the ultimate solution for an IPHMS. Multiple models must be integrated intelligently to form an IPHMS with more reliability.

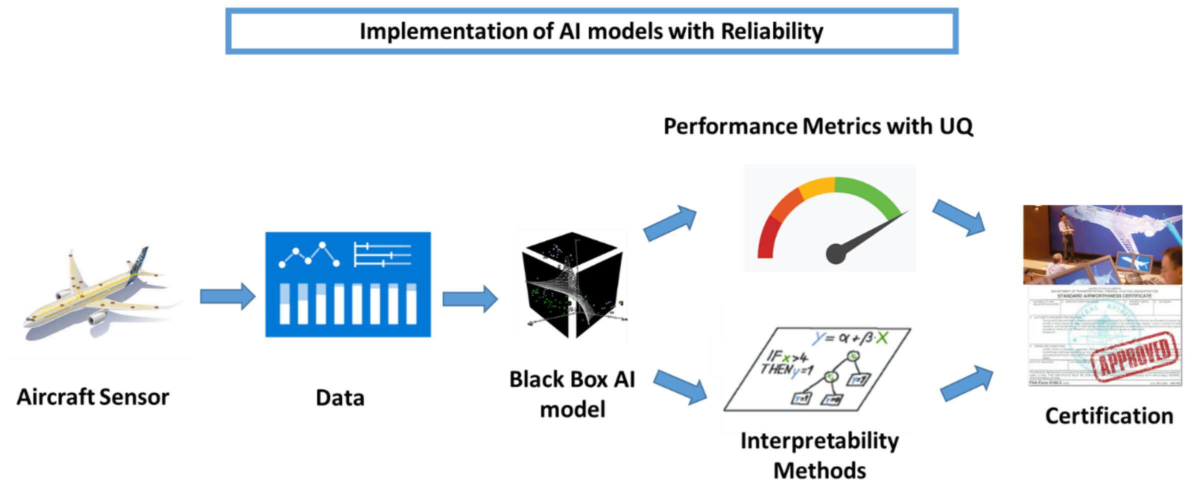

Figure 2.17 : Implementation of AI models with Uncertainty Quantification

2.5 Datasets Available

One of the essential inputs to build AI models is the data source. Unfortunately, many of the studies on composites have only been published as conference and journal papers. There is not much data available on composites, either in any of the domains of design, manufacturing, SHM and prognostics. The publicly available data sets as per our knowledge for SHM and prognostics of composites, to explore more AI models and develop insightful findings in composites are listed below.

- NASA Prognostics Dataset – CFRP Composites Dataset [151]
  https://ti.arc.nasa.gov/tech/dash/groups/pcoe/prognostic-data-repository/
- SNL/MSU/DOE database [152]

- Nathan Post Dataset – Virginia Tech [153]

  https://vtechworks.lib.vt.edu/handle/10919/26492

It is also recommended that researcher's create public datasets, for use of AI enthusiasts and to support PHM challenges.

2.6 COTF-IPHMS with IIoT

The real-world application of COTF-IPHMS would be a part of the aircrafts flight control system, where the application would provide the respective authoritative person (Pilot, Maintenance Engineer, Structural Inspector) with the information on damage, strength and life of the structure and recommended measures for the safety of the aircraft before tremendous damage to aircraft and life [154]. This could be achieved as:

1. During the startup of the aircraft, COFT-IPHMS assesses the airworthiness if the aircraft, by assessing the current state and past state values observed by the sensor systems.
2. During flight, the application continuously monitors the loads applied on the structure, damage state, and hence predicts the remaining strength and life of the composite structure. This is vital in military aircraft applications as the application assesses the reliability of the battle damage, and predicts the remaining values.
3. Any serious damage, exceeding the set threshold values would indicate the pilot to take control measures, and possible maneuvering procedures.
4. After landing, the application provides the authoritative person, with a complete report of the loads applied, induced damage, remaining strength and life of the structure and suggests the need for maintenance, or clears the aircraft for the next flight.

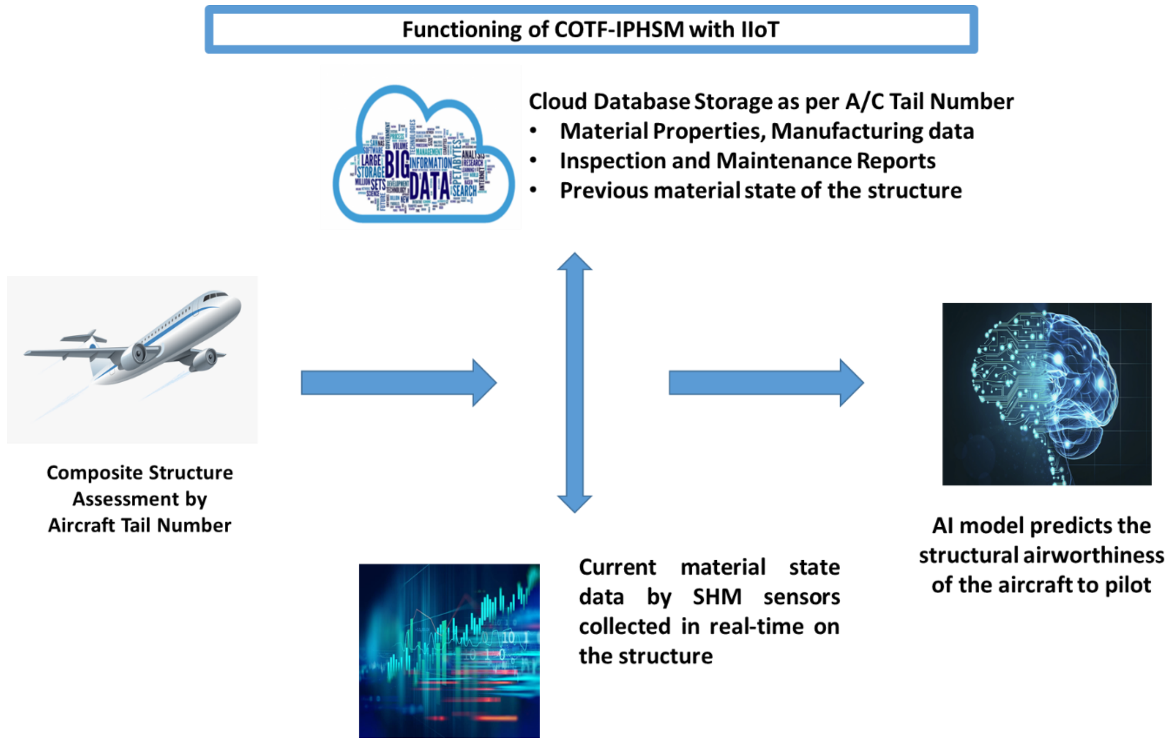

Figure 2.18: Functioning of IPHSM with IIoT

To build such a system, the authors suggest that the following research needs to be achieved in the materials sector using composites and AI.

1. Determination of sensor systems to be used in real-time for assessing the material state of the composite materials, and reliability of the sensor data
2. Creating a large cloud-based database of composite materials with all material properties data, SHM and prognostics data
3. Develop data-driven AI models to make predictions on the remaining strength and life of materials
4. Adaptive learning methods to predict unseen events must be developed.

5. Use the concepts of Transfer Learning and Multi-Task learning, to accelerate the process, and combine the data-driven AI models.
    a. Transfer learning is the concept where the learned parameters from one model can be used to build another model, with better accuracies, and faster learning time. For example, If one researcher A is working on Glass fiber composite materials, and have fatigue data for 1000 samples, and another researcher B is working on Carbon fiber composite materials and have fatigue data for 100 samples, the knowledge learnt on a AI model A, built with dataset A, can be used to develop an AI model B, with dataset B under some conditions.
    b. Multi-Task learning is the process where multiple AI models built for predicting different outputs, can be combined to a single AI model and to make a number predictions. Biologically, humans learn multiple related tasks instead of focusing on one specific task for a long time. This way, one task will help learning the other task, and vice versa, hence supporting each other.
6. If data-driven models, can be combined with physics-based models, hybrid models should be developed.
7. Develop Uncertainty Quantification methods for the AI models being developed

Also proper procedures need to be carried out during step 3, developing the data driven AI models, e.g.:

- Data mining – data cleaning and preprocessing techniques are necessary to separate “bad data” from the “good data”
- The data must be standardized to be used for faster model training and optimization

- Proper hyper-parameter tuning must be performed
- The thresholds for making predictions must be defined as per the industry requirements
- Proper use of Prognostic metrics must be employed to evaluate the model
- Due to the non-physics nature of AI models, it must be validated and tested with unknown uncertain instances, which are outside the training and testing datasets.

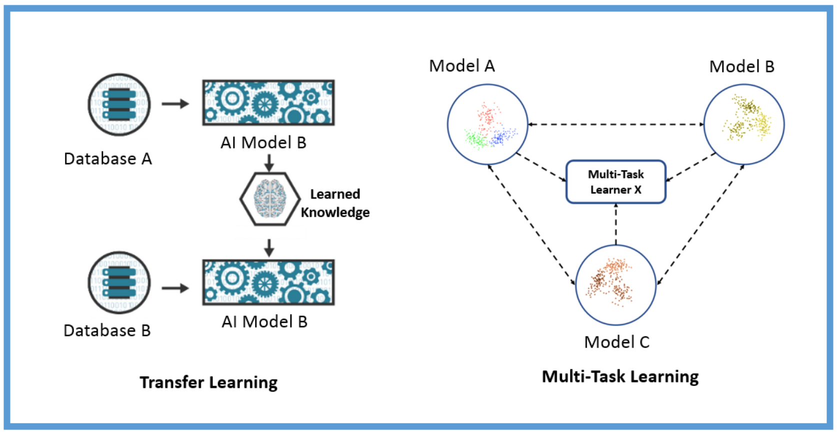

Figure 2.19: Transfer learning and Multi-Task learning

Figure 2.19 represents schematic of transfer learning and multi-task learning. It is to the surprise of the authors that such technologies have not been widely used by researchers in the field of composites. There is only one article as per the authors' knowledge that used transfer learning, on the CNN model to identify images with FOD, by using a publicly available pre-trained networks enabling its completion with a small number of training images [23]. Reinforcement learning has not been used widely in composites.

Finally, the birth to death approach for monitoring of composites using AI pipelines can be achieved by using compatible sensors, such as fiber optics, dielectrics, PZT embedded with the laminae during the manufacturing of the part. By embedded sensors in the composite during manufacturing, AI can keep track of the curing process, identify any defects in the material, and perform continuous health monitoring. Fiber optic sensors and dielectric methods have proven to be used in the life cycle monitoring of composites [52,155]. Integrating AI with such applications might improve the cost and maintenance of aircraft structures. However, the major limitation of sensors and other practical limitations on such methods such as secondary bonding needs to be considered.

This dissertation is focused on using AI with dielectric sensors and fiber optic sensors for i) identifying defects ii) predicting the characteristic damage state of the composite material iii) predicting the residual strength and life of composite materials - by developing interpretability models with AI. It also covers the topics of data fusion, statistical analysis and uncertainty of the models.

Chapter 3

METHODOLOGIES

In this chapter, an introduction is given for the composite manufacturing processes, quasi-static and fatigue testing equipment, and the state of the art sensor technologies of the Broadband Dielectric Spectroscopy Method and the Fiber Optic Sensing technique. Later, Weibull Statistical Analysis, and Artificial Intelligence methods are introduced and discussed in detail.

3.1 Manufacturing of Composites

In this section, we discuss the types of equipment and processes used for manufacturing the composite materials needed for the experiments. Three different composite specimens were manufactured for each type of experiments, which are described in their respective chapters. They were manufactured using the Compression Molding and Out of Autoclave Processes, using the equipment at the University of Texas at Arlington Research Institute (UTARI).

3.1.1 Compression Molding

Compression molding is a closed-mold composite manufacturing process that uses matched metal molds with the application of external pressure. In the compression molding process, an engineered composite layup is placed in the open mold cavity, the mold is closed, and consolidating force is applied. The pressure remains on the mold throughout the cure cycle, which usually occurs in an oven. The combination of heat and pressure produces a composite part with low void content and high fiber volume fraction—a near net shape finished component. Compression molding often yields composite parts that have the optimal mechanical properties possible from the particular combination of constituent materials. The WABASH compression molding press, model – VS50H-24-BCX at UTARI was used for the compression molding process of manufacturing composites for this work.

3.1.2 Out of Autoclave (OOA) Process

Out-of-Autoclave (OOA) composite manufacturing is an alternative to the traditional high-pressure autoclave (industrial) curing process commonly used by the aerospace manufacturers for manufacturing composite material. It is a process that achieves the same quality as an autoclave but through a different process. Many composite components have been manufactured using autoclave technology, which applies steam, heat, and high pressure in a liquid nitrogen environment to create the low-to-no void bonds necessary to combine two or more different materials to form a composite part. However, the extremely capital-intensive equipment costs, high operational costs, slow curing-cycle times, inability to make in-process adjustments, pressure-vessel size limitations, and other disadvantages associated with autoclave curing have caused manufacturers to seek less costly, more versatile, out of autoclave composite-curing technologies. OOA is considered a cost effective way to produce a part, and it avoids the financial investment in purchasing autoclaves and freezer storage. Today, low cost out-of-autoclave curing of aerospace-grade composite parts is possible using a vacuum bagging system with a walk-in batch oven. The process is precisely controlled and monitored to ensure void-free composite parts. At UTARI, the DESPATCH Complete Composite Curing – Walk-In Ovens TFD3-21-1E were used to manufacture very large composites panels. Thermocouples were used to monitor the temperature distribution during the manufacturing process.

3.2 Mechanical Testing Machine

All the quasi-static and fatigue cyclic testing was performed using an MTS Landmark servo hydraulic universal testing machine (Model 370.10). The Load cell capacity is 50KN, and it has a unique custom feature to test the composite materials at high strain rate. The MTS Series 647 hydraulic wedge grips were used which are specifically made for testing of the polymer composite materials. The MTS equipment at UTARI also has an Advantage environmental thermal chamber for operation between -129°C to 315°C; however the thermal chamber was not used in this dissertation experiments. MTS axial extensometers with 25 mm gage length were used to measure strain.

3.3 Sensor Technologies

Different SHM techniques were discussed in the review in chapter 2. Among them, the EIS technique of Broadband Dielectric Spectroscopy for measuring the dielectric constants, and another distributed sensing technique of Fiber Optic Sensing for measuring the strain are used in this dissertation. These techniques are explained in detail as follows in sections 3.3.1 and 3.3.2

3.3.1 Broadband Dielectric Spectroscopy (BbDS) Method

Dielectrics are electrically non-conducting materials such as glass, porcelain, and polymers etc. which exhibit the ability of an applied electric field to polarize the material creating electric dipoles. Fiber reinforced composites are naturally dielectric primarily due to the heterogeneous microstructure, interfaces and defects (voids, cracks etc.) that act as charge trapping sites.

The displacement of charged particles in atoms or molecules leads to development of a net dipole moments along the applied field direction. The net dipole moment per unit volume is termed as Polarization. Broadband Dielectric Spectroscopy (BbDS) is an established experimental tool that describes the interaction of electromagnetic waves with matter and reflects by that the underlying molecular mechanisms typically in the frequency range from a lower value of 10^{-6} Hz to a higher frequency of 10^{12} Hz. The frequency regime contains information about molecular and collective dipolar fluctuation; charge transport and polarization effects that occur at inner and outer boundaries in the form of different dielectric properties of the material under study.

Several polarization mechanisms can occur in a material system, i.e. electronic, ionic (molecular), atomic, dipolar (orientational), and interfacial polarizations. Figure 3.1 shows the effect of different charge displacement mechanisms on dielectric response and their corresponding effective frequency range and polarization mechanism.

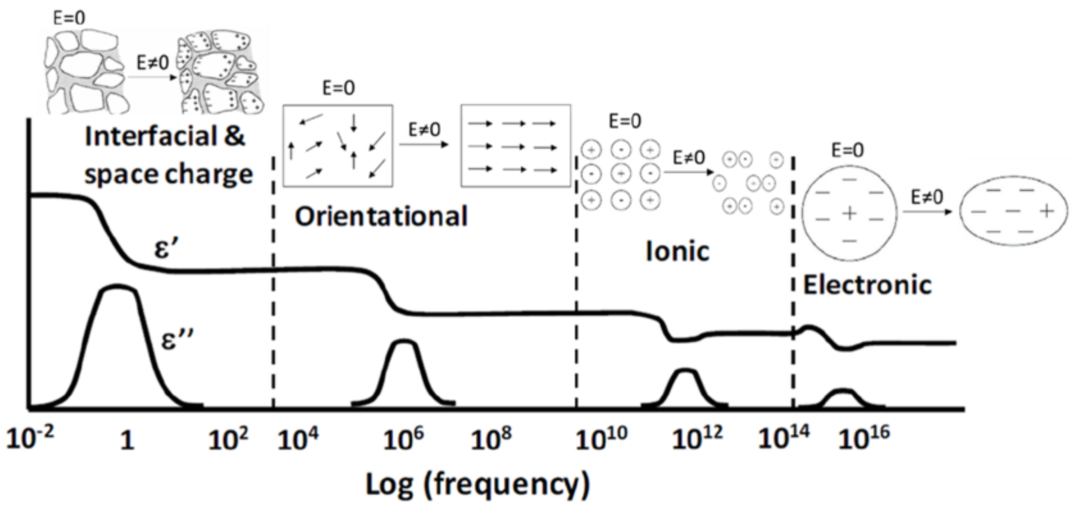

Figure 3.1: Dielectric Response to different polarization mechanisms in different frequency

At the atomic scale, the separation of effective centers of positive charges from effective centers of negative charge in the presence of an external electric field leads to creation of a net dipole moment and this mechanism of polarization is called electronic polarization. In ionic crystals, the anions and cations are arranged in a balanced structure that the net dipole moment of the structure is zero. However, under the influence of an electric field, a net dipole moment is induced because of the displacement of charges and this mechanism is termed as ionic polarization. In some crystals, the distribution of cations and anions are uneven and leads to creation of a net dipole moment because of the arrangement of these ions, termed as dipolar (permanent dipoles) molecules. In the presence of an electric field, these molecules tend to align in the electric field direction and leads to a net dipole moment. This mechanism of polarization in dipolar molecular structures is termed as orientational polarization. In the above mentioned polarizations, the charges are locally bound in atoms or molecules. There could be some charge carriers that are not bound and can migrate through the material under the action of a low frequency electric field. These charge carriers are displaced by the electric field and in the presence of multiple interfaces in the material system, these charge displacements are impeded at the interface and get trapped which results in charge accumulation. This mechanism is called as interfacial or space charge polarization. Based on this, it can be observed that different polarization mechanisms occur at different scales and using different frequency ranges, one can estimate the contribution of each of these different mechanisms.

The dielectric constant of a material can be measured using different techniques limited by the frequency at which the measurements are to be made. In this work, the complex permittivity is measured using the parallel plate capacitor technique. The setup is shown below in Figure 3.2. The dielectric material (laminate) is sandwiched between two conductive plates (electrodes) to form this setup. A sinusoidal voltage is input though one electrode and the output current is measured through the other electrode which could be in phase or out of phase with the input voltage signal based on the nature of the material.

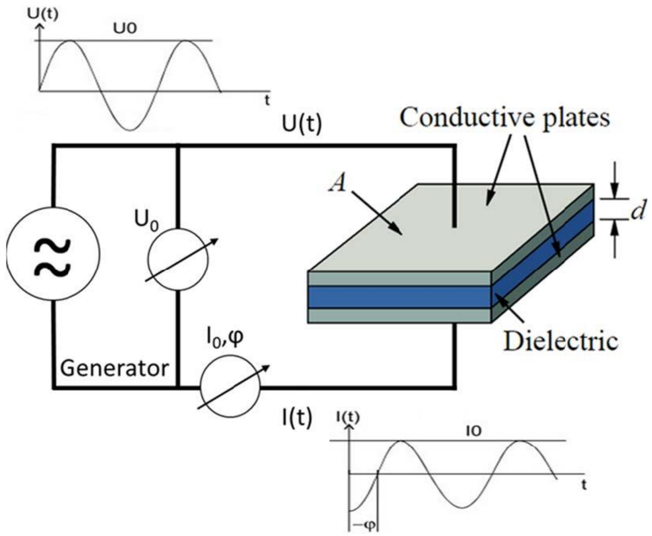

Figure 3.2: Principle of Broadband Dielectric Spectroscopy

A voltage $U_0(V)$ with a fixed frequency $(\omega/2\pi)$ is applied to the sample that causes a current $I_0(A)$at the same frequency but with a phase shift(φ). The relation between them can be expressed in complex notation by the relations shown below:

$$\mathrm{U(t)} = U_0 \cos(\omega t) = Re(U^* e^{j\omega t}) \tag{3.1}$$

$$\mathrm{I(t)} = I_0 \cos(\omega t + \varphi) = Re(I^* e^{j\omega t}) \tag{3.2}$$

Where $U^* = U_0$ and $I^* = I' + jI''$ is the complex representation of the current caused by the applied voltage. The magnitude of this current is given by $I_0 = \sqrt{I' + I''}$. The measured impedance and capacitance of the sample is given by:

$$\mathrm{Z}^*(\omega) = \mathrm{Z}' + j\mathrm{Z}'' = \frac{U^*}{I^*} \tag{3.3}$$

$$\mathrm{C}^*(\omega) = \mathrm{C}' + j\mathrm{C}'' = \frac{1}{j\omega \mathrm{Z}^*} \tag{3.4}$$

Where $\mathrm{Z}'(\Omega), \mathrm{Z}''(\Omega), \mathrm{C}'(\mathrm{F}), \mathrm{C}''(\mathrm{F})$ are the real and imaginary parts of measured impedance $\mathrm{Z}^*(\Omega)$ and capacitance $\mathrm{C}^*(F)$ respectively. The dielectric constant of the sample is given by:

$$\varepsilon_r^*(\omega) = \varepsilon_r' + j\varepsilon_r'' = \frac{C^*}{C_0} \tag{3.5}$$

$$C_0 = \varepsilon_0 \frac{A}{d} \tag{3.6}$$

Where $\varepsilon_r', \varepsilon_r''$ are the real and imaginary parts of measured complex dielectric constant ε_r^* and $C_0(F)$ is the capacitance of free space, $\varepsilon_0(\mathrm{F}/m)$ is the permittivity of free space, $A(\mathrm{m}^2)$ is the area of the electrodes, $d(m)$ is the distance between the electrodes (thickness of the laminate).

It can be observed that the measured dielectric state variable is dependent on the area A of the electrodes. Hence, as a best practice it is advised to use the same electrode configuration to measure the dielectric data of the samples being monitored. The question is how one can interpret the value of this variable? The effective way is to normalize the data w.r.t to initial dielectric data to understand the change in material state. To better understand, consider a material system as shown in Figure 3.3. In the initial state, the material comprises of some manufacturing defects and the initial dielectric constant of the as manufactured system is obtained. Under the application of a field (mechanical/electrical/thermal etc.) defects (cracks) develop in the material system. In the current state, the dielectric constant is obtained. Based on the theory of interfacial polarization, the creation of these new surfaces (cracks) would lead to charge accumulation and hence to a net increase in the measured dielectric constant with reference to the initial state of the material. The normalized value with respect to the initial state would give a representation of the intensity of damage.

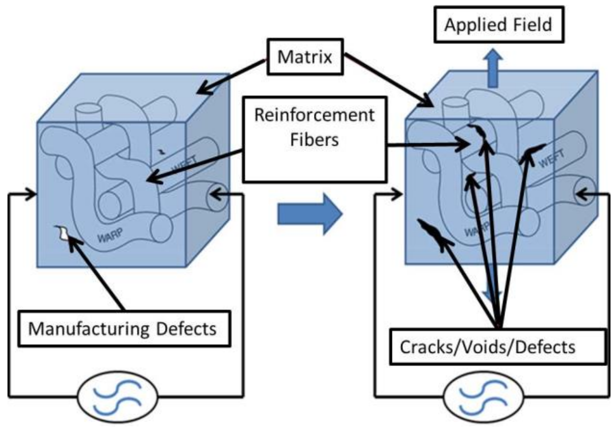

Figure 3.3: Different Material States for Interpretation of Dielectric State Variable

In this dissertation, the material behavior is characterized by broadband dielectric spectroscopy (BbDS) using the Novocontrol™ alpha analyzer. The alpha analyzer measures the complex dielectric properties of the material system as a function of frequency of applied electric field. The frequency range of the alpha analyzer is limited to (3μHz – 20MHz) with a phase accuracy of 0.002º and impedance range of ($10^{-3}\Omega$ - $10^{15}\Omega$) for the current work.

3.3.2 Fiber Optic Sensing (FOS) Method

The majority of FOS systems in the market today employ the use of fiber Bragg gratings to reflect light back to the interrogator. Each manufacturer utilizes a unique configuration and demodulation technique—the method used to obtain and interpret the optical signal provided by the sensors. Fiber Bragg gratings (FBG) operate as wavelength selective mirrors, meaning they reflect a single specific wavelength and transmit all others. The reflected wavelength is referred to as the Bragg wavelength. One way to think about this is with white light. White light consists of the entire color spectrum, or in other words, many different wavelengths. If white light was sent down a fiber with a FBG, one would see a single color reflected, while everything else is transmitted.

When a grating is stretched, compressed, or undergoes thermal expansion and contraction, the Bragg, or reflected wavelength changes. The interrogator then uses a demodulation technique to observe the change in wavelength and translate this into strain and temperature measurements. The relationship between mechanical strain and the Bragg wavelength is described in the Figure 3.4. Further, the demodulation techniques such as Wavelength Division Multiplexing (WDM) and Optical Frequency Domain Reflectometry (OFDR) are used.

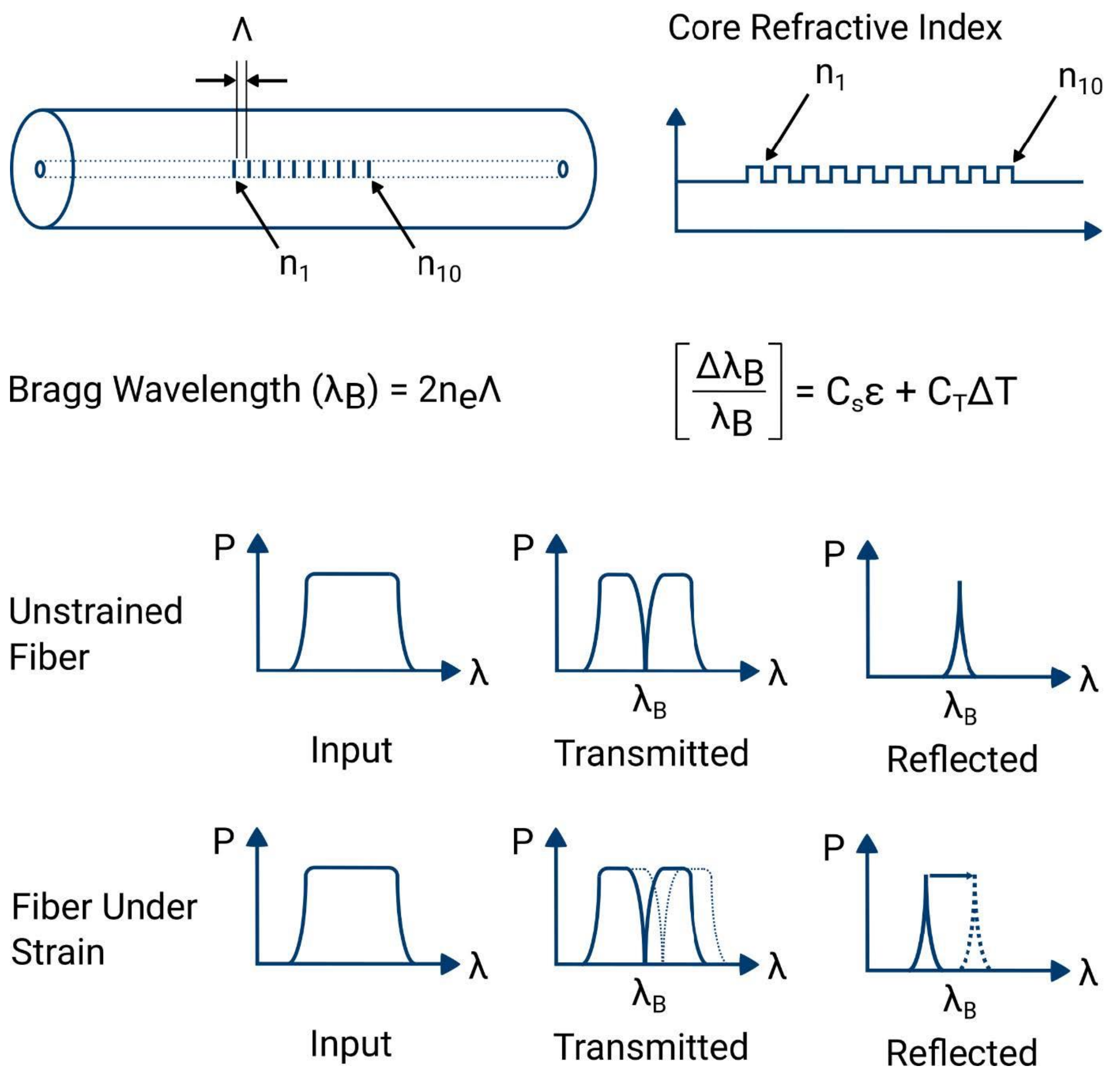

Figure 3.4: Working Principles of FBG in FOS

Optical frequency domain reflectometry (OFDR) can be applied to FBG-based sensors or to scattering technologies. Unlike WDM, when using OFDR, each grating is written at the same wavelength. Writing each grating at the same wavelength enables these systems to avoid the limitation on the number of sensors. Additionally, OFDR based fiber optic sensing systems can provide spatially continuous measurements instead of from a handful of points.

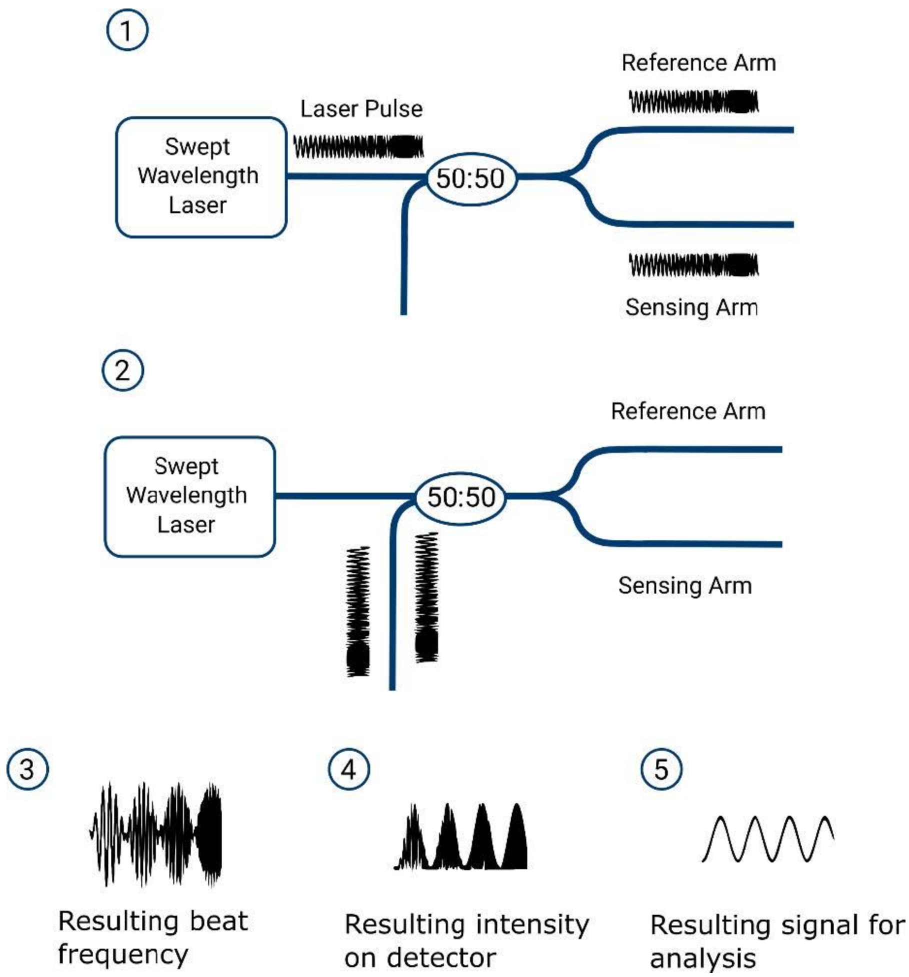

Figure 3.5: Operating Principle of OFDR

Multi-sensing platforms, simply put, are sensor technologies that can monitor multiple parameters (strain, temperature, deflection, etc.) simultaneously and are robust enough that they can be deployed in multiple applications across an organization and utilized throughout the product lifecycle. It's not just about being able to monitor different parameters using the same data acquisition hardware. More than that, a multi-sensing platform can consolidate sensing technology so the same hardware, with minor changes in application techniques and sensor packaging, can adapt to cover multiple testing and monitoring needs of an organization. In order to accomplish this, the sensing system must obtain spatially continuous information in real time, be capable of taking dynamic measurements, be able to easily integrate with a network and perform well in the lab or harsh applied environments. These features allow multi-sensing platforms to be deployed in lifecycle monitoring applications from design validation to providing operational data for critical components and equipment.

3.4 Weibull Statistical Analysis

Weibull statistical analysis is an important interpretive analysis method, especially for the prediction of the composite materials strength and life as per the ASTM standard. Waloddi Weibull proposed his work on the Weibull statistical distribution, and its family of distributions to be applied to a wide range of problems in 1951. He claimed that the function “may sometimes render good service”, and did not claim that it always worked, and it was the best choice. Today, Weibull analysis has many applications in many industries, particularly to Aerospace for the Life estimations.

The formula for the probability density function of the 2-Parameter Weibull distribution is

$$f(x) = \frac{\gamma}{\alpha}(\frac{x}{\alpha})^{(\gamma-1)}\exp(-\frac{x}{\alpha})^{\gamma} \quad x \geq 0; \gamma > 0$$

where γ is the shape parameter and α is the scale parameter.

3.5 Artificial Intelligence

In Chapter 2, section 2.2 a brief introduction was given to the AI and its methods. However the working principles of the different AI algorithms were not discussed. In this section, a complete explanation of the different AI algorithms used in this dissertation are presented, and the general AI model development process is explained.

3.5.1 Supervised Learning Algorithms

Linear Regression

In statistical data analysis, linear regression serves as an analytical technique to formulate the relationship between the dependent output based on the independent input variable. If the output variable depends on two or more input variables, it is defined as multivariate linear regression. The output of linear regression may be non-linear when the exponential powers of the input independent variables are additional input units. Linear regression is widely used in statistics, data analysis, machine learning, biological and industrial engineering to develop possible relationships when the physics of the data is unknown

Logistic Regression

The Logistic Regression or Classification algorithm was developed to classify the given data into the classes, obtain decision boundaries for the classes, and hence used to predict the class for any new input data.

Hypothesis

For Linear Regression with a given input vector X, the predicted output is

$$h(x) = W * X + b \tag{3.7}$$

For Logistic Regression with a given input vector X, the predicted output is

$$\hat{y} = g(W * X + b) \tag{3.8}$$

Where W and b are the parameters or weights. W is a vector of weights and b represents a scalar bias unit. g(z) represents the activation function

Cost function

For linear regression, we calculate the cost function from the loss function (also called as error function) as the mean of the squared errors.

For i^{th} example, the Loss Function is given by

$$L(h(x), y) = \frac{1}{2}\left(h\left(x^i\right) - y^i\right)^2 \tag{3.9}$$

Hence the Cost Function is given by J

$$J(W, b) = \frac{1}{2m}\sum_{i=1}^{m}\left(h\left(x^i\right) - y^i\right)^2 + \frac{\lambda}{2m}\sum_{j=1}^{n} {W_j}^2 \tag{3.10}$$

where, $h\left(x^i\right)$ is the predicted output and y^i is the actual output, and λ is the L2-regularization parameter. The accurate value of the L2- regularization parameter can be obtained by developing validation curves or error analysis curves.

For the Logistic Regression, the Loss function is defined as

$$L(\hat{y}, y) = -(\, y \log \hat{y} + (\, 1 - y\,) \log(1 - \hat{y})) \tag{3.11}$$

The cost function J is given by

$$J(W, b) = \frac{1}{m}\sum_{i=1}^{m} L\left(\hat{y}^i y^i\right) + \frac{\lambda}{2m}\sum_{j=1}^{n} {W_j}^2 \tag{3.12}$$

Where λ is the L2-Regularization parameter.

Gradient Descent Algorithm

As we need to determine the parameters W and b that will result in the very least cost function value, we use the batch gradient descent algorithm. In the batch gradient descent algorithm, every iteration performs the operations

$$W := W - \alpha \frac{\partial J(W,b)}{\partial w}$$

$$b := b - \alpha \frac{\partial J(W,b)}{\partial b}. \tag{3.13}$$

The batch gradient descent performs simultaneous updates of W and b, on all the examples in the training set. The parameters obtained, W and b are used to predict the output value for any new data set.

Random Forest Algorithm

An alternative approach, the random forest algorithm, also called random decision forests operates by the construction of decision trees during the training and outputs the mean of predictions of all the decision trees. The Random forest algorithm is the best fit to avoid the overfitting of the data. It was put forward by Leo Breiman as part of a statistical learning approach. It is an ensemble learning method, which can also predict the value and ranking of each feature.

The random forest algorithm involves two primary processes – Tree bagging (also known as Bootstrap aggregate bagging) and creation of the random forests. The number of trees in the model plays a vital role, as it increases the average value.

Tree Bagging

Given a dataset of m examples, B number of bags are created where each bag consists of the data of $\bar{m}$ examples. These bags are created by random selection of examples with replacement from the total data set (X,Y) such that an example may repeat in several bags. In general Machine learning usage, $\bar{m} \leq m$

Random Forests

From the Tree Bagging process, the input data X(m,n) is reduced to $X_1(\bar{m}, n)$ …. $X_b(\bar{m}, n)$. In the process of creation of random forests, the features to be used in each bag is selected in random, creating random subsets of features. Hence a massive number of tress is created to form the forest. Let $\bar{n}$ be the number of features in each tree, where $\bar{n} \leq n$. This process is defined as the feature bagging.

Each of these trees consists of a data set which is used in a machine learning algorithm (regression, classification or support vector machines) to predict the output of the tree. The output of the random forest is computed by the mean of the predicted output of the trees.

Artificial Neural Network

The Artificial neural networks (ANN) have been considered as the state of art technique for modeling and predicting non-linear system behavior. This non-linear behavior is obtained using hidden layers, which consist of units called neurons. The neurons in the hidden layers are connected to the input and output data by weights or parameters (W and b). The structure of an artificial neural network used in our model is depicted as follows. An N-layer neural network, consists of N-1 hidden layers.

In the mathematical theory of artificial neural networks, the universal approximation theorem states[10] that a feed-forward network with a single hidden layer containing a finite number of neurons, can approximate continuous functions on compact subsets of R^n, under mild assumptions on the activation function.

Activation functions

In the Linear Regression, we used the function $h(x^i)$ as cost function. It is called the linear activation function. There are also many other activation functions used by various machine learning methods and data scientists in the industry. The most commonly used functions are linear, sigmoid, tanh and ReLu – rectified linear unit, as defined below.

Let $h(x^i) = z$ be the input to the activation function

$$Linear = g(z) = z$$

$$Sigmoid = g(z) = \frac{1}{1 + e^{-z}}$$

$$Tanh = g(z) = \tanh(z)$$

$$ReLu = g(z) = \max(0, z)$$

Most of the algorithms use ReLu activation function in neural network model, because it greatly accelerates the convergence of our model compared to the other activation functions. [11]

Feed forward propagation

The feed forward propagation step is similar to the linear regression step to calculate the predicted output. The first layer of the ANN is the input layer.

Our hypothesis equation is

$$h(x) = z^1 = {W_1}^1 * X + b^1 \tag{3.14}$$

The superscript 1 represents the layer 1. a_k is used to calculate the values of the neurons in the hidden layer next to the input layer, given by the activation function used.

$$a_k{}^1 = g(z^1) \tag{3.15}$$

where k is the number of neurons in the respective hidden layer. $a_k{}^1$ serves as the inputs to the hypothesis function, which is used to calculate the outputs of the next hidden layer. The process is repeated until the output layer, where the final output z^N is predicted.

Backward propagation

Back-propagation algorithms are used in the design of multilayer neural networks, and are used in various applications in regression, classification problems, speech recognition and image recognition techniques.

It computes the derivatives of the cost function J with respect to our parameters W and b.

If the Cost Function J for a Neural Network is given by

$$J(W^1, b^1, W^2, b^2 \ldots \ldots W^N, b^N) = \frac{1}{2m}\sum_{i=1}^{m}\left(\hat{y}^i - y^i\right)^2 + \frac{\lambda}{2m}\sum_{j=1}^{n} W_j{}^2 \tag{3.16}$$

The derivatives are given by

$$\partial z^N = a^N - y$$

$$\frac{\partial J(W^1, b^1, W^2, b^2 \ldots \ldots W^N, b^N)}{\partial w^N} = \frac{1}{m} * \partial z^N * a^{N-1} + \frac{\lambda}{m} W^N$$

$$\frac{\partial J(W^1, b^1, W^2, b^2 \ldots \ldots W^N, b^N)}{\partial b^N} = \frac{1}{m} * \partial z^N \tag{3.17}$$

L-BFGS Algorithm

Earlier for our linear regression, we discussed the Gradient Descent Algorithm, but there are many other algorithms which can be used for the optimization processes to obtain the parameters W and b, which can find the least value of the cost function. These optimization algorithms are selected based on the input data, number of samples, timing required, efficiency and computational requirements. The most commonly used algorithms are gradient descent algorithm, stochastic gradient descent algorithm, gradient descent with momentum, exponentially weighted averages algorithm, Adam algorithm, BFGS and L-BFGS algorithm.

Limited-memory BFGS or L-BFGS belongs to the family of quasi-Newton methods which approximate the Broyden–Fletcher–Goldfarb–Shanno (BFGS) algorithm using a limited amount of computer memory. L-BFGS uses an estimation to the inverse Hessian matrix to steer its search through variable space, but where BFGS stores a dense $n \times n$ approximation to the inverse Hessian, L-BFGS stores only a few vectors that represent the approximation implicitly. Due to its resulting linear memory requirement, the L-BFGS method is particularly well suited for optimization problems with many variables [12-14].

Adam Optimization Algorithm

Require: α: Stepsize
Require: $\beta_1, \beta_2 \in [0, 1)$: Exponential decay rates for the moment estimates
Require: $f(\theta)$: Stochastic objective function with parameters θ
Require: θ_0: Initial parameter vector
$m_0 \leftarrow 0$ (Initialize 1st moment vector)
$v_0 \leftarrow 0$ (Initialize 2nd moment vector)
$t \leftarrow 0$ (Initialize timestep)
while θ_t not converged **do**
$t \leftarrow t + 1$
$g_t \leftarrow \nabla_\theta f_t(\theta_{t-1})$ (Get gradients w.r.t. stochastic objective at timestep t)
$m_t \leftarrow \beta_1 \cdot m_{t-1} + (1 - \beta_1) \cdot g_t$ (Update biased first moment estimate)
$v_t \leftarrow \beta_2 \cdot v_{t-1} + (1 - \beta_2) \cdot g_t^2$ (Update biased second raw moment estimate)
$\widehat{m}_t \leftarrow m_t / (1 - \beta_1^t)$ (Compute bias-corrected first moment estimate)
$\widehat{v}_t \leftarrow v_t / (1 - \beta_2^t)$ (Compute bias-corrected second raw moment estimate)
$\theta_t \leftarrow \theta_{t-1} - \alpha \cdot \widehat{m}_t / (\sqrt{\widehat{v}_t} + \epsilon)$ (Update parameters)
end while
return θ_t (Resulting parameters)

Figure 3.6: ADAM optimization algorithm

Adam optimization has proved to be the best for our models being developed, which is one of the best optimizing algorithms in deep learning inherited from the RMSProp and AdaGrad [13]. The Parameters are updated in this algorithm, invariant to re-scaling of the gradient, hence greater performance is achieved. In the original paper, Adam was demonstrated empirically to show that convergence meets the expectations of the theoretical analysis. Adam was applied to the logistic regression algorithm on the MNIST character recognition and IMDB sentiment analysis datasets, a Multilayer Perceptron algorithm on the MNIST dataset, and Convolutional Neural Networks on the CIFAR-10 image recognition dataset. Being computationally efficient, and suitable for large systems in terms of data, Adam is used in both the neural network models being developed. The Algorithm is shown in Figure 3.6.

Recurrent Neural Network

Recurrent Neural Network (RNN) is a supervised learning algorithm, and is a class of the artificial neural networks in which the connections between neurons in each layer form a directed graph along a sequence. RNNs are most commonly used in language modelling and generating text, machine translation, speech recognition, generating image descriptions and time series data, where the model depends on the previous data value to make a prediction.

Long Short-Term Memory (LSTM) networks, are a particular type of recurrent neural networks that has gotten immense attention recently within the data driven community. These networks have internal contextual state cells that acts as long-term or short-term memory cells. These memory cells are used for predicting a long sequence of data with less memory requirements and achieve greater performance. LSTM networks were discovered by Hochreiter and Schmidhuber in 1997 and set accuracy records in multiple applications domains [16]. LSTM networks keep contextual information of the inputs by integrating over a loop that allows information to flow from each previous step to the current, and further. Hence these loops make RNNs seem magical. The limitation of RNN is the vanishing gradient problem, which is solved by LSTM.

3.5.2 Unsupervised Learning Algorithms

Unlike traditional methods of Supervised Machine learning, where the input data are matched to their corresponding output data, Unsupervised methods take only the input data and perform the mathematical formulations on them to give significant information. Unsupervised learning is of two types – clustering and dimensionality reduction. Clustering is further divided into several types such as centroid based clustering, connectivity-based clustering, Gaussian mixture models, and density-based clustering. Based on the type of data, the best algorithm needs to be selected.

Dimensionality reduction of the data is used when there is a huge number of features and the best features are needed to be known as the inputs to the data. Feature selection is one technique for this purpose, but in the process of feature selection, several features are eliminated. In dimensionality reduction, the feature data is not eliminated. Also, applying dimensionality reduction improves the speed of learning for the model. Principal Component Analysis (PCA) is the most commonly used dimensionality reduction technique. Several other methods include random projection method, independent component analysis, feature agglomeration, neural auto-encoders, and linear discriminant analysis. The selection of these techniques also depends on the nature of the data. For instance, for the time-dependent data, the neural auto-encoders are used due to their time-distributed functions.

Principal Component Analysis

PCA is an important method in the field of machine learning, statistics, and data science. By definition, it is the linear dimensionality reduction using Singular Value Decomposition (SVD) of the data to project it to a lower-dimensional space. It combines the input features into a single value or vector, by retaining the most important knowledge of all the features. This was invented as an analog of the principal axis theorem in mechanics, by Pearson (1901) and Hotelling (1933), whilst the best modern reference is Jolliffe [9]. PCA is the process of transforming original features into a new coordinate system, creating new features called the principal components. These are linear functions of original features and are not correlated. The highest variance by any projection of the data comes to lie on the first coordinate, the second-highest variance on the second coordinate, and so on. This is achieved by calculating the covariance matrix for the entire data set, computing the eigenvectors and eigenvalues for the covariance matrix, and sorting them according to decreasing eigenvalue. The algorithm is shown in Figure 3.7. It is vital to note that PCA's bias is not always appropriate; features with low variance might have high predictive relevance, depending on its application.

1. Compute the mean feature vector

   $\mu = \frac{1}{p}\sum_{k=1}^{p} x_k$, where, x_k is a pattern ($k = 1$ to p), p = number of patterns, x is the feature matrix

2. Find the covariance matrix

   $C = \frac{1}{p}\sum_{k=1}^{p}\{x_k - \mu\}\{x_k - \mu\}^T$ where, T represents matrix transposition

3. Compute Eigen values λ_i and Eigen vectors v_i of covariance matrix

   $Cv_i = \lambda_i v_i$ $\quad$ ($i = 1, 2, 3, \ldots q$), q = number of features

4. Estimating high-valued Eigen vectors

   (i) Arrange all the Eigen values (λ_i) in descending order

   (ii) Choose a threshold value, θ

   (iii) Number of high-valued λ_i can be chosen so as to satisfy the relationship

   $\left(\sum_{i=1}^{s}\lambda_i\right)\left(\sum_{i=1}^{q}\lambda_i\right)^{-1} \geq \theta$, where, s = number of high valued λ_i chosen

   (iv) Select Eigen vectors corresponding to selected high valued λ_i

5. Extract low dimensional feature vectors (principal components) from raw feature matrix.

   $P = V^T x$, where, V is the matrix of principal components and x is the feature matrix

Figure 3.7: PCA Algorithm

Selecting the number of features that are needed for the model is a critical step of PCA. It is done either by the domain knowledge, if the user knows how many principal components are required, or by the proportion of variance that the user wants to maintain from their entire dataset. For example, if we want to retain 90% of the variance of the dataset, we select the top features whose sum of the variances equals or exceeds 90%. There is also another method called the elbow method, using the scree plot but it is not widely used. The main disadvantage of PCA is that, since the features are changed to principal components, it’s not possible to obtain meaningful information for engineering analysis or to get the inverse relationship from the model being developed. But few other techniques exist that can be carefully implied into PCA to get useful information from the data.

K-MEANS CLUSTERING

K-Means clustering [10], [11] is the most commonly used simple clustering algorithm, which aims to combine ‘n’ observations into ‘k’ clusters, where each observation belongs to the cluster with the nearest mean center or centroid. It is a type of centroid based clustering. It is often confused with the K-nearest neighbor algorithm due to the name. It uses the Euclidean distance function. It often gives the best result when the data set is distinct.

The K-Means algorithm is as follows:

- Choose the number of clusters (K) and obtain the data points
- Place the centroids c_1, c_2, ... c_k randomly
- Repeat steps below until convergence or until the end of a fixed number of iterations
- for each data point x_i:

  - find the nearest centroid(c_1, c_2 .. c_k)

  - assign the point to that cluster
- for each cluster j = 1..k

  - new centroid = mean of all points assigned to that cluster

The disadvantage of K-Means clustering is that it requires a prior specification of the number of clusters. However, by using the distortion or inertia data, we would be able to use the elbow method to find the optimal number of clusters. In some cases, the clustering accuracy is also used in the elbow method to determine the number of clusters. It has few other disadvantages in their application to the real world datasets as the algorithm provides the local optima of the squared error function. However, there are alternatives to the algorithm that are available with the increased research use of these methods. Also, it is to be noted that due to their iterative nature and random initialization of centroids, it is recommended to run the algorithm using different centroid initialization and select the results yielding the least sum of squared distance.

3.5.3 Performance Metrics

Once the model has been developed, the performance of the model is evaluated by the mean squared error function (MSE) and the R^2 score or R^2 coefficient.

R^2 coefficient

The R^2 coefficient is defined as the ratio of the residual sum of squares to the total sum of squares of output, subtracted from unity.

$$MSE = \frac{1}{2m}\sum_{i=1}^{m}\left(\hat{y}^i - y^i\right)^2 \tag{3.18}$$

$$R^2 = 1 - \frac{\sum_{i=1}^{m}\left(\hat{y}^i - y^i\right)^2}{\sum_{i=1}^{m}(mean(y^i) - y^i)^2} \tag{3.19}$$

An R^2 coefficient of 1 indicates a best model, and a negative R^2 indicates a worse model. When the R^2 score tends to 0, it indicates that our model is a constant model, and will always give 0 for any input. This R^2 coefficient determines the uncertainty of the model being developed.

Also in random forest regression algorithm and XG-boost, and other decision tree based algorithms, we can obtain the depth of each feature, which is the relative importance of that particular feature to the prediction of the output. These are defined by the expected fraction of samples they contribute.

Additionally, for the Logistic Regression models, additional Performance Metrics are used.

Confusion Matrix

Confusion matrix is used to evaluate the quality of the output of a classifier. The diagonal elements represent the number of points for which the predicted label is equal to the true label, while off-diagonal elements are those that are mislabeled by the classifier. The higher the diagonal values of the confusion matrix the better, indicating many correct predictions.

Precision

The precision is the ratio tp / (tp + fp) where tp is the number of true positives and fp the number of false positives. The precision is intuitively the ability of the classifier not to label as positive a sample that is negative.

Recall

The recall is the ratio tp / (tp + fn) where tp is the number of true positives and fn the number of false negatives. The recall is intuitively the ability of the classifier to find all the positive samples.

F1- Score

The F-beta score can be interpreted as a weighted harmonic mean of the precision and recall, where an F-beta score reaches its best value at 1 and worst score at 0. The F-beta score weights recall more than precision by a factor of beta. Beta == 1.0 means recall and precision are equally important.

Accuracy

In multi-label classification, Accuracy represents subset accuracy: the set of labels predicted for a test Set must exactly match the corresponding set of labels in test set

Accuracy = Number of correct classifications / Number of samples in the dataset

3.5.4 AI Model Development Process

Data Preparation

Normalization of the Data

Normalization is defined as the process of scaling individual sample data to have unit norm. This process is useful to quantify the similarity of any pair of samples. Normalization was done by using the scikit-learn normalizer package, by setting the norm parameter as “l2”, to obtain the Euclidian norm and normalizing each sample. By normalizing the data, the optimization algorithm runs better and faster, as the loss value is minimized.

Padding of Variable Length data

For few experiments, especially for fatigue experiments, since the data were obtained from the experimental testing of composite materials, the length of the data was not uniform for all the samples. As the data must be of uniform length, all the input and output data were padded with zeros, to make the length of the data set to be a vector of uniform size for each sample for both input and output.

Splitting of Training and Test Set

The total data set was split into training and test sets, by setting the test size parameter to be 0.2, using the scikit-learn[12] python package. The train data is used for the model development process, and its further split for cross-validation purposes. Finally, after the model is developed, the test data, which is the unseen data is used to test the model's predictions.

Cross Validation and Hyper Parameter Tuning

For each of the data-mining algorithms to be developed, there are certain parameters called Hyper-parameters which are not directly learned within estimators. In scikit-learn they are passed as arguments to the constructor of the estimator classes. Typical examples include number of neighbors, weights and p value for K-Neighbors Classifier, alpha for Neural Networks, etc. It is possible and recommended to search the hyper-parameter space for the best cross validation score. When the performance of the model is poor, the model will require proper tuning. The problem of bias and variance is first identified by learning curves, between the training set and cross-validation set. Based on it, the recommended tuning process is executed. The tuning of a neural network is complicated compared to the machine learning models, as the neural network has a number of hyper parameters.

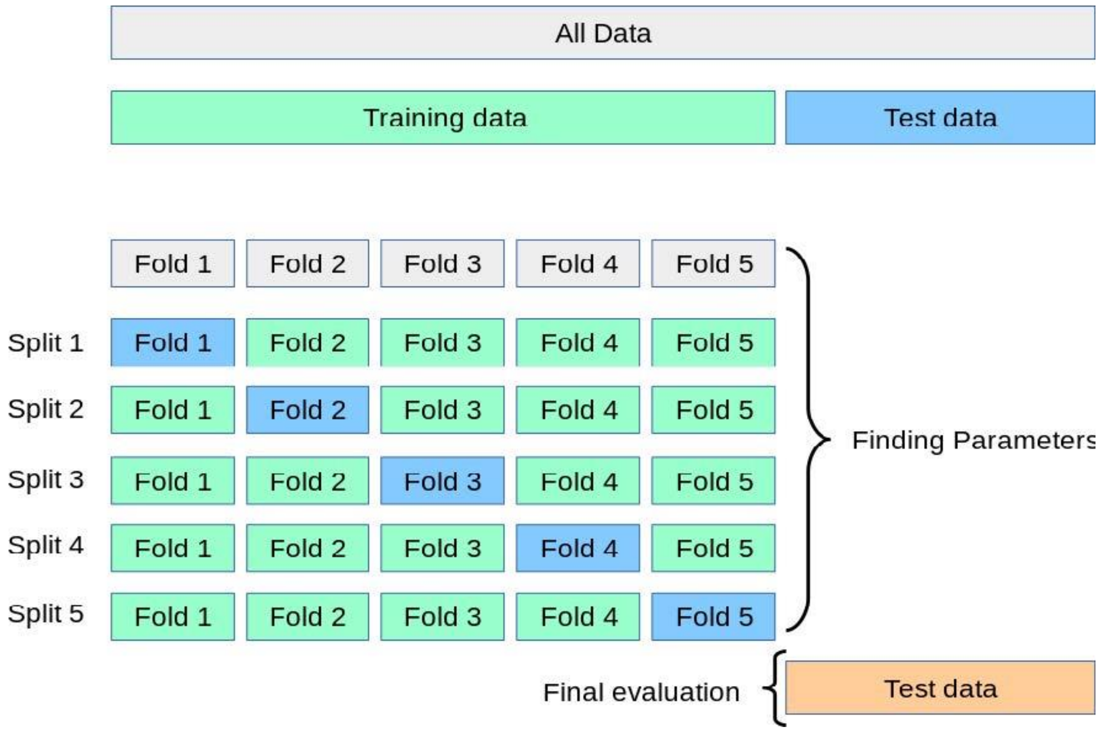

Figure 3.8: Cross Validation with Hyper Parameter estimation

When evaluating different settings ("hyperparameters") for estimators, such as the n_neighbors setting that must be manually set for an K-Neighbors, there is still a risk of over fitting on the test set because the parameters can be tweaked until the estimator performs optimally. This way, knowledge about the test set can "leak" into the model and evaluation metrics no longer report on generalization performance. To solve this problem, yet another part of the dataset can be held out as a so-called "validation set": training proceeds on the training set, after which evaluation is done on the validation set, and when the experiment seems to be successful, final evaluation can be done on the test set

A test set should still be held out for final evaluation, but the validation set is no longer needed when doing CV. In the basic approach, called k-fold CV, the training set is split into k smaller sets (other approaches are described below, but generally follow the same principles). The following procedure is followed for each of the k "folds":

- A model is trained using k-1 of the folds as training data;
- The resulting model is validated on the remaining part of the data (i.e., it is used as a test set to compute a performance measure such as accuracy).

The performance measure reported by k-fold cross-validation is then the average of the values computed in the loop. This approach can be computationally expensive, but does not waste too much data (as is the case when fixing an arbitrary validation set), which is a major advantage in problems such as inverse inference where the number of samples is very small.

3.5.5 Interpretable Machine Learning Methods

The importance of using Interpretable Machine Learning (IML) models was discussed in the last section of chapter 2. The working principle of the IML models are explained here.

Throughout this dissertation, the focus is on Model-Agnostic explanation systems. Desirable aspects of a model-agnostic explanation system are[156]

Model flexibility: The interpretation method can work with any machine learning model, such as random forests and deep neural networks.

Explanation flexibility: You are not limited to a certain form of explanation. In some cases it might be useful to have a linear formula, in other cases a graphic with feature importances.

Representation flexibility: The explanation system should be able to use a different feature representation as the model being explained. For a text classifier that uses abstract word embedding vectors, it might be preferable to use the presence of individual words for the explanation.

Permutation Feature Importance

Permutation feature importance measures the increase in the prediction error of the model after we permuted the feature's values, which breaks the relationship between the feature and the true outcome. The concept was developed by measuring the importance of a feature by calculating the increase in the model's prediction error after permuting the feature. A feature is "important" if shuffling its values increases the model error, because in this case the model relied on the feature for the prediction. A feature is "unimportant" if shuffling its values leaves the model error unchanged, because in this case the model ignored the feature for the prediction.

The permutation feature importance algorithm based on Fisher, Rudin, and Dominici (2018) is as follows [157]

Input: Trained model f, feature matrix X, target vector y, error measure L(y,f).

1. Estimate the original model error $e^{orig} = L(y, f(X))$ (e.g. mean squared error)
2. For each feature $j = 1,...,p$ do:
    i. Generate feature matrix X^{perm} by permuting feature j in the data X. This breaks the association between feature j and true outcome y.
    ii. Estimate error $e^{perm} = L(Y,f(X^{perm}))$ based on the predictions of the permuted data.
    iii. Calculate permutation feature importance $FI^j= e^{perm}/e^{orig}$. Alternatively, the difference can be used: $FI^j = e^{perm} - e^{orig}$
3. Sort features by descending FI.

LIME

Local interpretable model-agnostic explanations (LIME) is a research article in which the authors propose a concrete implementation of local surrogate models. Surrogate models are trained to approximate the predictions of the underlying black box model. Instead of training a global surrogate model, LIME focuses on training local surrogate models to explain individual predictions.

The idea is quite intuitive. First, forget about the training data and imagine you only have the black box model where you can input data points and get the predictions of the model. You can probe the box as often as you want. Your goal is to understand why the machine learning model made a certain prediction. LIME tests what happens to the predictions when you give variations of your data into the machine learning model. LIME generates a new dataset consisting of perturbed samples and the corresponding predictions of the black box model. On this new dataset LIME then trains an interpretable model, which is weighted by the proximity of the sampled instances to the instance of interest. The interpretable model can be anything from the interpretable models chapter, for example Lasso or a decision tree. The learned model should be a good approximation of the machine learning model predictions locally, but it does not have to be a good global approximation. This kind of accuracy is also called local fidelity.

Mathematically, local surrogate models with interpretability constraint can be expressed as follows:

$$\text{explanation}(x)=\arg\min_{g\in G}L(f,g,\pi_x)+\Omega(g)$$

The explanation model for instance x is the model g (e.g. linear regression model) that minimizes loss L (e.g. mean squared error), which measures how close the explanation is to the prediction of the original model f (e.g. an xgboost model), while the model complexity Ω(g)Ω(g) is kept low (e.g. prefer fewer features)

The procedure for training local surrogate models:

- Select your instance of interest for which you want to have an explanation of its black box prediction.
- Perturb your dataset and get the black box predictions for these new points.
- Weight the new samples according to their proximity to the instance of interest.
- Train a weighted, interpretable model on the dataset with the variations.
- Explain the prediction by interpreting the local model.

SHAP

SHAP (SHapley Additive exPlanations) by Lundberg and Lee (2016) is a method to explain individual predictions. SHAP is based on the game theoretically optimal Shapley Values. A prediction can be explained by assuming that each feature value of the instance is a "player" in a game where the prediction is the payout. Shapley values -- a method from coalitional game theory -- tells us how to fairly distribute the "payout" among the features.

The goal of SHAP is to explain the prediction of an instance x by computing the contribution of each feature to the prediction. The SHAP explanation method computes Shapley values from coalitional game theory. The feature values of a data instance act as players in a coalition. Shapley values tell us how to fairly distribute the "payout" (= the prediction) among the features. A player can be an individual feature value, e.g. for tabular data. A player can also be a group of feature values. For example to explain an image, pixels can be grouped to super pixels and the prediction distributed among them. One innovation that SHAP brings to the table is that the Shapley value explanation is represented as an additive feature attribution method, a linear model. SHAP is further subdivided into KernalSHAP and TreeSHAP based on the type of model to be developed.

3.6 Summary

In this chapter, we gave the entire description of technical background of manufacturing the composites, the sensor equipment's used and the different AI algorithms used in this dissertation work. In further chapters, we will discuss the experiments performed and how these sensor systems, and AI methods are used for the Defect Analysis, Stiffness Degradation Measurements, Residual Strength and Residual Life Prediction in Composite materials.

Chapter 4

DEFECT ASSESSMENT IN COMPOSITES USING DIELECTRICS AND AI

In the previous chapter 3, we discussed the Electrochemical Impedance Spectroscopy (EIS) technique, and the various Artificial Intelligence (AI) algorithms, model development techniques and Interpretable Machine Learning (IML) methods. In this chapter, we discuss the implementation of the aforementioned methods to Identify and predict the defects in composite materials. These defects are foreign body objects, which are induced in the material during manufacturing. The outline of this chapter is as follows. Section 4.1 deals with the process of experimental methods and data collection. Section 4.2 describes the Supervised Learning problem with sub-sections 4.2.1 describing the data preparation, 4.2.2 on AI model developed, 4.2.3 on Model performance and 4.2.4 on the use of Interpretable machine learning techniques. Section 4.3 describes using the real part of permittivity and imaginary part of permittivity with Un-supervised learning techniques.

4.1 Experimental Methods

4.1.1 Manufacturing

Four composite panels of 254 mm x 254 mm planar dimension were manufactured using Rockwest 120 Glass Fiber (E-glass) woven prepreg. The laminate sequence was $[0]_4$. The Panels were manufactured with defects induced in them in between the middle layers. Each panel was divided into 8x8 cells for the experimental readings, as shown in Figure 4.1. These panels were manufactured as per the manufacturer’s recommended cure cycle at 408 K for the NP301 Resin system, using the WABASH compression molding presses, at the University of Texas at Arlington Research Institute.

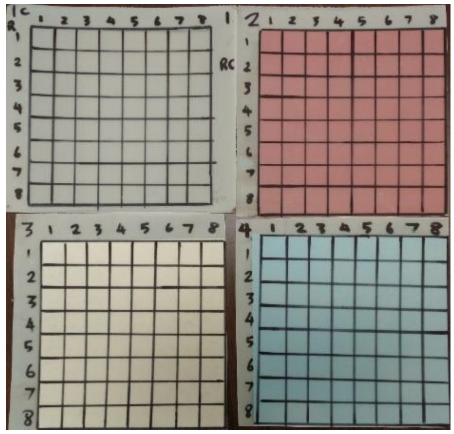

Figure 4.1: Panels manufactured for BbDS Testing

Table 4-I Defects induced in each panel manufactured

PANEL No.	DEFECT	Material description
1	No Defect	-
2	Release Film	Non-Perforated High Temperature
3	Backing Paper	Prepreg backing paper attached in Glass Fiber
4	Release Paper	Top Release paper from the prepreg

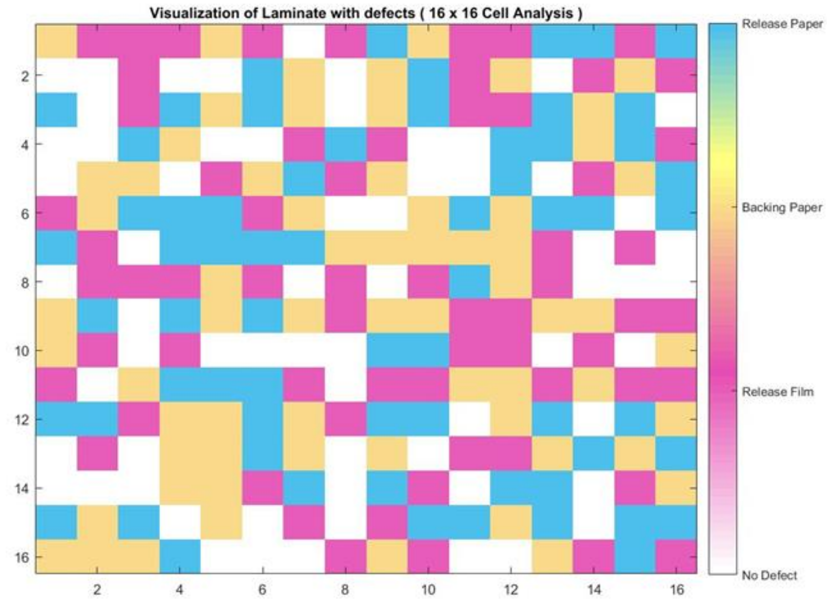

Figure 4.2. Composite laminate with the defects

Figure 4.2 represents a composite laminate with 3 different types of defects in it, and some regions with no-defects. As per our experimental data, measurements were taken for 256 points, represented in the figure by a 16 x 16 cell analysis.

4.1.2 Obtaining Dielectric parameters using Broadband Dielectric Spectroscopy

Dielectric property measurements were measured using the Novo Control Broadband Dielectric Spectrometer at the University of Texas at Arlington Research Institute. A 12.7 mm square electrode was used. The Panels were placed in between electrodes within the closed environmental chamber, and the measurements were observed at each cell for all the four panels. The measurements were obtained by a frequency sweep from 1 MHz to 0.1 Hz, with a scaling factor of 1.4. Figure 4.3 depicts the setup of the equipment which was used to carry out the experiments.

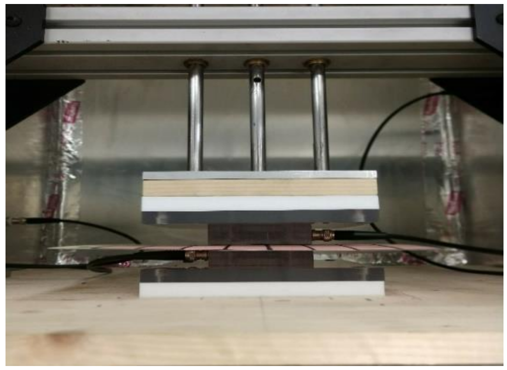

Figure 4.3: Experimental test setup for BbDS measurement

14 dielectric parameters were obtained from the experiments. They are the Real, Imaginary and Modulus of the Dielectric Permittivity, Electric Modulus, Conductivity and Impedance respectively. The Tan loss and conductivity ratio was also calculated. Each of these dielectric parameters were measured through the thickness of every single cell, at 49 different frequencies. Hence there are 14 dielectric parameters at 49 frequencies which form the 686 features. As there are 4 different panels and 64 cells in each panel, which form the 256 samples of data points. The average frequency sweep of these 14 dielectric parameters for each panel type are shown in Figure 4.4.

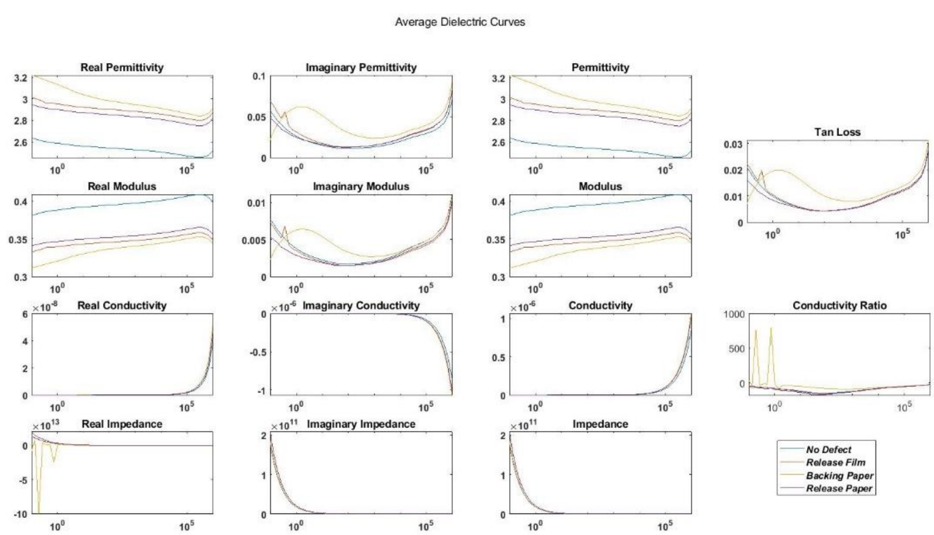

Figure 4.4: Average Curves of Dielectric Parameters for each defect

4.2 Supervised Learning Model and Interpretability

4.2.1 Data preparation

The dataset considered consists of 256 samples and 686 features, as discussed in the previous session. To build a logistic regression model, for the classification purposes, it is important to remove all of the redundant features. Hence, the Pearson Correlation Coefficients (PCC) were calculated for all the 686 features, and the correlation matrix was developed. Later, the features which had an absolute PCC value greater than 0.95 were removed, which reduced the number of features drastically to 16 features. These features obtained were found to be mostly in the lower frequency ranges between 0.1 Hz to 30 Hz. This reduction of features, implies that there is not significant change in values among the 4 different panels at higher frequencies. As it is difficult to visualize a 686 x 686 correlation matrix, a correlation matrix is shown in Figure 4.5, indicating the correlation of the frequency sweep of the 14 dielectric parameters.

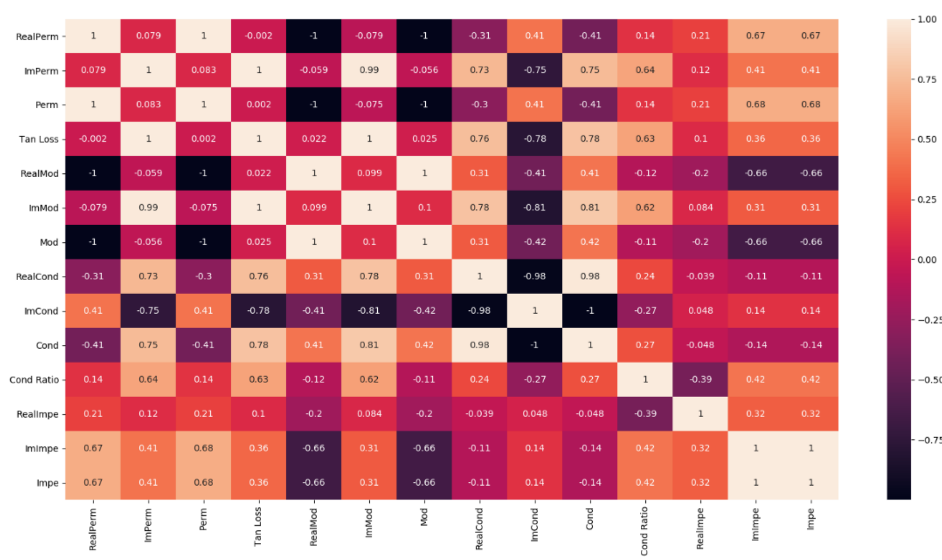

Figure 4.5: Correlation among the Dielectric Parameters

4.2.2 AI model development

Once the data reduction was performed by removing the highly correlated features, the data set was split into training and testing tests. The training set consisted of 204 samples and the test set consisted of 52 samples. It was randomly split using the sklearn train_test_split algorithm. The training set was further during split as per the K-Fold cross validation process. Four different AI models were developed – logistic regression, random forest classifier, XGboost classifier and artificial neural network. The algorithms of these AI models are discussed in the previous chapter. As per the procedure for developing an AI model discussed in previous chapter, section 3.5, the hyper parameter tuning was performed using the GridSearch Algorithm, to identify the best parameter set for each AI model developed. Unless specified, all other defaults parameters were used from the sklearn package.

4.2.2.1 Logistic Regression

The default parameters were used and the best value for maximum number of iterations was found to be 100. Increasing this parameter for logistic regression, did not improve the model performance.

4.2.2.2 Random Forest Classifier

The best value for the number of estimators was found to be 100 as per the hyper-parameter tuning for the random forest classifier. All other default parameters of the sklearn random forest classifier were used.

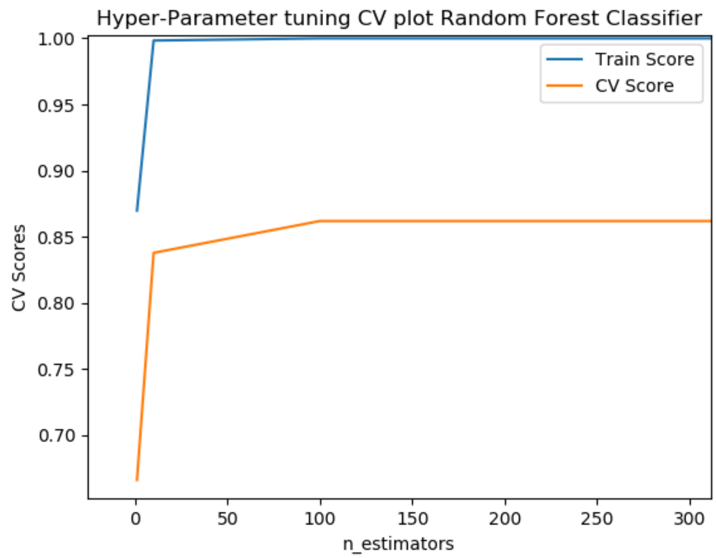

Figure 4.6: Hyperparameter tuning for Random Forest Classifier

4.2.2.3 XGBoost Classifier

The best value for the number of estimators was found to be 1000 as per the hyper parameter tuning for the random forest classifier.

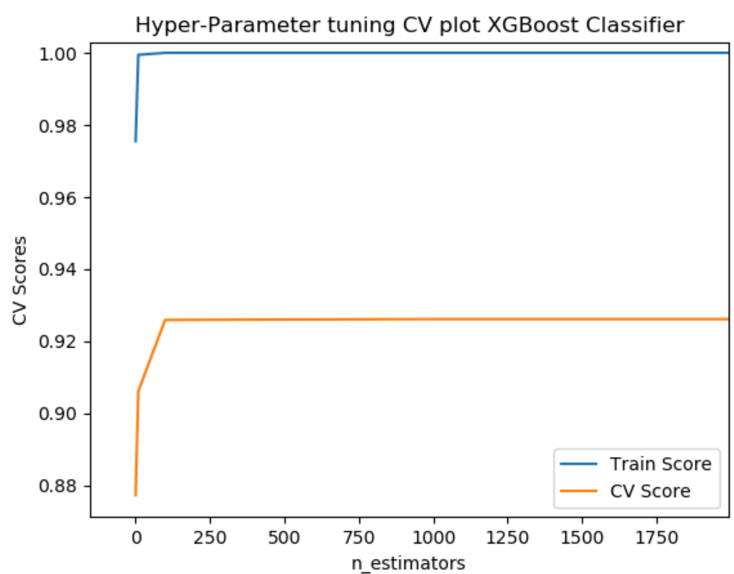

Figure 4.7: Hyper parameter tuning for XGBoost Classifier.

4.2.2.4 Artificial Neural Network

The best network was found to be a 2-Layer Neural Network which was developed, with 100 neurons in the Hidden layer and with an alpha value of 0.0003. The input layer had 16 inputs, and the output layer had four class output. The ReLu activation function was used for the hidden layers, and sigmoid activation function was used for the output layer. Optimization was done by the L-BFGS Algorithm.

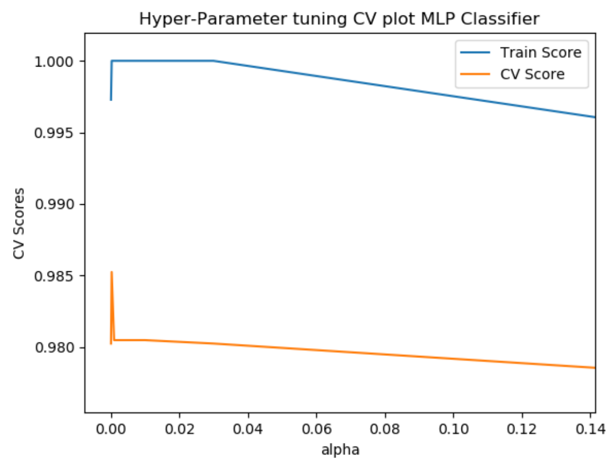

Figure 4.8: Hyper Parameter Tuning for Artificial Neural Network.

4.2.3 Model Performance

The performance metrics and their equations are discussed in chapter 3.

4.2.3.1 Performance Metrics

Table 4-II: Accuracy of the AI models developed

AI Model	Training Accuracy	Cross-Validation Accuracy	Test Set Accuracy
Logistic Regression	0.838 (+/-0.022)	0.832 (+/-0.185)	0.8269

Random Forest Classifier	1.000 (+/-0.000)	0.862 (+/-0.142)	0.8269
XG Boost Classifier	1.000 (+/-0.000)	0.926 (+/-0.066)	0.9423
Artificial Neural Network	1.000 (+/-0.000)	0.985 (+/-0.045)	0.9615

The Table 4-II values list the accuracy for the training, cross validation and the test data for the 4 different AI models developed. We can see that the Artificial Neural Network model has the highest accuracy on the Cross validation and the test data.

Additionally, the classification report for each of the AI models developed is as follows.

Detailed classification report of Logistic Regression :

	precision	recall	f1-score	support
No Defect	1.00	0.93	0.96	14
Release Film	0.67	0.55	0.60	11
Backing Paper	0.84	0.84	0.84	19
Release Paper	0.73	1.00	0.84	8
accuracy			0.83	52
macro avg	0.81	0.83	0.81	52
weighted avg	0.83	0.83	0.82	52

Detailed classification report of Random Forest Classifier :

	precision	recall	f1-score	support
No Defect	1.00	0.93	0.96	14
Release Film	0.67	0.55	0.60	11
Backing Paper	0.89	0.89	0.89	19
Release Paper	0.64	0.88	0.74	8
accuracy			0.83	52
macro avg	0.80	0.81	0.80	52
weighted avg	0.84	0.83	0.83	52

Detailed classification report of XGBoost Classifier :

	precision	recall	f1-score	support
No Defect	1.00	0.93	0.96	14
Release Film	0.91	0.91	0.91	11
Backing Paper	1.00	0.95	0.97	19
Release Paper	0.80	1.00	0.89	8
accuracy			0.94	52
macro avg	0.93	0.95	0.93	52
weighted avg	0.95	0.94	0.94	52

Detailed classification report of MLP Classifier :

	precision	recall	f1-score	support
No Defect	1.00	0.93	0.96	14
Release Film	1.00	0.91	0.95	11
Backing Paper	1.00	1.00	1.00	19
Release Paper	0.80	1.00	0.89	8
accuracy			0.96	52
macro avg	0.95	0.96	0.95	52
weighted avg	0.97	0.96	0.96	52

Figure 4.9: Classification Report on the Test Data.

4.2.3.2 Confusion Matrix

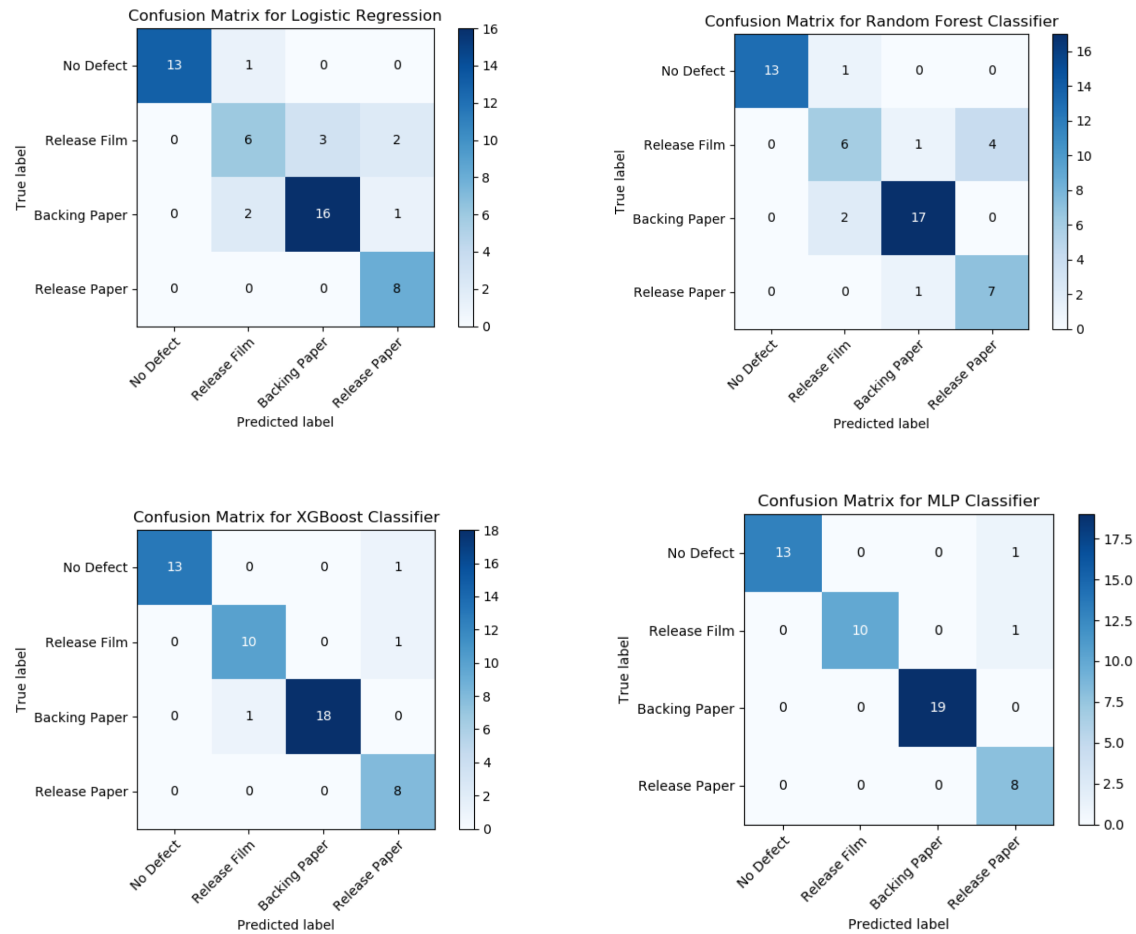

Figure 4.10: Confusion Matrix from the AI Classification models.

4.2.4 Interpretability of the AI models

As discussed in our previous chapter, here we deal with explainability of the AI models that were developed. The permutation importance's, LIME and SHAP techniques are used to explain the global and local interpretability of the predictions and to learn which dielectric parameter at which frequency makes the most significant contribution to identify the presence of defects in composite materials. All these explanations are on the unseen – test dataset.

4.2.4.1 Global Feature Importance – Permutation Importance

Weight	Feature
0.2346 ± 0.0449	RealPerm 0.1 Hz
0.2308 ± 0.1287	ImImpe 0.1 Hz
0.0923 ± 0.0449	TanCond 1.99989 Hz
0.0115 ± 0.0462	ImPerm 0.1 Hz
0.0077 ± 0.0188	TanCond 0.520588 Hz
0.0077 ± 0.0188	ImPerm 0.520588 Hz
0 ± 0.0000	TanCond 1.4285 Hz
0 ± 0.0000	TanCond 0.728824 Hz
0 ± 0.0000	TanCond 0.371849 Hz
0 ± 0.0000	TanCond 0.189719 Hz
0 ± 0.0000	TanCond 0.135513 Hz
-0.0038 ± 0.0154	TanCond 0.265606 Hz
-0.0038 ± 0.0154	TanCond 0.1 Hz
-0.0154 ± 0.0288	ImPerm 0.371849 Hz
-0.0269 ± 0.0392	TanCond 29.5142 Hz
-0.0423 ± 0.0377	TanCond 1.02035 Hz

a) Logistic Regression

Weight	Feature
0.1731 ± 0.1192	ImImpe 0.1 Hz
0.1577 ± 0.0615	RealPerm 0.1 Hz
0.0115 ± 0.0392	ImPerm 0.1 Hz
-0.0038 ± 0.0288	TanCond 0.135513 Hz
-0.0077 ± 0.0188	TanCond 0.371849 Hz
-0.0115 ± 0.0188	TanCond 0.728824 Hz
-0.0115 ± 0.0188	ImPerm 0.520588 Hz
-0.0115 ± 0.0392	TanCond 29.5142 Hz
-0.0154 ± 0.0288	TanCond 1.4285 Hz
-0.0154 ± 0.0288	TanCond 0.1 Hz
-0.0154 ± 0.0154	ImPerm 0.371849 Hz
-0.0192 ± 0.0243	TanCond 0.520588 Hz
-0.0192 ± 0.0000	TanCond 0.265606 Hz
-0.0192 ± 0.0243	TanCond 0.189719 Hz
-0.0231 ± 0.0565	TanCond 1.02035 Hz
-0.0231 ± 0.0288	TanCond 1.99989 Hz

b) Random Forest Classifier

Weight	Feature
0.3192 ± 0.1323	ImImpe 0.1 Hz
0.3077 ± 0.0973	RealPerm 0.1 Hz
0.1423 ± 0.0392	TanCond 29.5142 Hz
0.1038 ± 0.0897	ImPerm 0.1 Hz
0.0346 ± 0.0154	TanCond 0.1 Hz
0.0192 ± 0.0000	TanCond 0.135513 Hz
0.0115 ± 0.0188	TanCond 0.371849 Hz
0.0115 ± 0.0188	ImPerm 0.371849 Hz
0.0077 ± 0.0308	ImPerm 0.520588 Hz
0.0038 ± 0.0154	TanCond 1.99989 Hz
0.0038 ± 0.0154	TanCond 1.4285 Hz
0.0038 ± 0.0154	TanCond 1.02035 Hz
0 ± 0.0000	TanCond 0.728824 Hz
0 ± 0.0000	TanCond 0.520588 Hz
0 ± 0.0000	TanCond 0.265606 Hz
0 ± 0.0000	TanCond 0.189719 Hz

c) XGBoost Classifier

Weight	Feature
0.5308 ± 0.0392	RealPerm 0.1 Hz
0.4885 ± 0.1472	ImImpe 0.1 Hz
0.0692 ± 0.0462	TanCond 1.99989 Hz
0.0385 ± 0.0000	ImPerm 0.1 Hz
0.0154 ± 0.0377	TanCond 1.02035 Hz
0 ± 0.0000	TanCond 29.5142 Hz
0 ± 0.0000	TanCond 0.728824 Hz
0 ± 0.0000	TanCond 0.371849 Hz
0 ± 0.0000	TanCond 0.265606 Hz
0 ± 0.0000	TanCond 0.189719 Hz
0 ± 0.0000	TanCond 0.135513 Hz
0 ± 0.0000	ImPerm 0.371849 Hz
-0.0077 ± 0.0188	TanCond 0.520588 Hz
-0.0077 ± 0.0188	ImPerm 0.520588 Hz
-0.0154 ± 0.0154	TanCond 1.4285 Hz
-0.0462 ± 0.0308	TanCond 0.1 Hz

d) Artificial Neural Network

Permutation Importance

Figure 4.11: Permutation Importance’s of the predictions.

These permutation importance’s are obtained using the Eli5 package in Python. We can see that the Real Permittivity and Imaginary Permittivity at 0.1 Hz are the most highly contributing features to the prediction of the output. The next highest contributing feature is the Conductivity Ratio at 2 Hz and 30 Hz.

4.2.4.2 LIME

The local predictions are obtained for two observations from the test dataset, and their predictions are explained using LIME. Figure 4.12 shows the LIME prediction for a sample from the test dataset, whose actual prediction is for Backing Paper. Figure 4.13 shows the LIME prediction for a sample, whose actual prediction belongs to the class “No Defect”

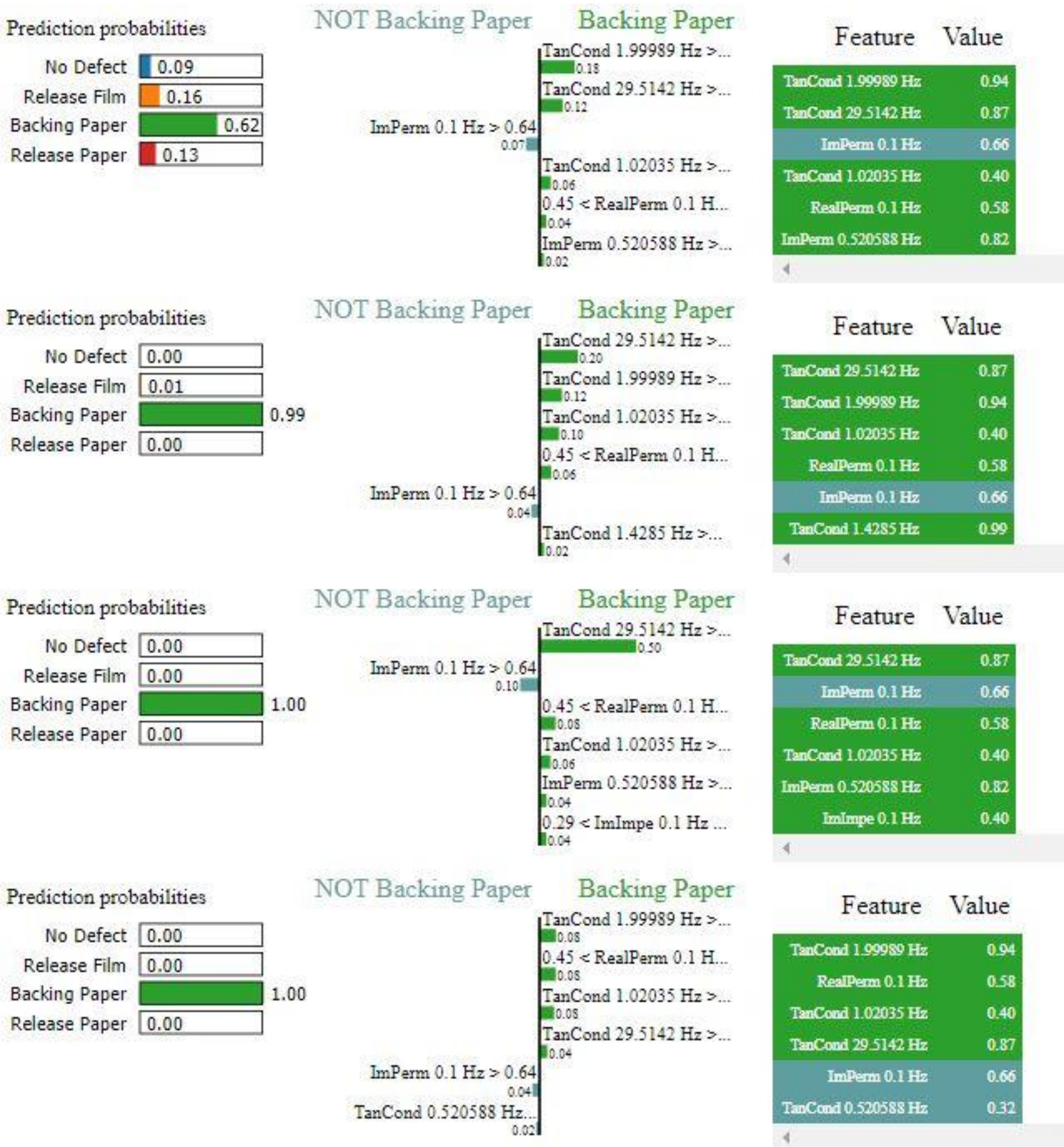

Figure 4.12: LIME Predictions for Observation 1.

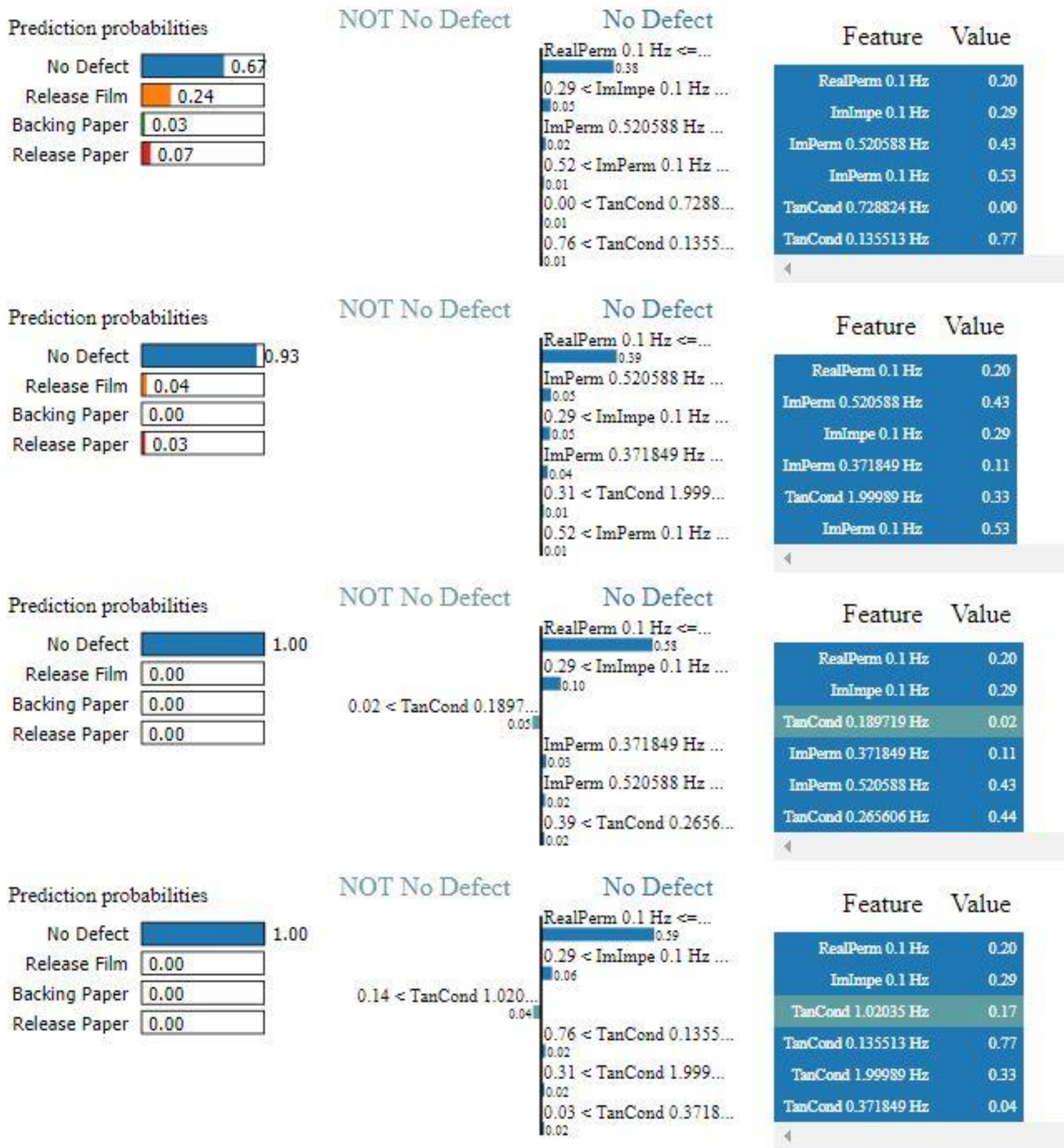

Figure 4.13: LIME Prediction for observation 2.

It can be noted that, for observation 1, where the actual class is Backing Paper, the conductivity ratio at 2 Hz and 30 Hz are the most contributing features, whereas for observation 2, where the actual class is “No Defect”, the contributing features are the Real Permittivity and Imaginary Impedance at 0.1 Hz.

4.2.4.3 SHAP

The SHAP values are obtained and the Summary Plots are plotted for each of the AI models. These plots represent the global behavior of the model based on the test data.

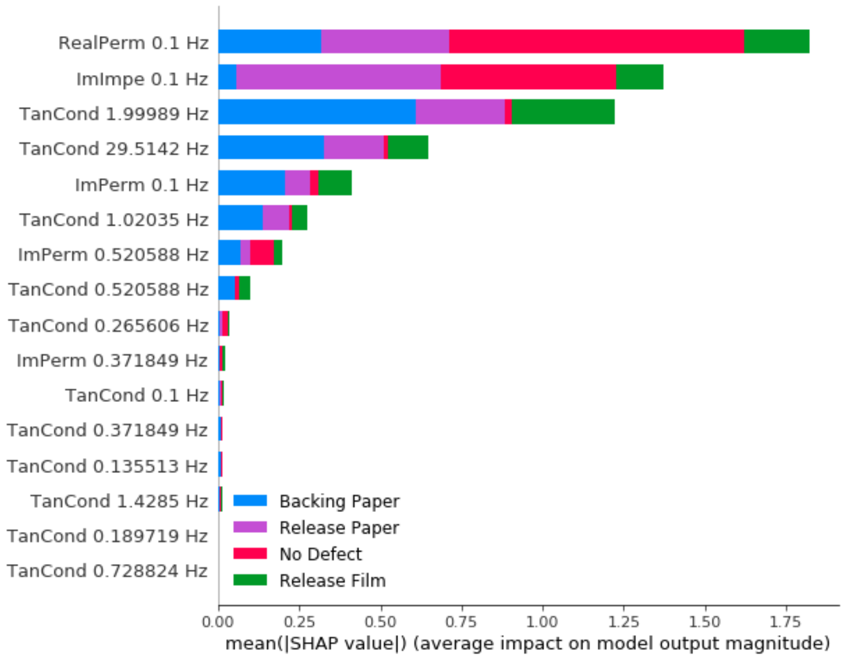

Figure 4.14: SHAP Summary Plot for Logistic Regression

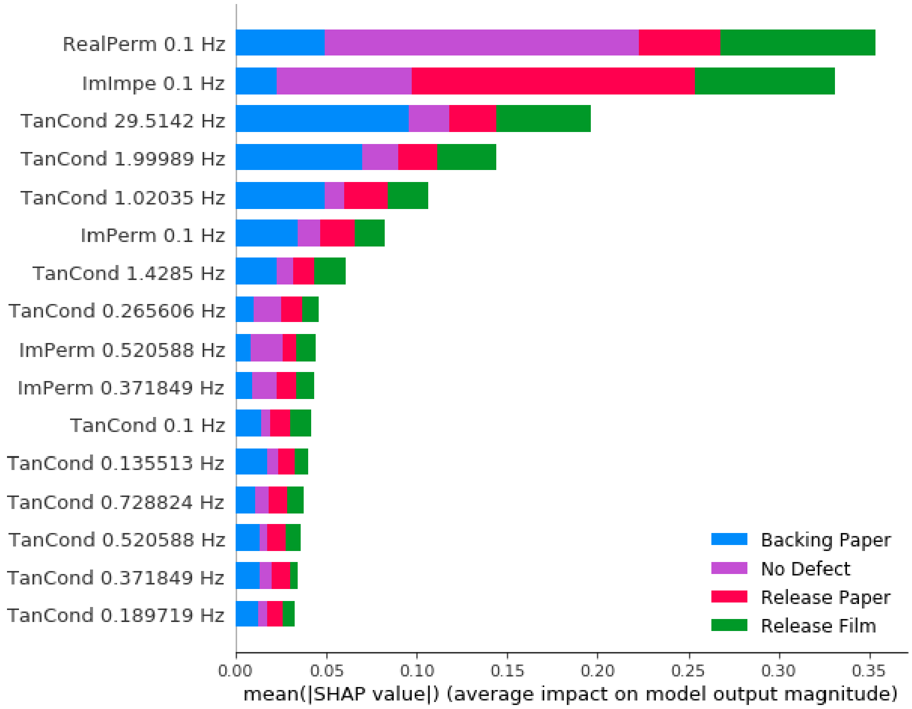

Figure 4.15: SHAP Summary Plot for Random Forest Classifier

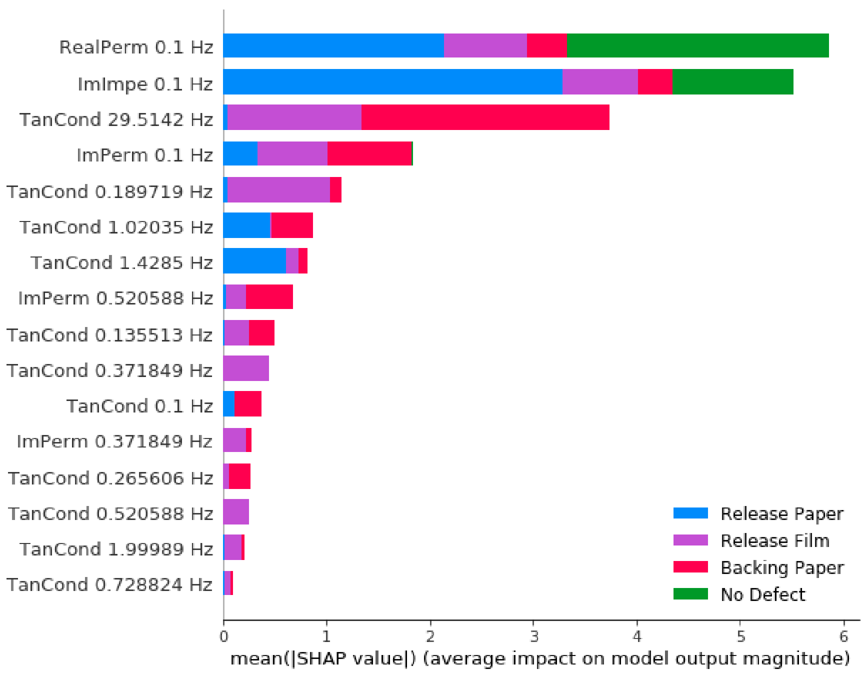

Figure 4.16: SHAP Summary Plot for XGBoost Classifier

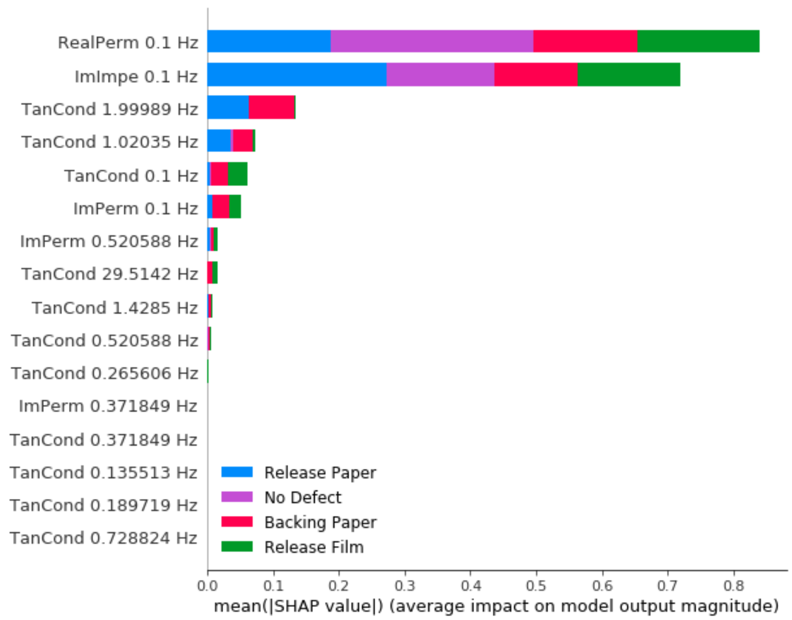

Figure 4.17: SHAP Summary Plot for Artificial Neural Network

As we can notice from above four figures, the Real Permittivity and the Imaginary Impedance at 0.1 Hz are the top contributing factors, with each model having different SHAP Values to identify the prediction classes. The individual –local predictions for observation 1 are shown in figures 18,19,20,21. Comparing to the LIME results, the Conductivity ratio at 2 Hz and 30 Hz, Real and Imaginary permittivity at 0.1 Hz are the most strongly contributing features for the prediction of “Backing Paper”

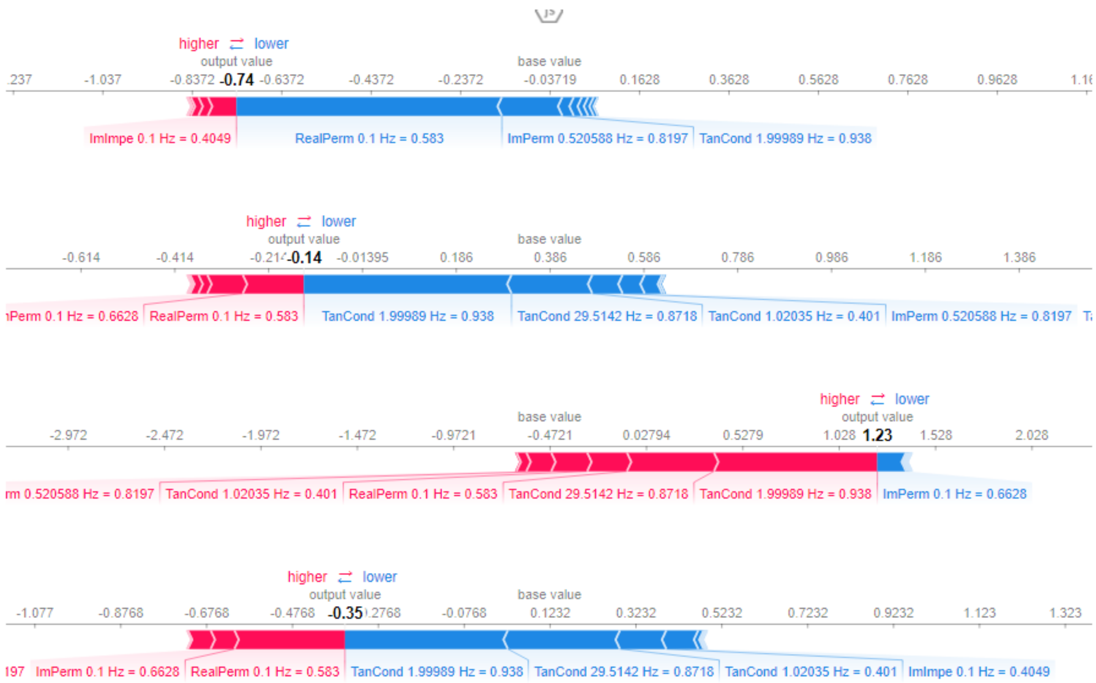

Figure 4.18: SHAP Prediction of Logistic Regression for Class 3 – Backing Paper

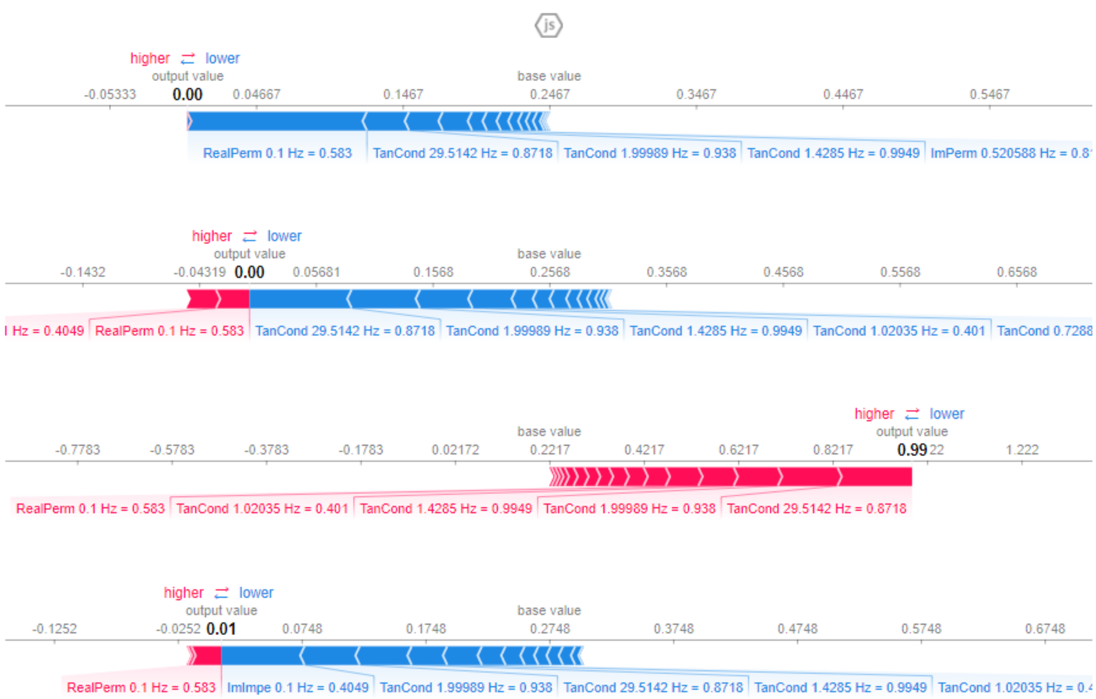

Figure 4.19: SHAP Prediction of Random Forest Classifier for Class 3 – Backing Paper

Figure 4.20: SHAP Prediction of XGBoost Classifier for Class 3 – Backing Paper

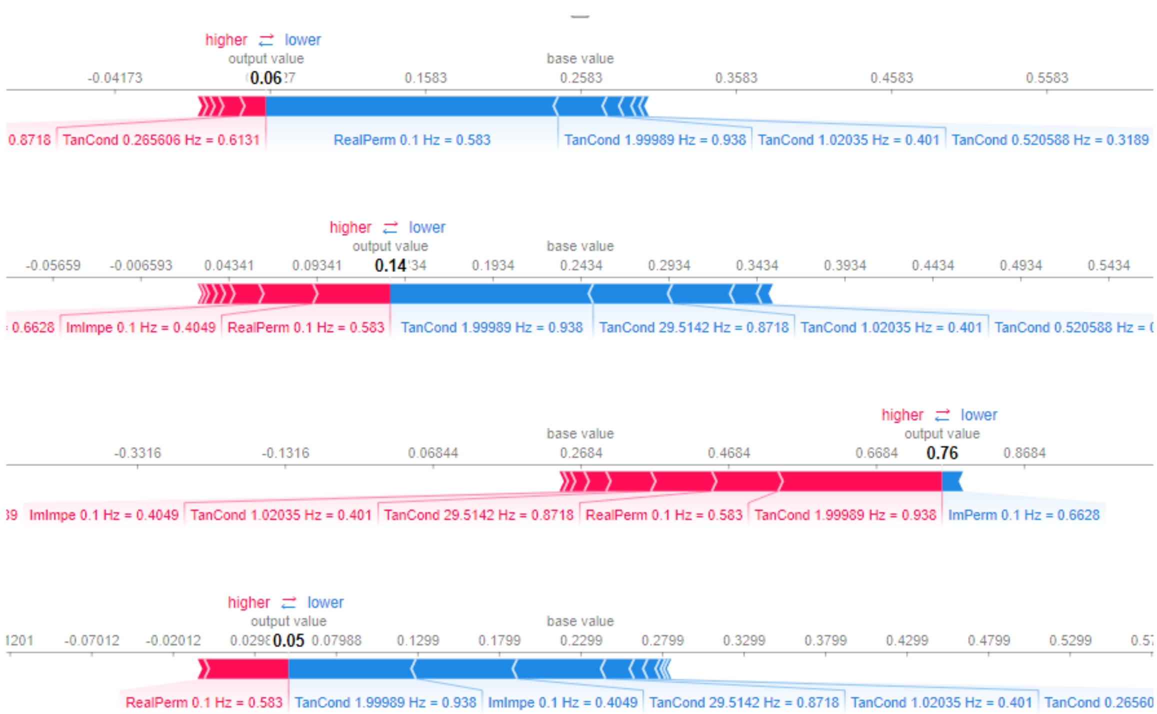

Figure 4.21: SHAP Prediction of ANN for Class 3 – Backing Paper

4.3 Unsupervised Learning Algorithms

Using the same experimental setup and data collected as discussed in the above sections, the frequency sweeps of the real and imaginary parts of permittivity alone were used to develop unsupervised learning algorithms. Hence, 98 features indicating the real and imaginary permittivity are used for dimensionality reduction using Principal Component Analysis (PCA) and K-Means Clustering algorithms. These data clustered, was further used to drive supervised learning algorithms such as Random forest classifier to understand the principal components.

4.3.1 Principal Component Analysis (PCA)

4.3.1.1 PCA with 99% Variance

A PCA model was developed to obtain a 99% variance of the input features and 5 principal components were obtained. These principal components had variances as shown in Figure 4.22, which sums up to be 0.9975

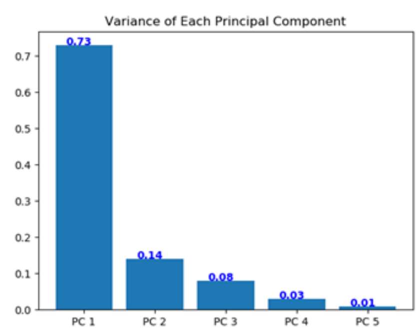

Figure 4.22: Variance of PC's in 5 PC dataset

4.3.1.2 PCA with 2 Di-Electric Principal Components

As the 5 principal components obtained earlier, contain information from the data, but do not represent the data directly i.e as no physical meaning can be obtained, we developed a new approach to obtain Di-electric principal components. The 49 features of the real part of permittivity were given as an input to the PCA algorithm, and a single principal component called the "Real Permittivity Principal Component (RP-PC)" was obtained. Similarly, the 49 features of the imaginary part of the permittivity were used to develop "Imaginary Permittivity Principal Component (IP-PC)". Hence these 2 are the Di-electric Principal Components (PC), which are used in the further model development process. From Figure 4.23, it can be observed that the RP-PC was still able to obtain 98.75% of the variance, and the IP-PC was able to obtain a 74.35% variance of their original feature vectors.

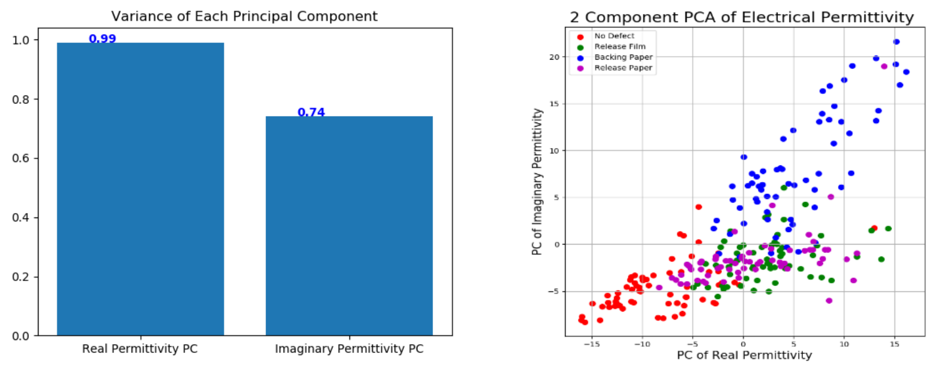

Figure 4.23: Variance of Dielectric PC's and Cluster Plot of Dielectric PC's.

4.3.1.3 PCA with K-Means Clustering

The two datasets, one with 5-PC's and another with 2 PC's were clustered using the K-Means clustering algorithm. The algorithm is designed to find the optimal number of clusters from the inertia data obtained. The inertia is the sum of the squared distances of samples to their closed cluster center. Later, the elbow method plot was created for the number of clusters vs. inertia as shown in Figure 4.24. Surprisingly for both the 5-PC and 2 Dielectric-PC datasets, the same inertia plot was obtained, with difference only in the magnitude of the inertia.

From Figure 4.24, it can be seen that there is not a sharp elbow and it lies between the values of 4-6 number of clusters. From domain knowledge, it is known that 4 different types of laminate defects were inspected, we can conclude that 4 is the optimum number of clusters for this dataset. Also, as per the elbow method, the number of clusters can be 6, as the curve begins its linearity when K=6. The actual clusters for the Dielectric 2-PC data, with the clusters obtained by K-Means when K=4 and K=6 are plotted in Figure 4.25.

Hence, by this method of PCA with K-Means clustering, and by cross-validating with the human visual inspection data of the laminates, a labeled database is created. This labeled database can be further used in supervised learning methods for making predictions on the type of foreign object defect present in the composite material, as we discussed in our previous sections.

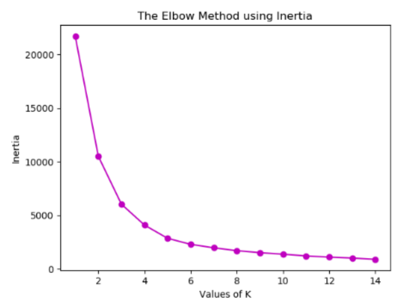

Figure 4.24: Elbow Curve for determining K.

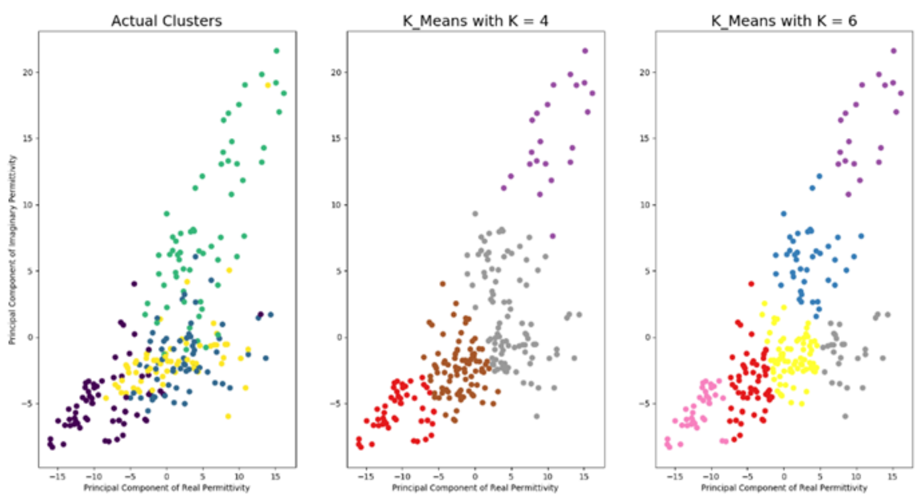

Figure 4.25: Clusters obtained using K-Means clustering algorithm

4.3.1.4 PCA with Supervised Learning

As the supervised learning algorithms are discussed in chapter 3, we have used a few of the popular techniques, such as K-Nearest Neighbors, Decision Trees, Adaboost model, Random forest Classifier and Artificial Neural Network, to use the data from unsupervised learning algorithms. The main difference between the section 4.2 and 4.3 is that the previous section did not have the principal component analysis and unsupervised clustering algorithms applied to them.

Table 4-III: Hyper-parameters for the supervised learning algorithms

	5 PC dataset	**2 Dielectric PC dataset**
K-Nearest Neighbors	n_neighbors: 6	n_neighbors: 9
Decision Tree	max_depth: 6	max_depth: 7
Adaboost	n_estimators :10000	n_estimators :100
Random Forest	n_estimators: 100	n_estimators: 1000
Neural Network	alpha: 1, hidden_layer_sizes: (25, 25), solver: 'lbfgs'	alpha: 1, hidden_layer_sizes: (25), solver: 'lbfgs'

For each of these algorithms, both the datasets were split into training and testing sets, where 80% of the data is used for training and 20% is used for testing. A python function was created to perform the K-Fold cross-validation and grid search for determining the best hyper-parameters for the supervised learning model.

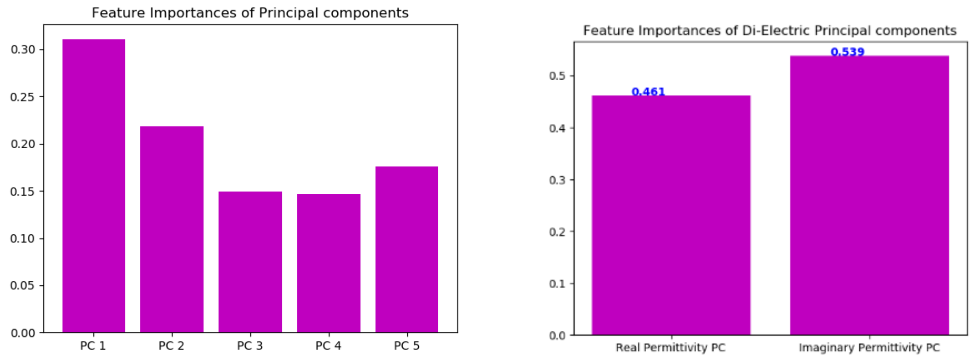

Figure 4.26: Feature Importance's obtained using Random Forest Regression

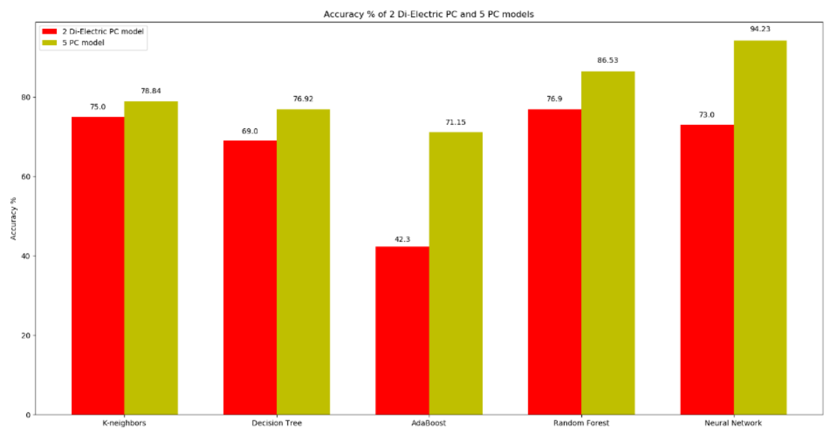

Figure 4.27: Test Accuracy of the Supervised Learning models.

It can be observed from the elbow method of K-Means clustering that the optimal number of clusters K is from 4-6. Although by using our prior knowledge we can select K=4 as there were 4 different composite laminate panels from which the data were collected, it can be observed by comparing the figures that the PC's indicating the release film and release paper are together. This might be due to their indistinguishable dielectric properties from the dataset. Also because the value of K is selected based on the point at which the elbow starts its linearity, and then the value of K will be 6. From Figure 4.25, K = 6, we can see that the clusters are grouped more evenly. This brings another intuition that as the dielectric properties are measured through the thickness of the composite laminate, this thickness, and resin flow, or curing of the laminate are contributing factors to the two additional clusters.

In the hybrid model of using supervised learning, one significant advantage of using ensemble-learning methods such as decision trees, Adaboost, and random forest classifier algorithms, is the capability to obtain feature importances. These are the impurity-based feature importances of the ensemble forests algorithm. Due to the high accuracy of the random forest classifier models, we obtain feature importances for the five PC's and two dielectric PC's dataset as shown in Figure 4.26. It is vital to note that the RP-PC had higher variance than IP-PC as shown in Figure 4.26 but the feature importance of IP-PC is higher than the RP-PC, while the tradeoff is small.

Figure 4.27 illustrates the overall testing accuracy of the five different supervised models developed with the 2 Dielectric PC dataset and 5 PC dataset. The five PC data models have more accuracy and better performance in all the different supervised models being developed than the 2 Dielectric PC dataset. Hence, for visualization, or to obtain a meaningful analysis of their real and imaginary permittivity values, the 2 dielectric PC data can be used. For the real-time classification of defects and further identifying the damages, the five PC model can be used.

4.4 Summary of Results

From this research work, we identified that the BbDS – EIS technique is able to identify the defects caused during manufacturing of composite materials. Moreover, using the AI algorithms, we were able to predict the defects and label them. A combination of the supervised and unsupervised algorithms were used, and the Interpretable Machine Learning was used to explain the predictions of the AI model.

As this work focused on developing machine learning models for classification of the foreign object defects present in the composite laminate, the future work will attempt to create algorithms to identify the different damage types during the service life of composite laminates, and hence to predict the remaining strength and life of the composite structure, topics which are discussed in the subsequent chapters.

Chapter 5

DAMAGE PRECURSOR IDENTIFICATION UNDER STATIC LOADING

In the previous chapters, we have discussed the literature, background and the methodologies used in this dissertation. This chapter explains the experimental process and the results, which are used to conclude that the damage precursors can be identified using the dielectric spectroscopy and the artificial intelligence methods.

5.1 Experimental Methods

5.1.1 Manufacturing

In this work, unidirectional glass fiber reinforced composites (Newport 301 epoxy resin/E-Glass fibers (volume fraction 55%)) were manufactured in house at UTARI using a compression-molding technique. In order to induce matrix dominated failure, off axis lamina were chosen and the laminate layup was $[+45/-45]_s$. Two laminate panels were made wherein the temperature was ramped up at a rate of 3 °F/min from 70 °F to 275 °F, cured at 275 °F for 60 minutes and cooled at a rate of 3 °F/min from 275 °F to 120 °F, as per the manufacturer recommendations. Cured panels were cut into coupons as per ASTM D 3039 recommendations [7]. The final average dimensions of the unidirectional specimens are 203.2 mm (L) * 18.54 mm (W) * 0.86mm (T).

5.1.2 In-Situ Monitoring with Tensile Loading

The coupons were loaded in tension using MTS Landmark™ unit under displacement control. Simultaneously, the dielectric properties are measured by attaching an electrode block to the coupon in the form of a parallel plate capacitor and is connected to the analyzer of the Novocontrol™ unit. The schematic of the setup is shown in Figure 5.1. A rate of 0.3 mm/min was used for testing the specimens and for the dielectric response a sinusoidal AC signal with a potential of 1VRMS at a frequency of 10 Hz was applied. The insitu testing was done in the low frequency regime to capture the redistribution of charges (interfacial polarization) due to local damage mechanisms [4, 8]. Also, edge replication techniques were used to capture the damage patterns developed during loading to correlate the changes in dielectric response to damage growth. Replicas were obtained at every 250 N by holding at that load level for 4 minutes.

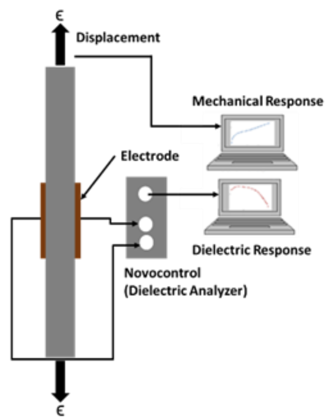

Figure 5.1: Schematic of the In-Situ Setup for Measuring Mechanical and Dielectric Response.

5.2 Experimental Analysis and Results

The stress-strain curves for the coupons are shown in Figure 5.2(a) and Figure 5.2(b). The data just before failure are plotted. The mechanical and dielectric response for one specimen is shown below in Fig. 3 [9]. From Figure 5.3, it is evident that with increasing strain and damage, there is a variation in the dielectric response. To better understand the variations, the dielectric response data are fitted using a fourth order polynomial as shown in Figure 5.3 and the first and second slope of the fitted curves are plotted in Figure 5.4 and Figure 5.5[9]. Since, dielectric response varies with damage, the first slope represents the damage growth and second slope indicates the rate of damage. The edge replication images for a coupon are shown below in Figure 5.6 and a fractured specimen is shown in Figure 5.8 [9].

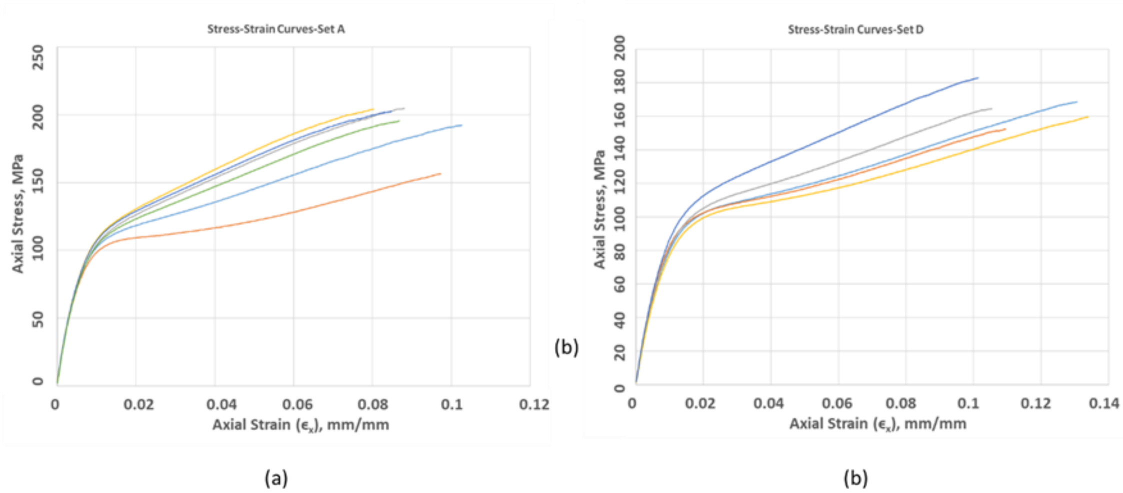

Figure 5.2: (a) Stress-Strain curves for Set A, (b) Stress-Strain curves for Set D

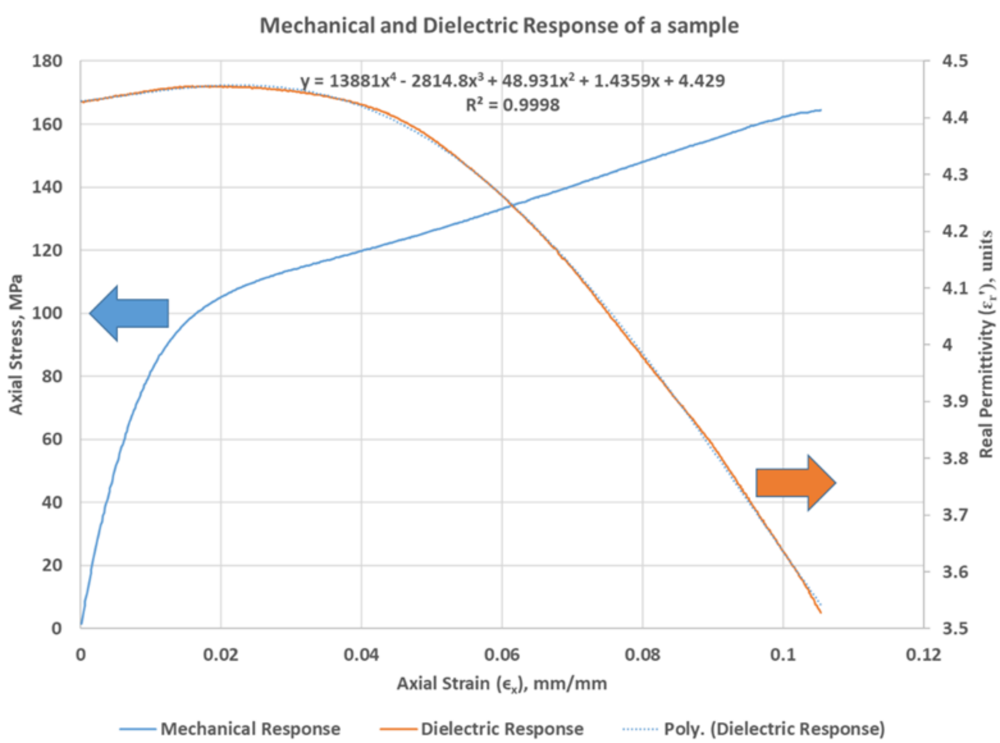

Figure 5.3: Mechanical and Dielectric Response of a Composite Sample

From Figure 5.4, the strain at which the first slope changes from positive to negative or the strain at which the real permittivity ε'_r saturates was determined to be the Characteristic Damage State (CDS) of the material system. Characteristic Damage State (CDS) is a material state where the primary cracks saturate and the secondary cracks initiate in the neighboring plies followed by coupling of those cracks [9]. This can be observed in edge replication images (1750 N) in Figure 5.6[9]. With increasing strain, these secondary cracks initiate at multiple sites leading to interaction of these cracks creating interlaminar cracks or local delamination that are thin strip like lines shown in Figure 5.7. During this stage, the 'rate' of these interactions increases at such pace, that the local failures aided by fiber fractures lead to global failure of the material [9]. From Figure 5.5, it can be observed that at a certain stage the second slope or 'rate' of damage changes shape indicating an accelerating growth of damage events. Also, from Figure 5.5, it is evident that the strain at which the rate of damage accelerates is in the zone where there is an inflection in the stress strain curve.

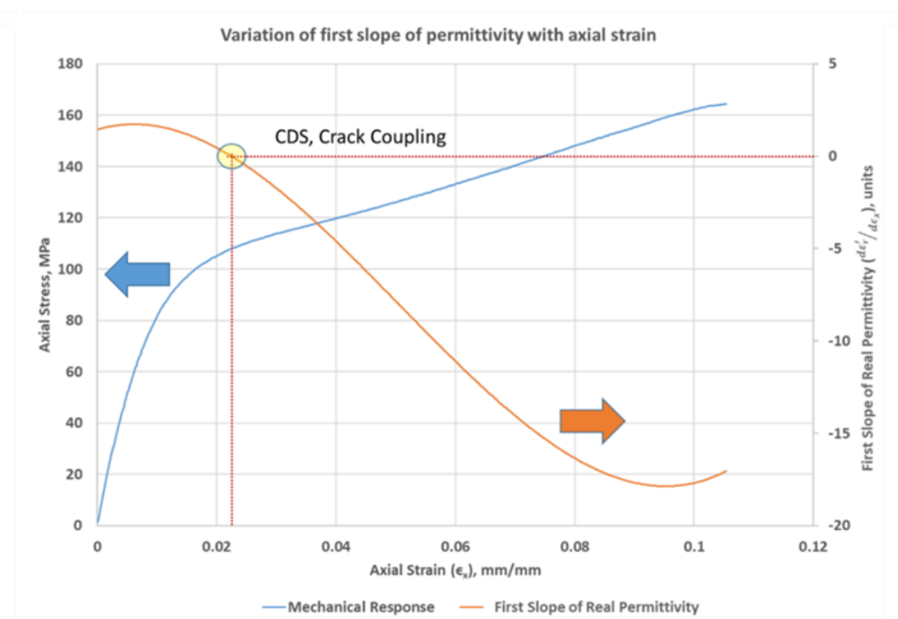

Figure 5.4: Variation of 1st slope of Permittivity with Axial Strain [9]

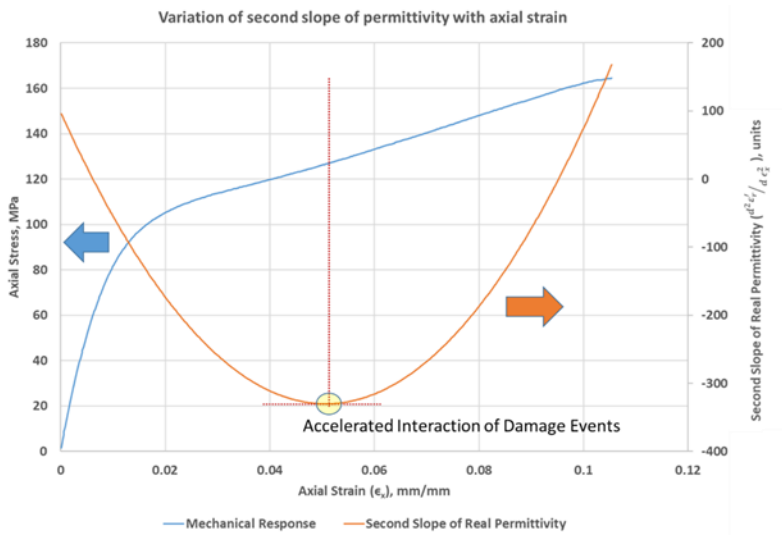

Figure 5.5: Variation of 2nd slope of Permittivity with Axial strain [9]

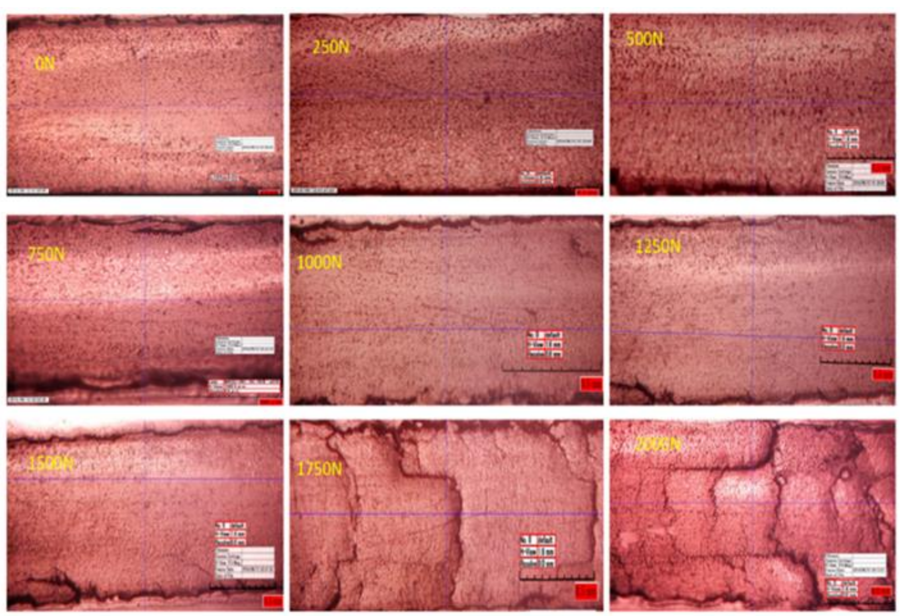

Figure 5.6: Edge replication images of the composite specimen at various load levels [9]

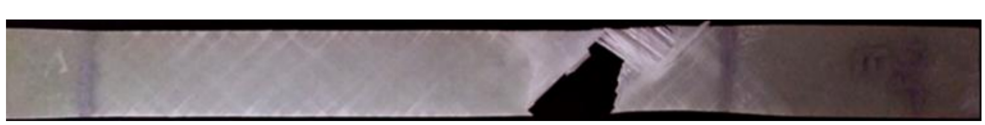

Figure 5.7: Fractured Specimen depicting distributed damage [9]

5.3 Damage Precursor Identification using Artificial Intelligence

In this section, we describe the method to use the dielectric compliance measurements in the artificial intelligence algorithm that can then predict the state of the material, and the initiation of failure based on the experimental observables. A pictorial representation of this research work is shown in Figure 5.8.

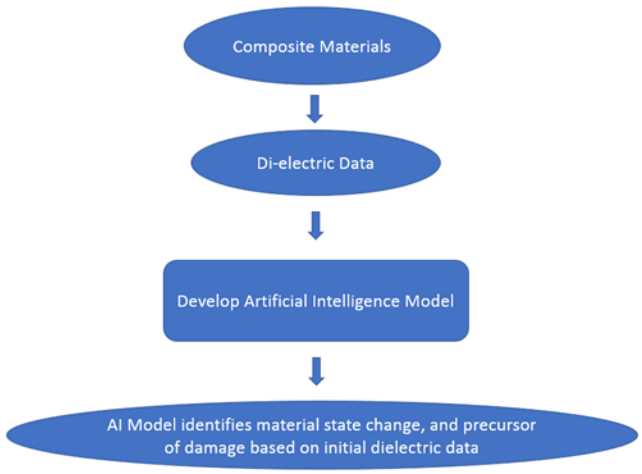

Figure 5.8: Flowchart of the Damage Precursor Identification

5.3.1 Data Pre-Processing

5.3.1.1 Data Visualization

The first stage of developing a machine learning and neural network model was to understand the data. Visualizing the data, gives a clear overview of what is being expected from the model, and helps to develop the model correctly. The input data set and output data set over time are plotted in Figure 5.9(a) and (b) for several samples

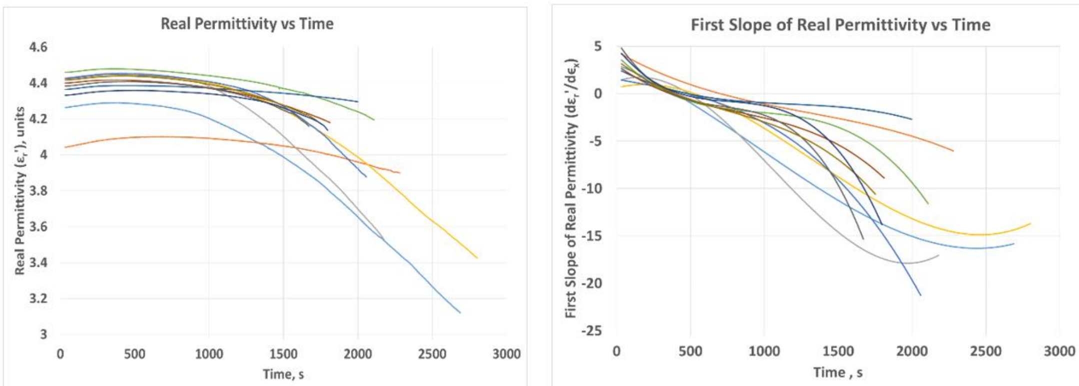

(a) (b)

Figure 5.9: (a) Input data of Real Permittivity and (b) Output data of 1st slope

5.3.1.2 Padding of data

Since the data were obtained from the experimental testing of composite materials, the length of the data was not uniform for all the samples. As the data must be of uniform length, all the input and output data was padded with zeros, to make the length of the data set to be a vector of size (1, 1000) for each sample for both input and output.

The data is then normalized and further split into the train and test sets for the development of the AI model.

5.3.2 Model Parameters

In this experiment, three different AI models – Artificial Neural Network, Random Forest Regressor and Recurrent Neural Network Models were developed. All the model parameters were obtained by following the hyper-parameter analysis as mentioned in the procedures of chapter 3.

5.3.2.1 Multi-Layer Perceptron (MLP) Model

For our given dataset, we developed a 3-Layer MLP model, as shown in Fig 10. As per the dataset, the input and output layers had 1000 values. Both the hidden layers had 1500 neurons in each. Adam optimization algorithm and the ReLU activation function was used. The learning rate was 0.001 and the L2- regularization parameter was chosen to be 0.0003. This parameter was obtained by plotting the training vs. cross validation curve on various L2-regularzation parameter values.

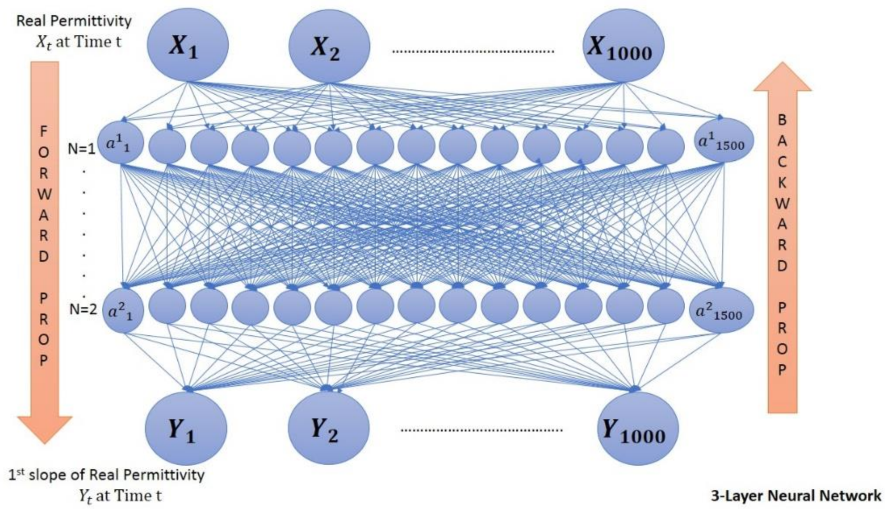

Figure 5.10: Multi-Layer Perceptron Model

5.3.2.2 Random Forest Regressor

With our previous experiments on using random forest regression models to learn about the behavior of the model from the feature importance's [11], a random forest regression model was developed. It was a part of the error analysis process. Our model was developed by setting the number of estimators to be 3000, which is thrice the size of our input features. All other parameters were set as default by the scikit-learn [12] python package. The results obtained from these models, played a vital role in the development of our next model.

5.3.2.3 Recurrent Neural Network Model

Masking Layer

From the results obtained from the previous model, it was realized that padding with zeros had an effect on the models' performance and hence affected the R2-score of the predictions. RNN or LSTM does not have the requirements for the data to be of the same input length. Also, by masking these networks with a masking layer, and by setting the mask value parameter to be zero, the LSTM model skips the particular mask value. Hence the weights are not affected.

3D Input Shape

For LSTM, the input needs to be in a 3D shape. Hence the 2D input of (m, 1000) was reshaped into the form of (m, 1000, 1) where the 1000 represents the time steps. Now as per the input data, for every sample m, there are 1000 time steps and each time step has a single feature. In certain other examples, it can have multiple features for a single time step, such as considering the real permittivity, imaginary permittivity, material properties or stress and strain value for a sample.

Model Development Parameters

The LSTM model was developed using keras[17] package sequential model as shown in Figure 5.11 . First the input was converted from 2D to 3D, then the masking layer was set on the sequential model, which is an embedding layer. The LSTM layer had 1000 units, and the return sequences parameter was set to be false, hence we predict the output as a many- to- one- problem. This is more beneficial in the real time implementation of the model, because the entire input set of values was used to make the prediction at every time step. The model was ran for 2500 epochs, to ensure the convergence of the training loss and testing loss. 4,008,000 parameters were trained.

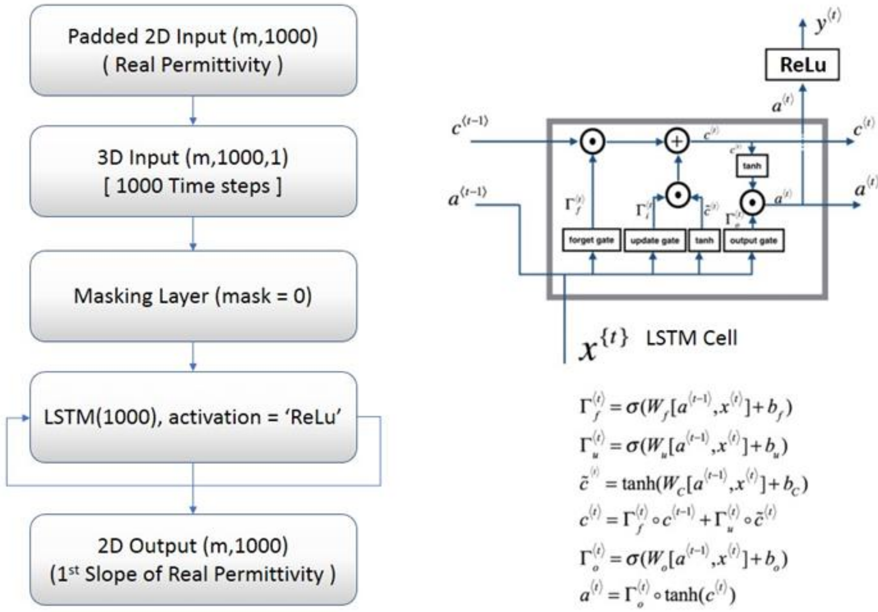

Figure 5.11: RNN model for predicting the Characteristic Damage State

5.3.3 Results from AI models

5.3.3.1 MLP model results

From the MLP model developed, it was observed that the model was over-fitting. It had an excellent R2-score on the training data, but a very moderate R2-score on the test data. Also, from the results obtained, it was observed that the model predicted outputs even when the input data was zero as observed in Figure 5.12(a), which means that the zero padding was inversely affecting the model. Also the R^2-score on the test data was moderate, because it could very well learn the initial set of data, up to the first 250 features, by which this model still predicts the 1st slope of permittivity to classify if the specimen has achieved the Characteristic Damage State as shown in Figure 5.12(b). Because when the predicted 1st slope of permittivity reaches zero, and changes from positive to negative, we believe that the material state changes from damage initiation stage to damage accumulation and growth stage.

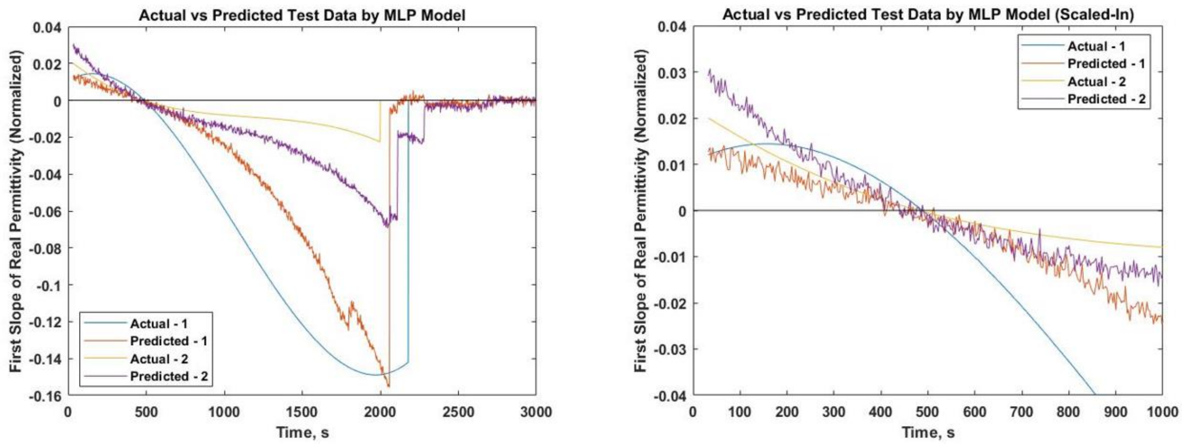

(a) (b)

Figure 5.12: (a) Actual test data vs. predicted data by Multi-Layer Perceptron model (b) Scaled-in version of (a)

5.3.3.2 Random Forest Regressor Results

The Random forest regression model that was developed, did not outperform the MLP model. It had a lesser R^2-score on both the training and testing compared to the MLP model. Although the R^2-score was quite a bet less, the model had the same behavior of predicting the output values for the padded region of input data as well. While examining the features importance's, this behavior was verified that the weights were higher in the regions where there was a change in the length of the data. This is depicted in Figure 5.13(a), from which it can be observed that the weights are high at approximately the 150th feature instance, which is the average instance where the characteristic damage state occurs as seen in Figure 5.13(b). It is also high approximately at instances 550, 775 and 890 which are the regions were the input data has no value, and zero padding begins as observed from Figure 5.13(b). Once this issue was realized, it was planned to develop the RNN model instead of improving this model to overcome the effect of zero padding and sequential nature of the data.

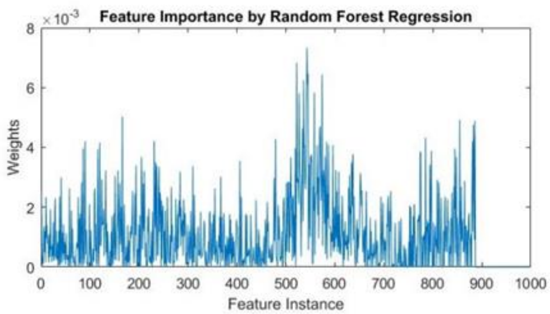

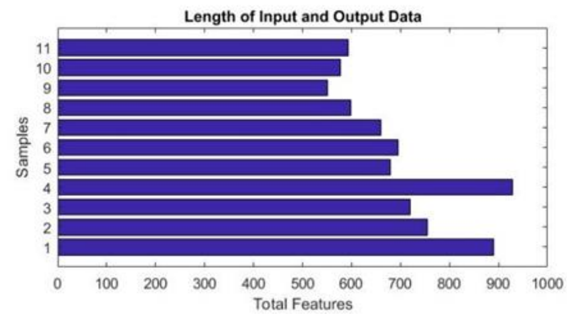

(a) (b)

Figure 5.13 (a) Feature Importance's (b) Size of Input and Output Data

5.3.3.3 Recurrent Neural Network model results

The LSTM model had tremendous performance on our dataset. The training R^2-score was much similar to that of the MLP model, and the testing R^2-score was significantly improved. Although a highest testing R^2-score was not obtained, the LSTM model developed does not have bias and variance issues. The training loss and the test loss gradually began decreasing after the first few iterations, when our model started learning, as shown in Figure 5.14. After 1500 iterations, both the losses converged, and the difference between the losses were of the order of 10^{-5}.

Also from Figure 5.15, it can be observed that the predicted values match closely with the actual test data values. It can also be observed that there is no zero padding effect due to the masking layer in the LSTM model being developed.

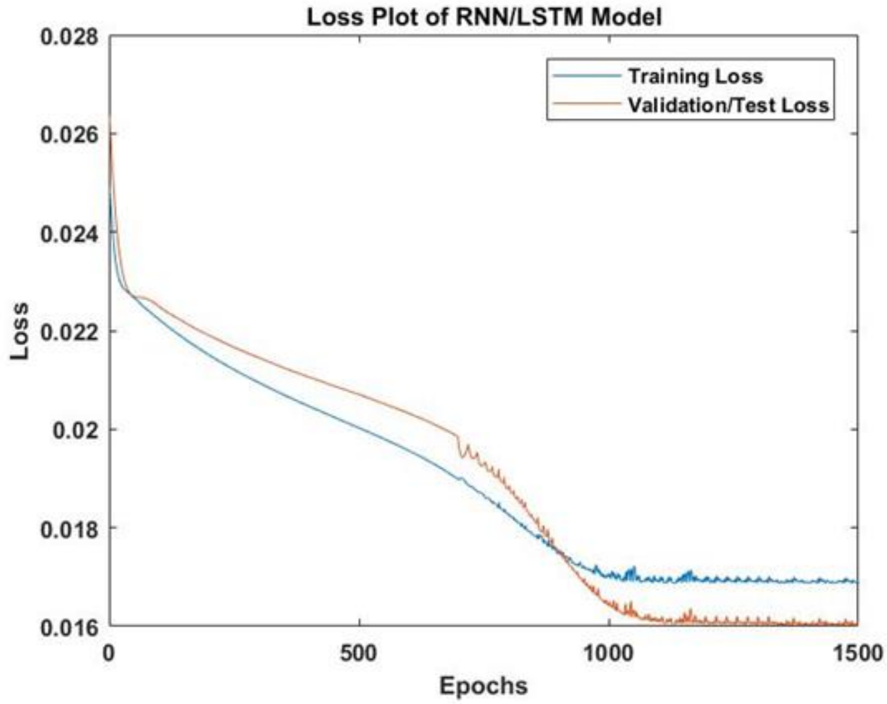

Figure 5.14: Loss Plot of the LSTM model

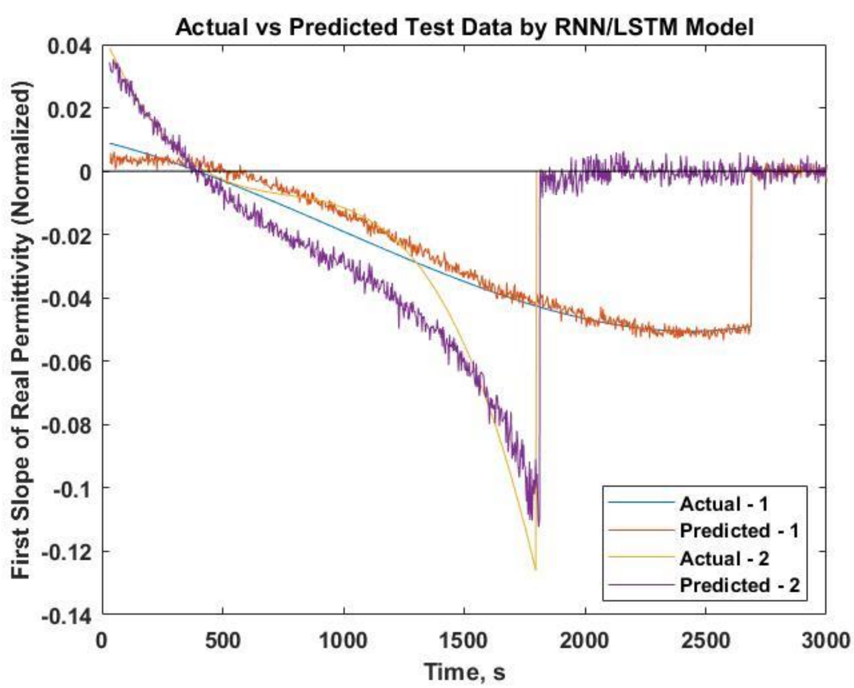

Figure 5.15: Test Data vs. Predicted Data by LSTM model

5.3.3.4 R^2 – Score of Data Driven Models

As defined earlier, the model's accuracy is the R^2-score value. Table 5-I represents the R^2 score of the three different models developed.

Table 5-I. R^2-Score of Data Driven Models

Model	Training Score	Testing Score
Multi-Layer Perceptron (MLP)	0.9831	0.7322
Random Forest Regression	0.9168	0.6840
Long Short Term Memory Network (LSTM)	0.9528	0.8713

5.4 Summary of the Work

An in-situ testing technique was used to measure the variation in dielectric response as a function of damage growth in 4 ply unidirectional off axis glass fiber reinforced polymer composites. An increase in normalized real permittivity was observed during the micro cracking stage followed by saturation that correlated with the Characteristic Damage State (CDS) of the material system. These were validated using edge replication images and it was observed that when the value of 1st slope of normalized real permittivity was 0, the material state was CDS. Also from the 2nd slope of normalized real permittivity it was observed that the point at which there was a curvature change, there was an inflection point observed in the stress strain response indicating acceleration of damage events.

Three different supervised learning algorithms were developed to predict the 1st slope of real permittivity, for the given real permittivity input values over time. By these predictions, the CDS of the material system could be identified from the dielectric data. The Multi-Layer Perceptron and Random Forest Regression model developed reflected in the over fitting of the model. It also lacked success due to the zero padding done on the input data. However these models can be used to classify data between the damage initiation and damage growth stages. The Long-Short Term Memory network model developed as a part of the Recurrent Neural Network, demonstrated better performance on both training and test data and can be used for predicting the CDS of the material system.

Chapter 6

RESIDUAL STRENGTH AND LIFE PREDICTION IN COMPOSITES

In the previous chapters, we discussed the use of the dielectric parameters for assessing the defects in composites, and to predict the characteristic damage state under the quasi-static loading condition. This chapter is focused on Tension-Tension Fatigue experiments, with In-situ monitoring using the dielectric and fiber optic sensors. The Stiffness Degradation, Residual Strength and Residual Life are important parameters of interest in this chapter.

6.1 Manufacturing of Composite specimens

In this study, GFRP composite laminate was manufactured using the Rockwest unidirectional E-glass prepreg. An 8-ply quasi-isotropic laminate with stacking sequence $[-45°/0°/-45°/90°]_s$ was manufactured using the out-of-autoclave (OOA) process in a Despatch composite curing oven. The manufacturer recommended cure cycle[158] was followed and the laminate was cured at 135° C. These laminates were cut using a Protomax water jet cutter to prepare the specimens in the dimensions of 254 mm × 38.1 mm as per the ASTM D3479 standard [159], where the width was determined as needed for the experiments. The samples had an average thickness of 1.9 mm. Seven different panels were manufactured and used for testing and analysis, hence this creates a large variation in the dataset.

6.2 Determination of the Ultimate Tensile Strength under Static Loading

Initially, 21 specimen (3 from each panel) were subjected to quasi-static loading, to determine the ultimate tensile strength of the composite specimens as per ASTM D3039. These tests were performed in the displacement control mode, at a rate of 0.03 mm/s. Once the breaking load for the samples was obtained, average ultimate tensile strength was calculated and a Weibull analysis was carried out, and the 95% confidence levels were obtained as shown in Table 6-I.

Table 6-I: Results of Quasi-static Tensile Tests

Mean Ultimate Tensile Strength (MPa)	Scale Parameter (Mpa)	Shape Parameter	95 % Confidence Limit – Lower (Mpa)	95% Confidence Limit – Upper (Mpa)
314.12	323.54	16.37	314.71	332.62

6.3 Determination of the Number of cycles to Failure under Cyclic Loading

6.3.1 Experimental Design

Based on the Average Strength and Average Area (73.25 mm^2) from our initial static tests, the Average breaking load was obtained to be 23 KN, and hence the fatigue test experiments were designed as shown in Table 6-II. The fatigue tests were performed at a constant amplitude of 20% stress loads. Three different mean stress conditions are used.

Table 6-II: Fatigue Test Parameters

Mean Stress %	Mean Stress (MPa)	Max Stress (MPa)	Min Stress (MPa)	R ratio
75 %	235.58	298.41	172.76	0.578
50 %	157.06	219.88	94.23	0.428
25 %	78.53	141.35	15.70	0.111

6.3.2 Fatigue Test Results and Weibull Analysis

As per the parameters in Table 6-II, run-to-failure fatigue tests were carried out and the number of cycles to failure were obtained for three different mean stress conditions. The results are shown in Table 6-III

Table 6-III: Initial Fatigue Test Results

Mean Stress % Condition	Shape Parameter	Mean Cycles to Failure – Scale Parameter	95 % Confidence Limit – Lower	95% Confidence Limit – Upper
75 %	1.7392	764.70	**500.51**	1168.34
50 %	2.6236	60504.49	**49756.22**	73574.57
25 %	4.2211	456882.75	**390979.68**	533894.37

6.4 State Variable Change with Damage Development

For the fatigue data of the composite specimens tested, the evolution of state variables (stiffness and permittivity) were obtained. In this work, secant stiffness is used as the mechanical state variable. These curves were normalized with respect to initial values, so a normalized value of 1 indicates initial stiffness and initial permittivity. The life was also normalized with respect to the number of cycles to failure, so a normalized value of 1 indicates the failure of the specimen. A fifth order polynomial was then used to fit these curves, and from these curves, the first and second derivative of the state variables were calculated. The fifth order polynomial was selected, rather than the other orders because it was able to provide a better fit in terms of R^2 value and the correlation of mechanical and dielectric response was clear. In general, the first derivative represents the instantaneous rate of change, and second derivate represents the acceleration. These curves represent significant behavior, which helps us identify the damage precursors and beginning of the end of life of the composite material. Primarily, the instantaneous rate of change is triggered by damage development, and acceleration of response is dependent on acceleration of damage development and can be an indicator of impending failure. For each of the composite specimens, the coefficients of polynomial equation for the state variables were obtained and average coefficients were calculated to generate a representative curve for the entire dataset. The slopes of this representative curve are then used to understand the evolution of these state variables with damage development.

6.5 Residual Strength Determination

6.5.1 Experimental Design

Based on the results from Table 6-III, the experiments were designed in such a way that, for each of the mean stress levels, to apply fatigue loading for a number of cycles determined as the 95% lower confidence limit of that particular stress level, and then unload it to the zero load level and perform a quasi-static test to determine the residual strength of that particular specimen. These tests are carried out with both the dielectric sensor and FOS placed in them as shown in Figure 6.1. In this experiment, the dielectric sensors are used with the polycarbonate blocks as shown in Figure 6.2. The Installation of fiber optic sensors are shown in that figure.. The sensor data collected during tests were correlated with the residual strength obtained.

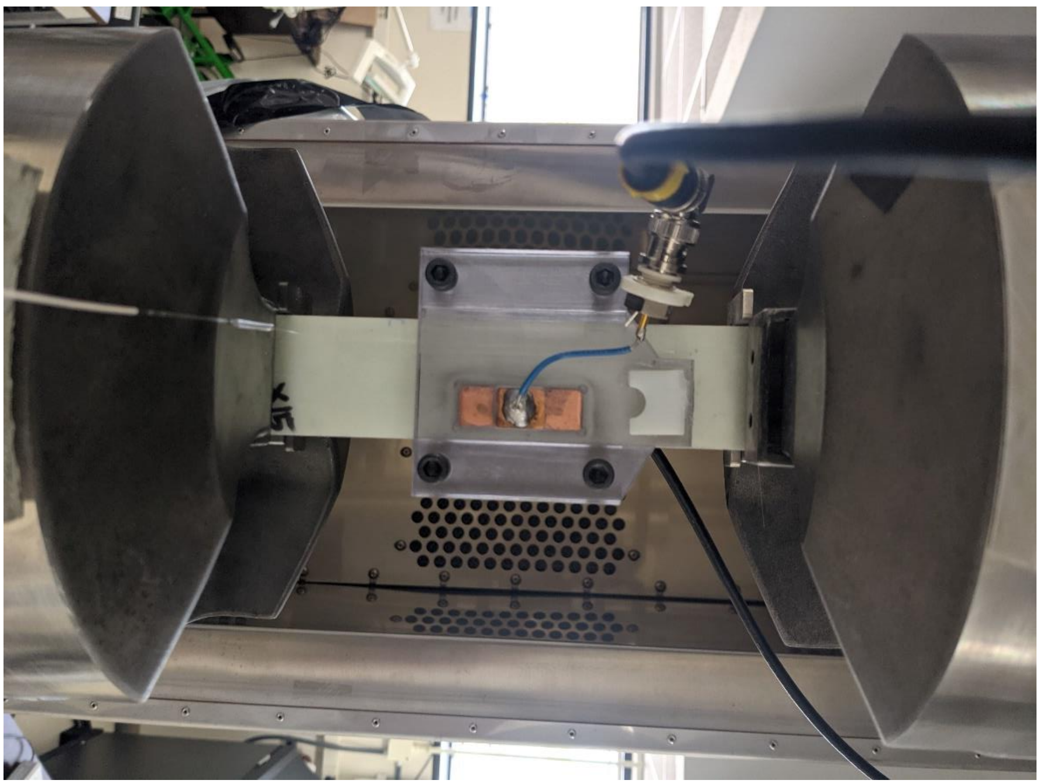

Figure 6.1: Composite Specimen under Fatigue with Dielectric and FOS Sensor

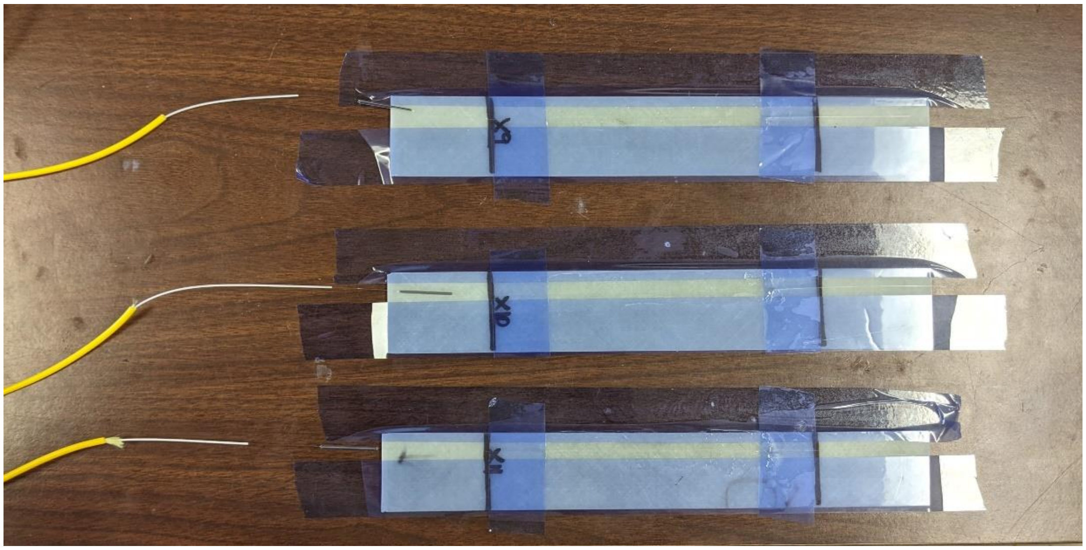

Figure 6.2: Installation of FOS Sensors on the Composite Specimen

The Figure 6.3 shows the Input Mechanical Response over time, Figure 6.4 shows strain response over time, and Figure 6.6 the Output Stress-Strain response for a Sample which is fatigued at 75% Mean stress level. The Dielectric Response for the entire Residual Strength test is shown in Figure 6.7

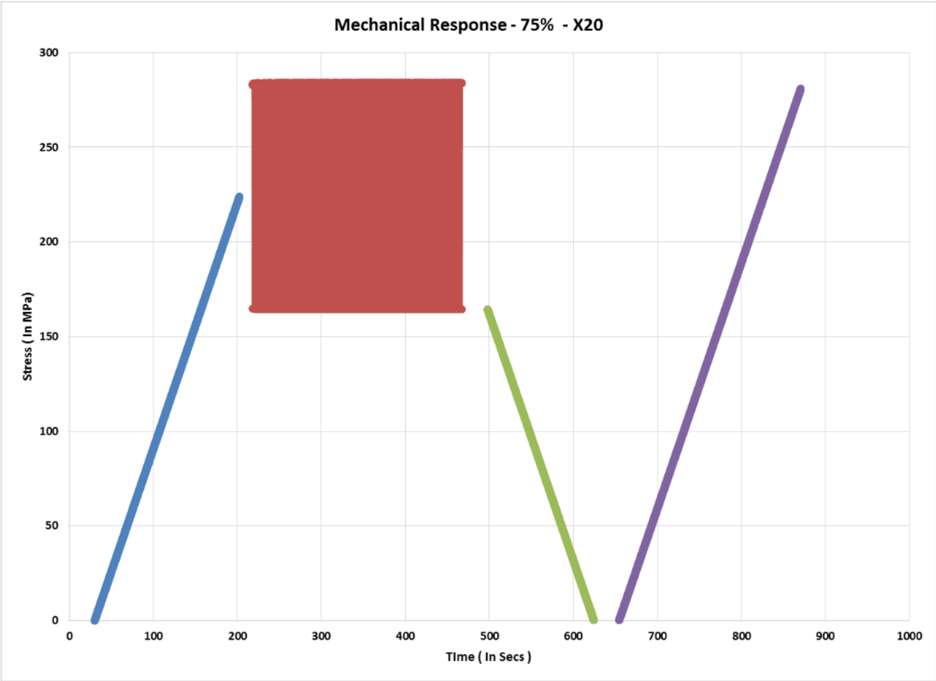

Figure 6.3: Input Stress over time during Fatigue

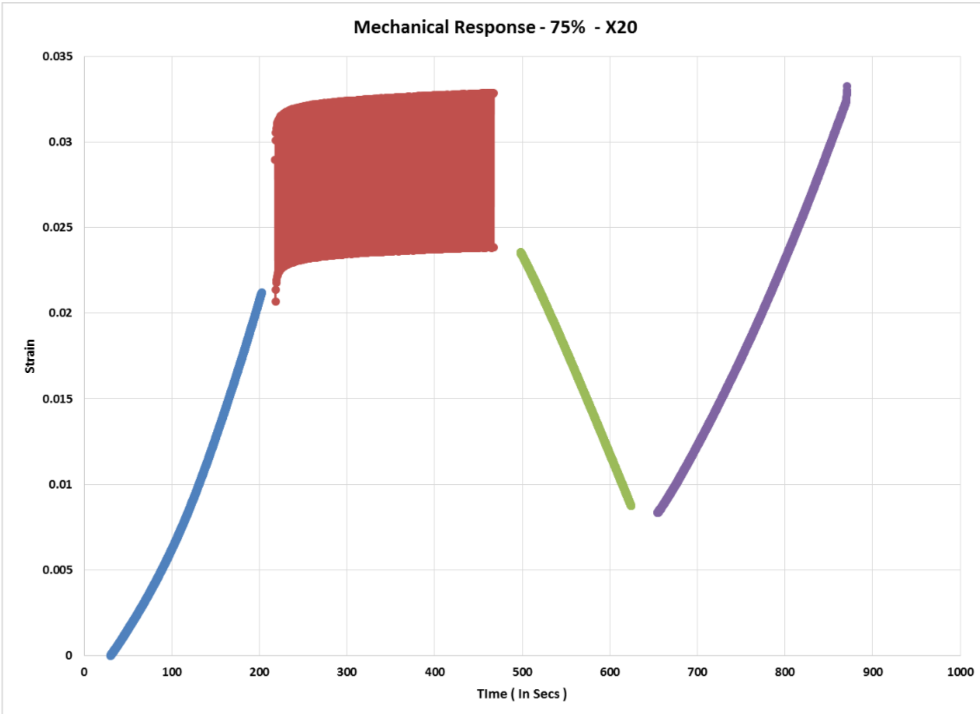

Figure 6.4: Strain response over time during Fatigue

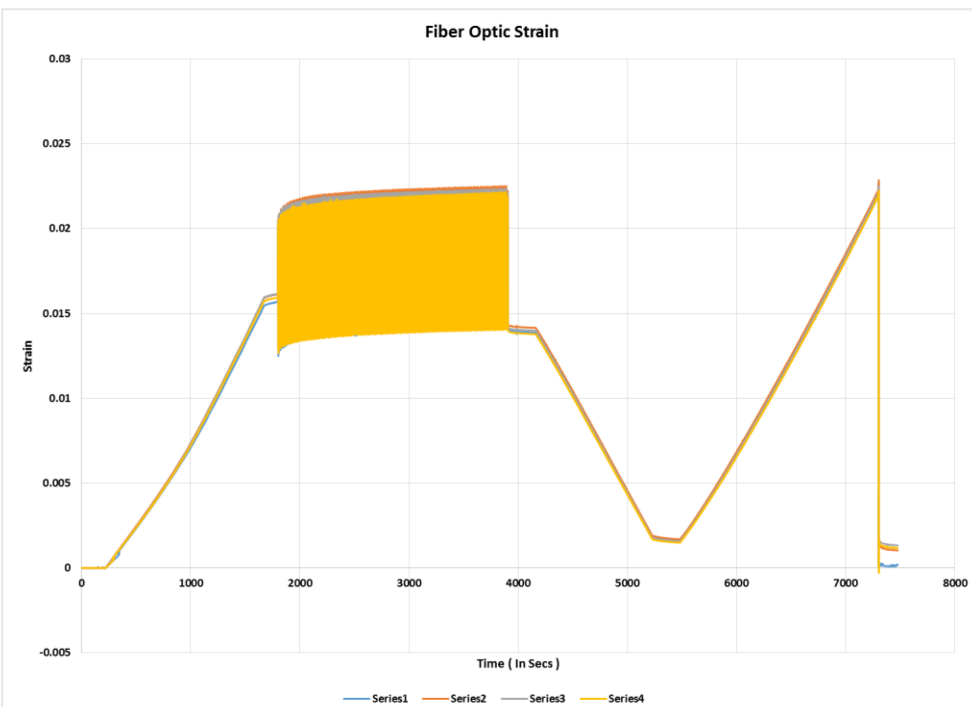

Figure 6.5: Fiber Optic Strain response for Fatigue

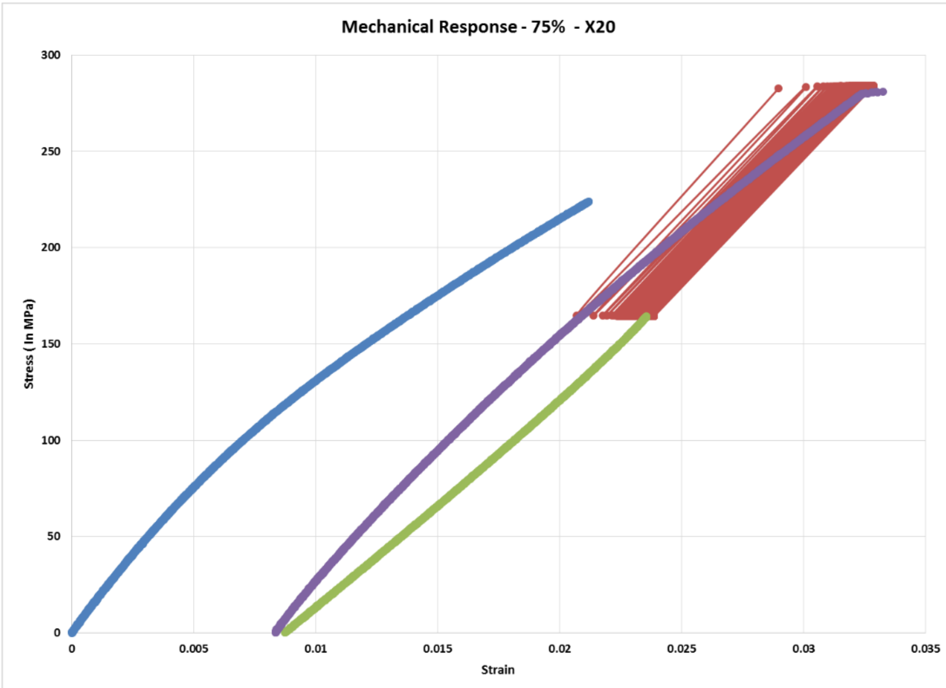

Figure 6.6: Stress-Strain response during residual strength determination test

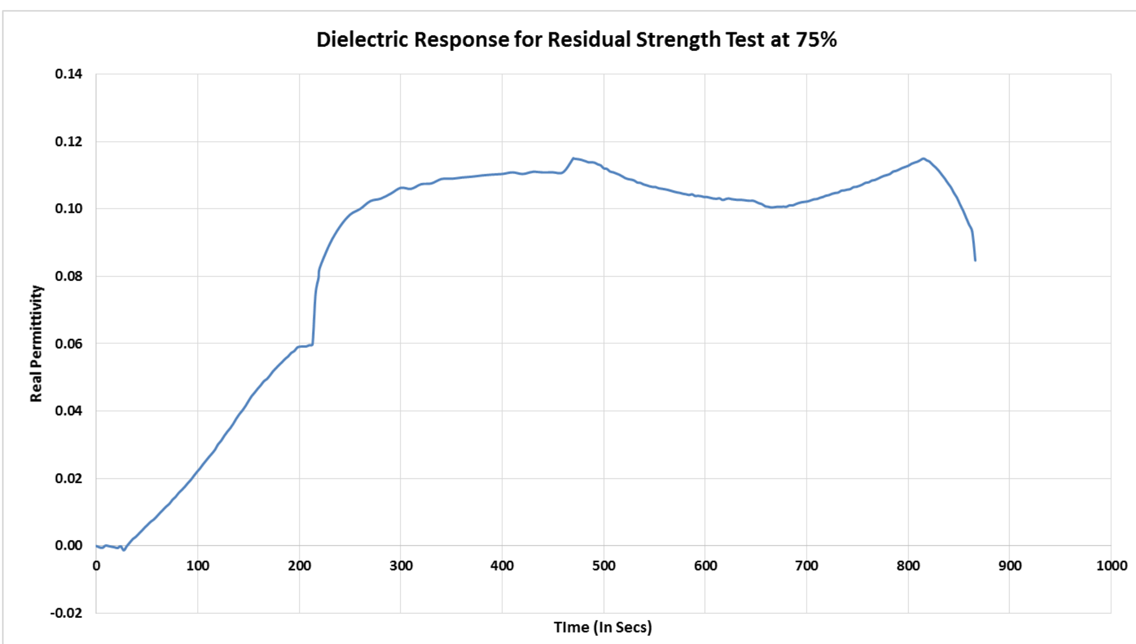

Figure 6.7: Dielectric Permittivity response for residual strength determination test

From the above figures, it can be observed that the dielectric response has a certain correlation with the strain response, during the initial static ramp up and during fatigue. However the curves are different for the ramp down and the second ramp up for residual strength determination. This gives us another intuition that the dielectric response behaves differently when there is damage in the material, validating our prior theories.

The results of the residual strength calculations are shown in Table 6-IV.

Table 6-IV: Residual Strength Values for different fatigue loading conditions

Mean Stress Condition	Average Residual Strength (MPa)	Shape Parameter	Weibull Scale Parameter (MPa)	95% Lower Residual Strength (MPa)	95% Upper Residual Strength (MPa)
75 %	326.50	13.60	339.1871	320.22	359.27
50 %	262.24	21.48	269.446	259.06	280.03
25 %	248.18	16.93	255.661	238.13	274.47

6.6 Life Prediction with ECSEA Bonded Sensors

Being a popular characterization technique, dielectric properties of composite materials have been measured using different established techniques as discussed above using copper electrode blocks. However, due to the clamping force of the blocks on the composite specimen under testing, stress concentrations at the contact sites are common. In addition, if the clamping force isn't sufficient or the specimen surface is uneven, there would be poor surface contact. All these issues can lead to erroneous noise measurements. To get rid of these issues, a new approach has been carried out using Extremely Conductive Silver Epoxy Adhesive (ECSEA) paste manufactured by MG Chemicals. This method eliminates the possibility of having any stress concentration as well as maintains proper contact with the specimen surface (given proper curing of the silver epoxy). By bonding copper electrodes using ECSEA paste to the composite, continuous contact is established. The composite specimens where first marked with the location of the sensor and taped all around with a masking tape, to avoid any excess adhesive on the specimen. The part A and part B of ECSEA pastes were mixed in 1:1 ratio and applied evenly on the particular location on both sides of the composite sample, and thin copper sheets were placed on top and bottom of the ECSEA paste. This setup was cured at 60° C for 2 hours as per the manufacturer's recommendation. Later, BNC connectors were soldered to the sensor using copper wires. The composite specimen with the bonded dielectric sensor is shown in Figure 6.88.

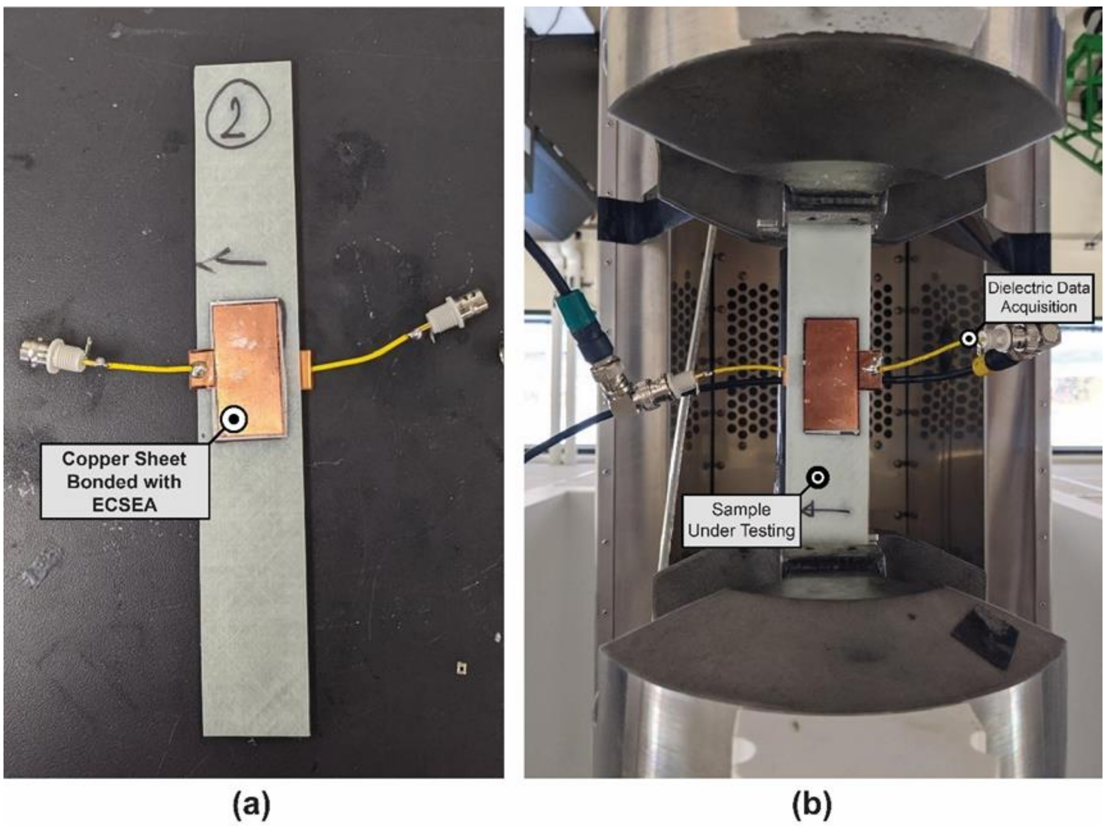

Figure 6.8: a) Composite sample with copper sensor bonded using ECSEA paste b) sample under testing in MTS machine.

All the mechanical tests were carried out using MTS Landmark Servo-hydraulic test systems. The composite specimens were subjected to the fatigue test at the mean load level of 50% of the lower confidence interval bound of the breaking load. These fatigue tests were designed at a constant amplitude of 20% and frequency of 2 Hz. The fatigue parameters are as mentioned earlier in Table 2. Both the tensile and fatigue in-situ tests were carried out using the ECSEA paste based dielectric sensors. The real and imaginary part of permittivity were measured simultaneously during these mechanical tests using the NoVoControl Dielectric Spectrometer as described earlier. These ex-situ dielectric measurements were carried out between the frequency of 1 MHz to 0.1 Hz and the in-situ measurement was carried out at a frequency of 100 Hz. 11 composite specimens were used in this particular experiment.

6.6.1 Dielectric response using ECSEA under quasi-static loads

Since a new methodology of using ECSEA with the copper plate was used to measure the dielectric properties of the composite material using the BbDS method, the sensors were first validated by measuring the ex-situ response of the composite as shown in Figure 6.9; it was observed that the behavior is similar to using the traditional electrode block setup[160]. Then another validation was performed by analyzing the in-situ behavior of the composite panel with SEA bonded sensors, under quasi-static loading as shown in Figure 6.10 and was similar to using the traditional electrode block setup[160]

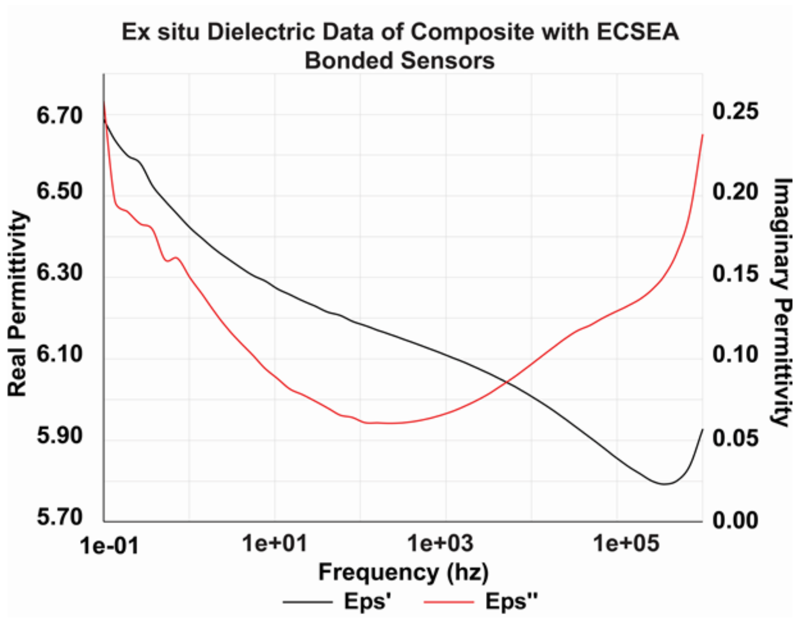

Figure 6.9: Ex-Situ Dielectric data of composite bonded with ECSEA sensors

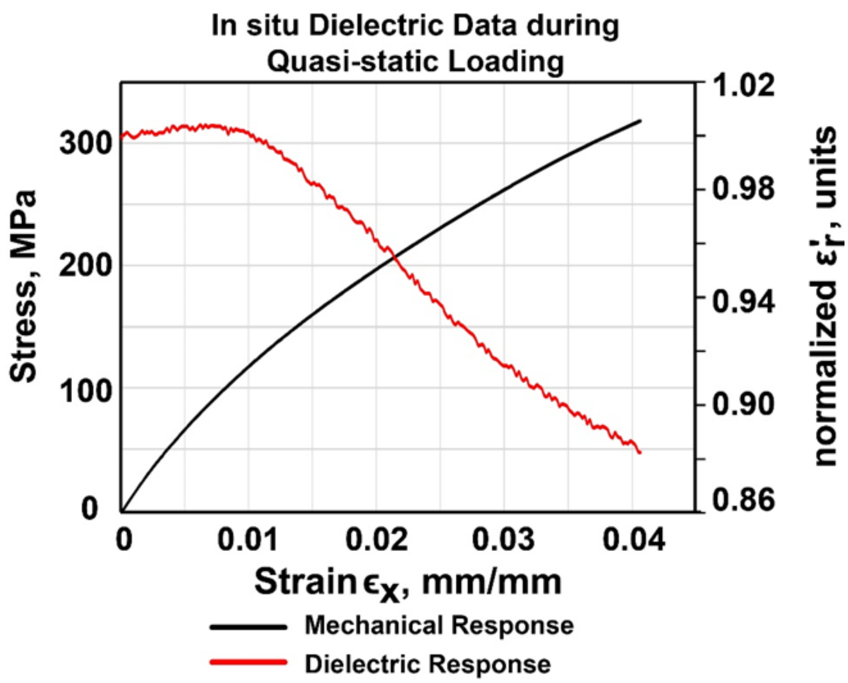

Figure 6.10: In-situ dielectric data of composite with SEA bonded sensors under quasi-static loading

6.6.2 Dielectric response under fatigue loading

Figure 6.11 represents the mechanical (stiffness) and dielectric (permittivity) response during fatigue loading of a specimen. The stiffness vs. life curve (normalized), is similar to observations made in the literature (Figure 2.3), except a for few artifacts. A sharp decrease in the beginning and end of the fatigue is notable, which is primarily due to the 50% mean stress level. At this stress level, and considering the amplitude of fatigue loading, the material would have attained the CDS (Characteristic Damage State crack spacing), resulting in this initial sharp decrease in stiffness unlike the behavior in Figure 2.3. From Figure 6.11, it is seen that there is an accelerated decrease in the permittivity at about 75% of the life of the composite material, which could serve as a precursor for indicating the beginning of the end of life of the material.

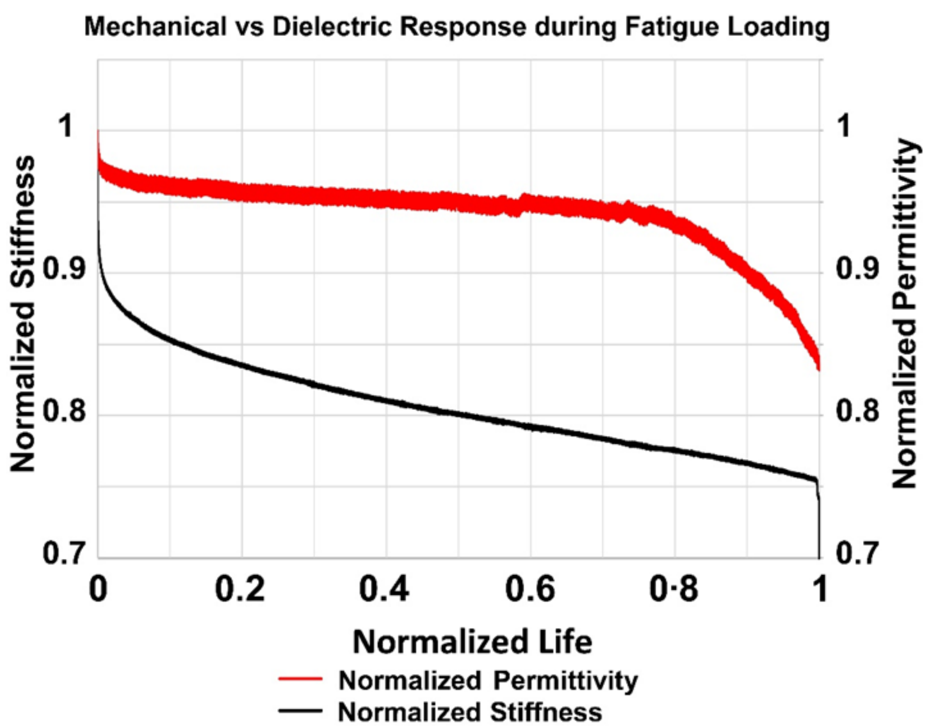

Figure 6.11: Mechanical vs. Dielectric Response of Composite under Cyclic loading

6.6.3 Evolution of state variables with damage development

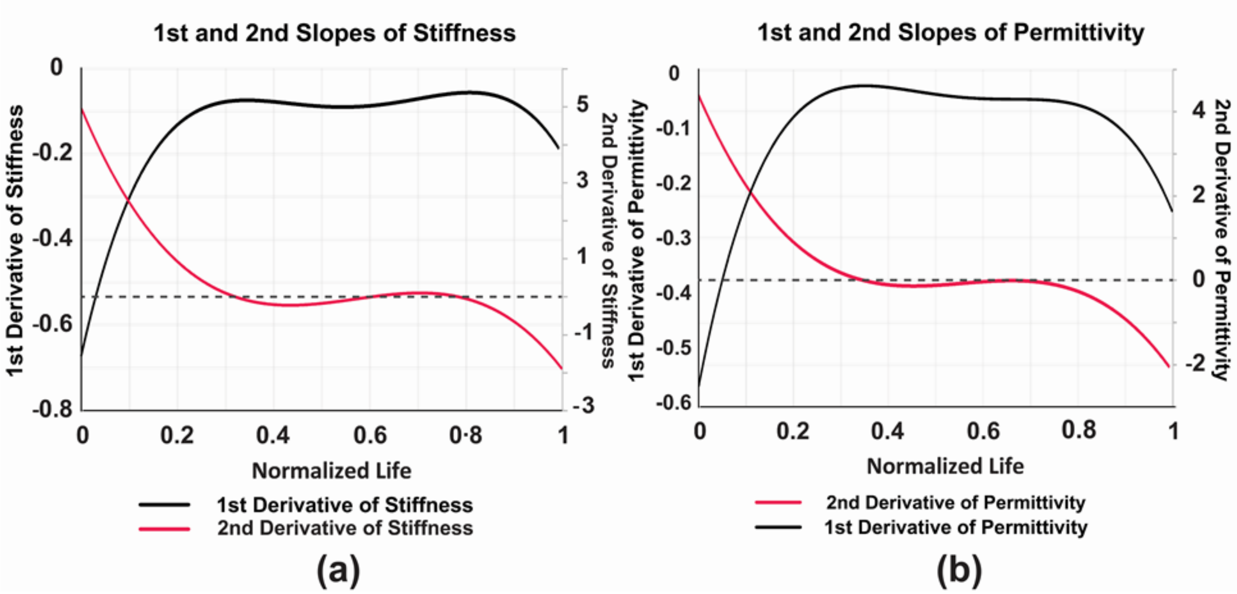

Figure 6.12: 1st and 2nd derivatives of a) stiffness and b) permittivity

To get a better understanding of the material behavior with damage development, curve fits were obtained for the mechanical and dielectric representative curves and their slopes were analyzed. Figure 6.12 represents the derivatives for the state variables of the representative curve. As described above in State Variable Change with Damage Development section, the first derivative represents the rate of change in behavior whereas the second derivate represents the acceleration in behavior [161,162]. The average acceleration of stiffness and permittivity are normalized with respect to their maximum values and compared as shown Figure 6.13. It can be observed that the acceleration of mechanical and dielectric state variables follow a similar trend until 50% of life, i.e. the magnitude of the acceleration is higher in the beginning and starts to decrease gradually followed by saturation. We observe the second inflection point in the acceleration curve at around 70% of life where the magnitude of acceleration in dielectric response starts to increase earlier than the mechanical response which increases around 75% of life and then both decrease, hence providing an earlier warning of beginning of failure. Based on this second point of inflection, which indicates the beginning of end of life, the percent of life and hence the number of cycles at that point of inflection was obtained for all the 11 composite specimens. The average percent of life is predicted as 68.78% and average number of cycles is predicted as 53655 based on permittivity, at which the failure is imminent for this laminate under the given loading conditions. Based on the 2nd point of inflections calculated from stiffness, the percent of life is 71.74% and the number of cycles is 59669. Weibull analysis was carried out for these data, indicating the reliability of this dielectric in-situ monitoring method. A shape factor of 10.30 was obtained.

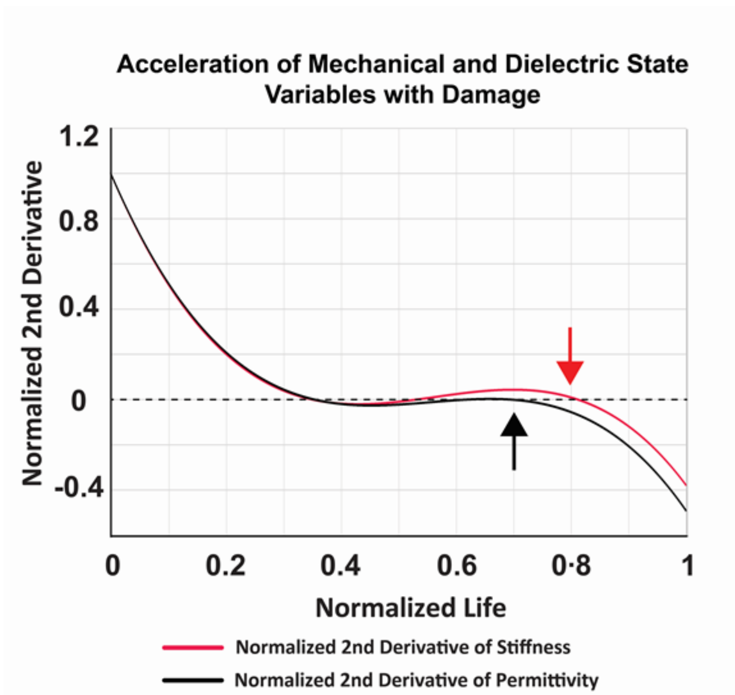

Figure 6.13: Acceleration of Mechanical and Dielectric state variables

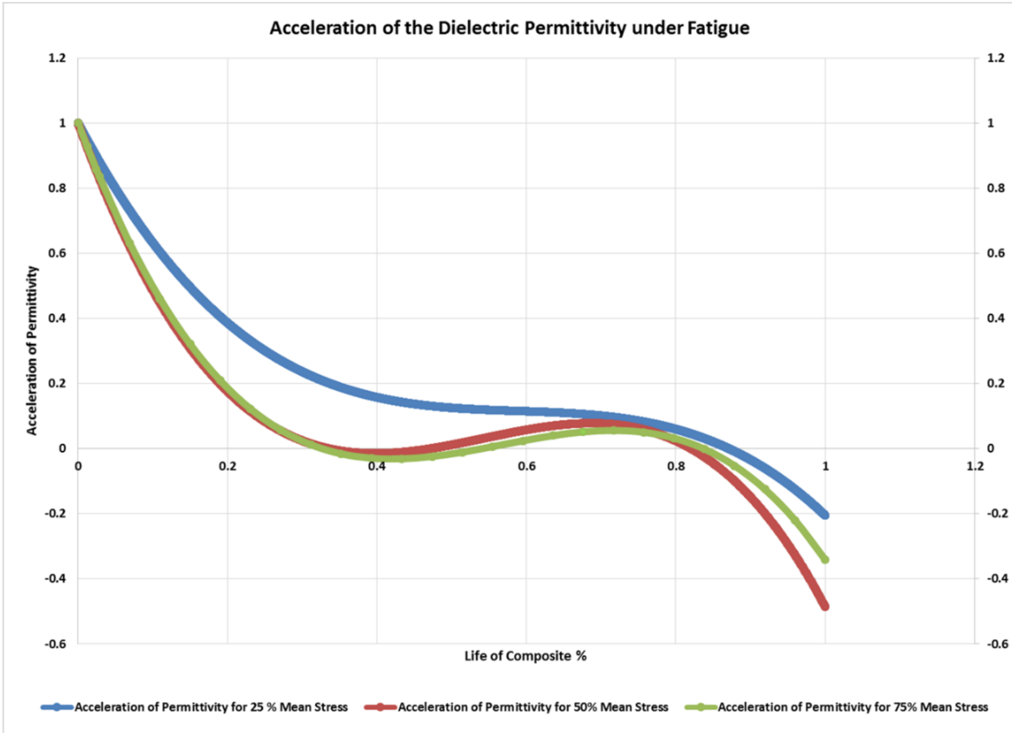

Figure 6.14: Acceleration of Dielectric Permittivity under Fatigue for different load levels

Figure 6.14 shows how the acceleration of the permittivity changes for the 3 different fatigue loading conditions based on the dielectric permittivity response as an input. It can be clearly observed that, for all the 3 different loading conditions, we are able to identify the inflection point at about 75-80% of the material's failure, indicating the beginning of the end of failure of the composite specimen.

Hence with this in-situ monitoring of the composite material using the SEA bonded sensors, it is possible to predict the beginning of the end of life of the material. Based on these observations, we propose the following framework shown in the Figure 6.15 for in-situ monitoring of composite structures using BbDS. Here, the dielectric property is measured at regular time intervals, the rate of change and acceleration are calculated and based on the design, the structure can be called for maintenance, repair and operation. Based on this framework, by continuous monitoring of dielectric data, maintenance scheduling will be more effective leading to reliable and safer structures. It is to be noted that, all of these results were obtained with the fifth order polynomial curves and changing the order of curve might result in different results. Hence the future work will be focused to use data-driven artificial intelligence methods for in-situ monitoring using this methodology.

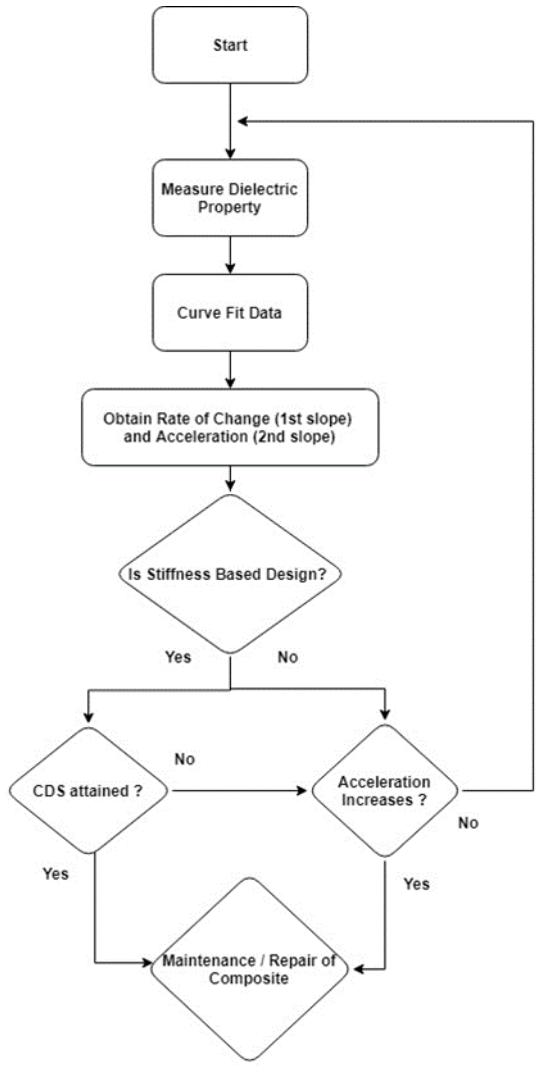

Figure 6.15: Proposed Di-electric in-situ monitoring framework

6.6.4 Artificial Intelligence Models for ECSEA bonded Dielectric Sensor Monitoring

Until now we discussed the physics based approach of using real-permittivity value and the stiffness value, over life. This section explains the development of an AI algorithm using the real-permittivity curve for each specimen, obtained over time and predicting the life at that instant, and the future life.

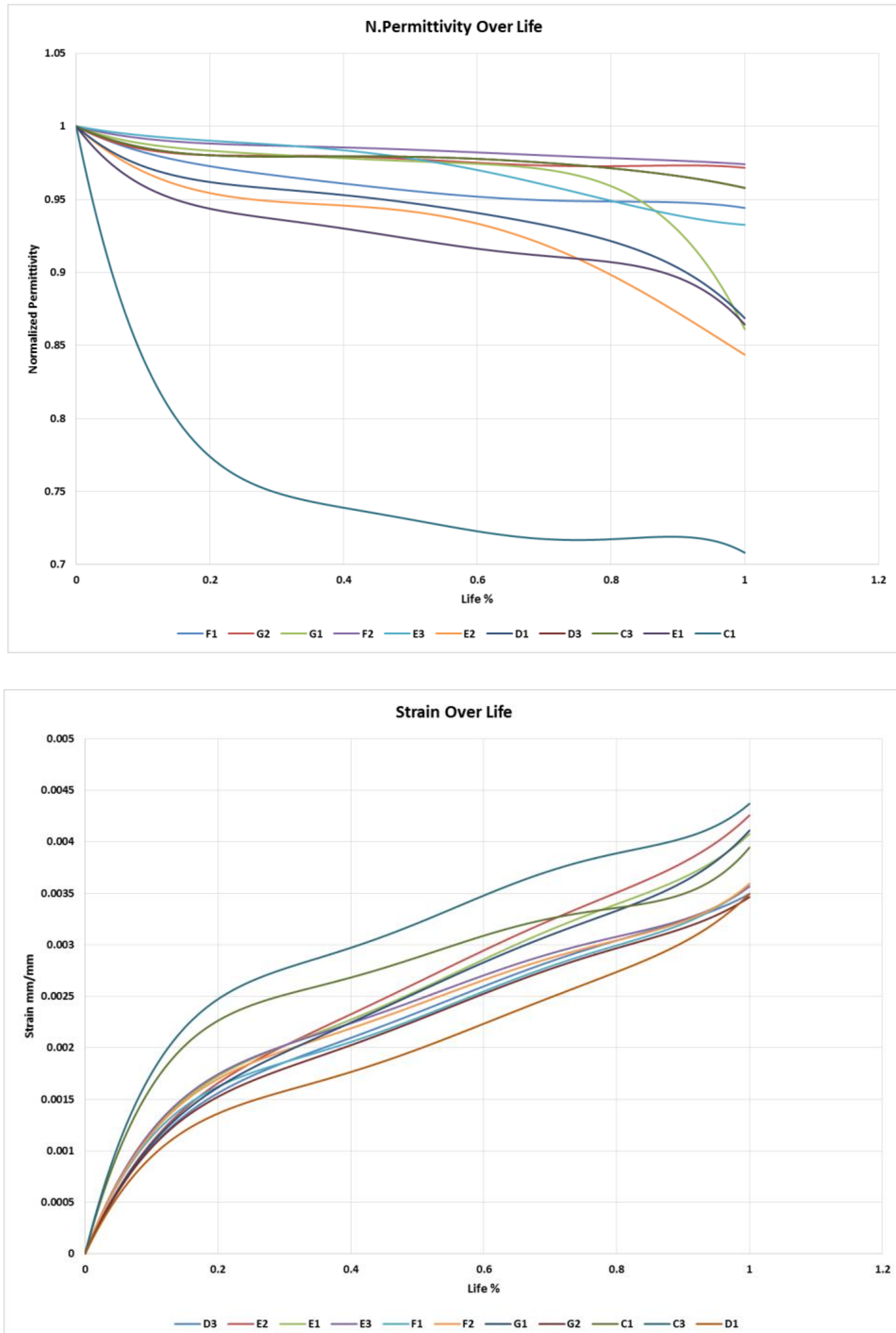

Figure 6.16: Interpolated representation of Permittivity and Strain over time

For the development of the AI model, we converted the input data into finite time steps of data by the process of interpolation. This helps us improve the model efficiency, and develop a model with the limited data points. Various approaches can also be taken by using the RNN-LSTM model, where the LSTM model takes care of the variable sequence length using the encoder-decoder approach.

An Artificial Neural Network model was developed, where the permittivity is provided as the input and the Life is obtained as the output. It's a 4-Layer Neural Network model, with 1000 neurons in each layer, with 500 outputs in the output layer. 8 samples were used for training and 3 samples were used for the testing. Validation was done from the training data set, with the validation parameter set to 0.2. For the output prediction, each sample in the test data set was split into 5 sub-samples, where these sub-samples had values only for 100,200,300,400 and 500 time steps, and the remaining values were made as 0. By this way, the output prediction curves were obtained from the ANN model for each sub-samples as shown in Figure 6.17

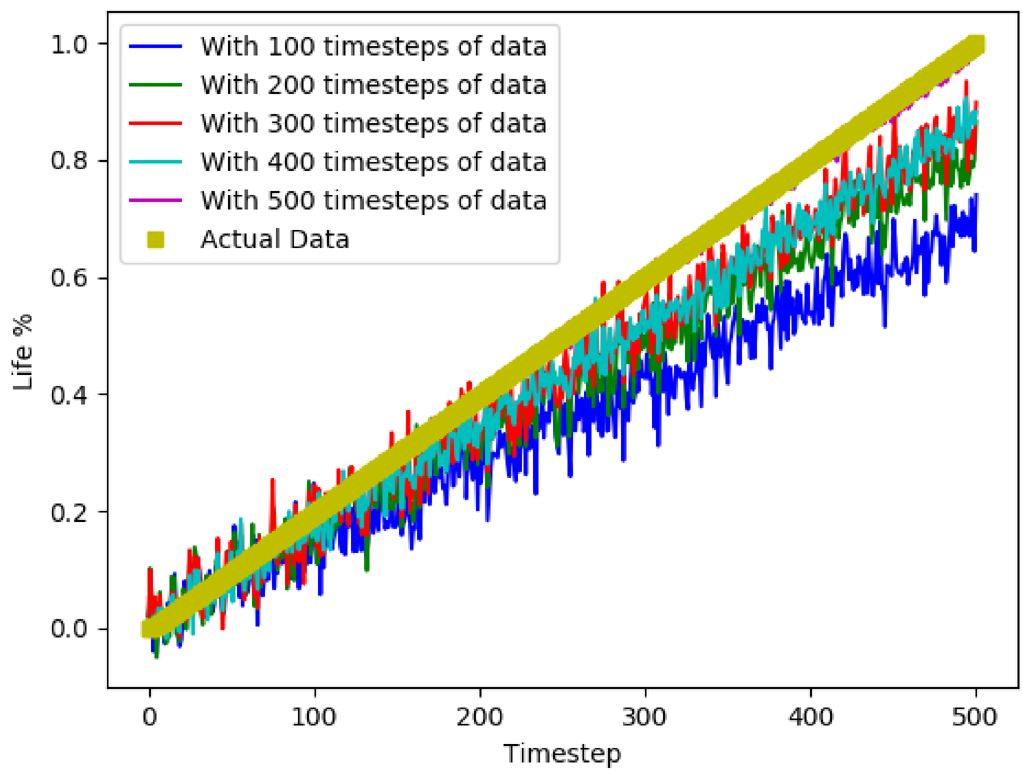

Figure 6.17 Prediction of a test data for ANN model with Permittivity as Input

Table 6-V: Results from the ANN model for a sample

X	100 Time steps	200 Time steps	300 Time steps	400 Time steps	500 Time steps
Actual Life % at X Time step	0.1932	0.3944	0.5956	0.7968	1
Predicted Life % at X Time step	0.1907	0.4020	0.5880	0.7522	0.9831
Predicted Life % at 500th Time step	0.74	0.8649	0.8831	0.9480	0.9831
Accuracy	74 %	86.49 %	88.31 %	94.80 %	98.31 %

From the results above, it can be observed that with the initial 100 time steps in-situ monitoring data of dielectric permittivity, the life prediction has a low accuracy, however as more ground-truth information in form of time-steps is obtained and the damage progression occurs in the composite materials and provided to the AI model, the life can be predicted with more than 90% accuracy. This will be helpful for the maintenance inspection technicians, to schedule timely condition based maintenance.

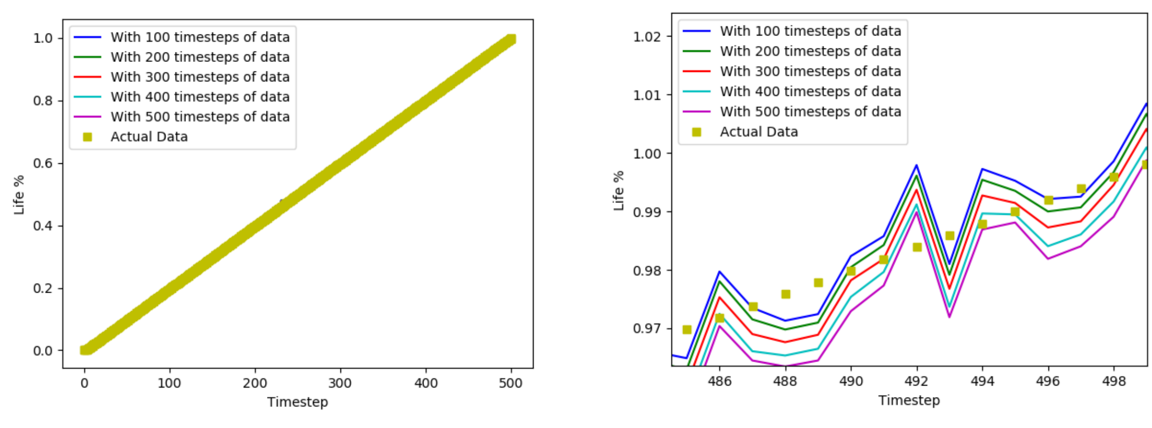

Figure 6.18: Prediction of a test data for ANN with Strain as Input

Figure 6.18 shows the output predictions of the ANN model. It can be seen that the output predictions matches the actual prediction so accurately. This is due to the fact that the strain response developed during a constant amplitude fatigue tests do not vary and follow similar pattern. Since the input data is smooth as shown in Figure 6.16

6.7 Summary of the work

In this work, in-situ dielectric spectroscopy was used to monitor evolution of state variables with damage development during fatigue. Quasi isotropic laminates made out of glass fiber reinforced polymer composites were loaded in tension-tension fatigue at a mean stress level of 75 %, 50 %, and 25% of ultimate tensile strength. The Number of cycles to failure were obtained for each fatigue condition. Residual strength determination tests were designed based on the Weibull parameters, and the residual strength of the specimens was obtained for each fatigue condition. As the change in the state variables is triggered by damage development, the rate of change of these state variables indicates the rate of damage interaction and can be effectively used to predict impending failure. For these laminates under the given loading conditions, it was predicted that failure is imminent after 53655 cycles (68.78 % of life) with a 95% confidence interval [41488 to 69390 cycles]. A framework was designed in this work based on in-situ monitoring to effectively schedule maintenance and hence make the composite structures more reliable. AI models are developed to predict the life during fatigue of composite materials using the dielectric permittivity value collected in real-time.

Chapter 7

CONCLUSION AND FUTURE WORK

With the increasing use of Artificial Intelligence based data-driven modelling in composite materials, and the need for reliable prognostic health management systems for condition based maintenance, it is necessary to identify the material state parameters that could give reliable information on the performance of the composite material under various loading conditions.

This work is summarized as the results of the four chapters, where the in-depth literature survey is performed, experiments are carried out using the state of the art material sensor systems for manufacturing, static and fatigue loading conditions, and the use of artificial intelligence techniques using these data is studied.

The major contributions from this dissertation are

- Proposed the methodology to adopt artificial intelligence based data-driven methods for prognostic health management, from the survey of the current methods available
- Established a method to identify the foreign object defects in the composite materials from dielectric properties and machine learning

• Established the use of Interpretable Machine Learning and Explainable Artificial intelligence techniques to identify which dielectric parameter, and at what frequencies, the defects are distinguishable in composites

• Developed Artificial Intelligence models to identify the Characteristic Damage State (CDS) of the composite material from the in-situ dielectric data under quasi-static loading

• Established a framework to predict the beginning of end of life of the material during in-life service, by in-situ monitoring with dielectric sensors

• Developed an Artificial Intelligence framework to predict the remaining useful life of the composite material using permittivity and strain measurements

The future work that can be carried out in various directions is suggested as follows:

- Research work on the advancement of using dielectric sensors for fatigue monitoring, by varying several other parameters that can be studied, such as spectrum loading conditions
- A complete life cycle monitoring of the composite structure can be done using the proposed sensors from manufacturing till failure, and the data can be studied.
- Adaptive data-driven models can be developed
- Interpretable methods to predict the regression – time series data can be used for the fatigue life monitoring of composite materials
- Develop classification models for identifying the different damage states under fatigue loading conditions
- Develop methods to correlate the damage state of the material based on the slope change of dielectric response, i.e correlated the initial stiffness, residual stiffness with the dielectric slope.

References

[1] Elenchezhian MRP, Vadlamudi V, Raihan R, Reifsnider K, Reifsnider E. Artificial Intelligence in Real-Time Diagnostics and Prognostics of Composite Materials and its Uncertainties – a Review. Smart Mater Struct 2021.

[2] Bowles KJ, Frimpong S. Void Effects on the Interlaminar Shear Strength of Unidirectional Graphite-Fiber-Reinforced Composites. J Compos Mater 1992;26:1487–509. https://doi.org/10.1177/002199839202601006.

[3] Talreja R. Damage and fatigue in composites. Compos Sci Technol 2008;68:2585–91. https://doi.org/10.1016/j.compscitech.2008.04.042.

[4] Raihan MR. Dielectric Properties of Composite Materials during Damage Accumulation and Fracture 2014.

[5] Vadlamudi V. ASSESSMENT OF MATERIAL STATE IN COMPOSITES USING GLOBAL DIELECTRIC STATE VARIABLE. 2019.

[6] K. L. Reifsnider, E. G. Henneke WWS and JCD. DAMAGE MECHANICS AND NDE OF COMPOSITE LAMINATES. Mech Compos Mater 1983:399–420.

[7] Reifsnider KL, Henneke EG, Stinchcomb WW, Duke JC. DAMAGE MECHANICS AND

NDE OF COMPOSITE LAMINATES., 1983. https://doi.org/10.1016/b978-0-08-029384-4.50032-8.

[8] Hufner DR. Progressive failure of woven polymer-based composites under dynamic loading; Theory and analytical simulation. Dr Diss 2008.

[9] Fathi-Torbaghan M, Kern H, Janczak J. AI in material design-an expert system for construction of composite material. [1991 Proceedings] Tenth Annu. Int. Phoenix Conf. Comput. Commun., IEEE Comput. Soc. Press; 1991, p. 828–34. https://doi.org/10.1109/PCCC.1991.113901.

[10] Sticklen, Jon;Kemel, Ahmed; Hawley MDJ. An artificial intelligence-based design tool for thin film composite materials. Appl Artif Intell 1992;6:303–13. https://doi.org/10.1080/08839519208949957.

[11] Sabouhi R, Ghayour H, Abdellahi M, Bahmanpour M. Measuring the mechanical properties of polymer-carbon nanotube composites by artificial intelligence. Int J Damage Mech 2015;25:538–56. https://doi.org/10.1177/1056789515604375.

[12] Yang C, Kim Y, Ryu S, Gu GX. Using convolutional neural networks to predict composite properties beyond the elastic limit. MRS Commun 2019;9:609–17. https://doi.org/10.1557/mrc.2019.49.

[13] Chen CT, Gu GX. Machine learning for composite materials. MRS Commun 2019;9:556–66. https://doi.org/10.1557/mrc.2019.32.

[14] Man H, Furukawa T, Herszberg I, Prusty G. IMPLICIT MODELING OF DAMAGE BEHAVIOR FOR COMPOSITE MATERIALS USING AN ENERGY-BASED METHOD. n.d.

[15] Ciupan E, Ciupan M, Jucan D-C. Determining the Mechanical Properties of a New

Composite Material using Artificial Neural Networks. vol. 66. 2018.

[16] Matos MAS, Pinho ST, Tagarielli VL. Application of machine learning to predict the multiaxial strain-sensing response of CNT-polymer composites. Carbon N Y 2019. https://doi.org/10.1016/j.carbon.2019.02.001.

[17] Su HB, Fan LT, Schlup JR. Monitoring the process of curing of epoxy/graphite fiber composites with a recurrent neural network as a soft sensor PERGAMON. vol. 11. 1998.

[18] Hsiao K-T, Devillard M, Advani SG. STREAMLINED INTELLIGENT RTM PROCESSING : FROM DESIGN TO AUTOMATION. 47 th Int. SAMPE Symp. Exhib., 2002, p. 454–65.

[19] Tsao CC, Hocheng H. Evaluation of thrust force and surface roughness in drilling composite material using Taguchi analysis and neural network. J Mater Process Technol 2008. https://doi.org/10.1016/j.jmatprotec.2006.04.126.

[20] Oromiehie E, Gangadhara Prusty B, Rajan G, Wanigasekara C, Swain A. Machine Learning Based Process Monitoring and Characterisation of Automated Composites. SAMPE Conf. Proceedings. Seattle, WA, May 22-25, 2017, 2017.

[21] Sacco C, Radwan AB, Harik R, Van Tooren M. Automated fiber placement defects: Automated inspection and characterization. SAMPE Conf. Proceedings. Long Beach, CA, May 21-24, 2018, vol. 2018- May, 2018.

[22] Sacco C, Radwan AB, Beatty T, Harik R. Machine Learning Based AFP Inspection: A Tool for Characterization and Integration. SAMPE 2019 - Charlotte, NC, vol. 2019- May, SAMPE; 2019. https://doi.org/10.33599/nasampe/s.19.1594.

[23] Blake S. Elements and mechanisms for applying artificial intelligence to composites fabrication. Int. SAMPE Tech. Conf., vol. 2019- May, Soc. for the Advancement of

Material and Process Engineering; 2019. https://doi.org/10.33599/nasampe/s.19.1435.

[24] Karnik SR, Gaitonde VN, Rubio JC, Correia AE, Abrão AM, Davim JP. Delamination analysis in high speed drilling of carbon fiber reinforced plastics (CFRP) using artificial neural network model. Mater Des 2008;29:1768–76. https://doi.org/10.1016/j.matdes.2008.03.014.

[25] Krishnamoorthy A, Rajendraaboopathy S, Palanikumar K. DELAMINATIONNPREDICTIONNINNDRILLINGGOFFCFRPP COMPOSITESSUSINGGARTIFICIALLNEURALLNETWORKK. vol. 22. 2011.

[26] Erkan Ö, Işık B, Çiçek A, Kara F. Prediction of damage factor in end milling of glass fibre reinforced plastic composites using artificial neural network. Appl Compos Mater 2013;20:517–36. https://doi.org/10.1007/s10443-012-9286-3.

[27] Wirtz SF, Beganovic N, Söffker D. Investigation of damage detectability in composites using frequency-based classification of acoustic emission measurements. Struct Heal Monit 2019;18:1207–18. https://doi.org/10.1177/1475921718791894.

[28] Argus P, Gurka M, Kelkel B. Development of a small-scale and low-cost SHM system for thin-walled CFRP structures based on acoustic emission analysis and neural networks 2019:49. https://doi.org/10.1117/12.2518439.

[29] Staszewski WJ. Intelligent signal processing for damage detection in composite materials. 2001.

[30] Fu T, Zhang Z, Liu Y, Leng J. Development of an artificial neural network for source localization using a fiber optic acoustic emission sensor array. Struct Heal Monit 2015;14:168–77. https://doi.org/10.1177/1475921714568406.

[31] Voth MM, Miller DA, Nunemaker JD, Murdy P, Samborsky DD, Cairns DS. Exploring

frequency based analysis methods for damage identification in fiberglass-epoxy composite systems. SAMPE Conf. Proceedings. Seattle, WA, May 22-25, 2017, 2017.

[32] Banerjee P, Palanisamy RP, Haq M, Udpa L, Deng Y. Data-driven Prognosis of Fatigue-induced Delamination in Composites using Optical and Acoustic NDE methods. 2019 IEEE Int. Conf. Progn. Heal. Manag., IEEE; 2019, p. 1–10. https://doi.org/10.1109/ICPHM.2019.8819426.

[33] Bhat C, Bhat MR, Murthy CRL. Characterization of failure modes in CFRP composites - An ANN approach. J Compos Mater 2008;42:257–76. https://doi.org/10.1177/0021998307086209.

[34] Dia A, Dieng L, Gaillet L, Gning B. Damage detection of a hybrid composite laminate aluminum/ glass under quasi-static and fatigue loadings by acoustic emission technique 2019. https://doi.org/10.1016/j.heliyon.2019.

[35] Refahi Oskouei A, Heidary H, Ahmadi M, Farajpur M. Unsupervised acoustic emission data clustering for the analysis of damage mechanisms in glass/polyester composites. Mater Des 2012;37:416–22. https://doi.org/10.1016/j.matdes.2012.01.018.

[36] Doan DD, Ramasso E, Placet V, Boubakar L, Zerhouni N, Dong DOAN D. Application of an Unsupervised Pattern Recognition Approach for AE Data Originating from Fatigue Tests on CFRP. 2014.

[37] Doan DD, Ramasso E, Placet V, Zhang S, Boubakar L, Zerhouni N. An unsupervised pattern recognition approach for AE data originating from fatigue tests on polymer-composite materials. Mech Syst Signal Process 2014;64–65:465–78. https://doi.org/10.1016/j.ymssp.2015.04.011.

[38] Crivelli D, Guagliano M, Eaton M, Pearson M, Al-Jumaili S, Holford K, et al.

Localisation and identification of fatigue matrix cracking and delamination in a carbon fibre panel by acoustic emission. Compos Part B Eng 2014;74:1–12. https://doi.org/10.1016/j.compositesb.2014.12.032.

[39] Al-Jumaili SK, Eaton MJ, Holford KM, Pearson MR, Crivelli D, Pullin R. Characterisation of fatigue damage in composites using an Acoustic Emission Parameter Correction Technique. Compos Part B Eng 2018;151:237–44. https://doi.org/10.1016/j.compositesb.2018.06.020.

[40] Boussetta H, Beyaoui M, Laksimi A, Walha L, Haddar M. Study of the filament wound glass/polyester composite damage behavior by acoustic emission data unsupervised learning. Appl Acoust 2017;127:175–83. https://doi.org/10.1016/j.apacoust.2017.06.004.

[41] Ramasso E, Placet V, Boubakar ML. Unsupervised Consensus Clustering of Acoustic Emission Time-Series for Robust Damage Sequence Estimation in Composites. IEEE Trans Instrum Meas 2015;64:3297–307. https://doi.org/10.1109/TIM.2015.2450354.

[42] Sawan HA, Walter ME, Marquette B. Unsupervised learning for classification of acoustic emission events from tensile and bending experiments with open-hole carbon fiber composite samples. Compos Sci Technol 2015;107:89–97. https://doi.org/10.1016/j.compscitech.2014.12.003.

[43] Ech-Choudany Y, Assarar M, Scida D, Morain-Nicolier F, Bellach B. Unsupervised clustering for building a learning database of acoustic emission signals to identify damage mechanisms in unidirectional laminates. Appl Acoust 2017;123:123–32. https://doi.org/10.1016/j.apacoust.2017.03.008.

[44] Tang J, Soua S, Mares C, Gan TH. A pattern recognition approach to acoustic emission data originating from fatigue of wind turbine blades. Sensors (Switzerland) 2017;17.

https://doi.org/10.3390/s17112507.

[45] Nair A, Cai CS, Kong X. Studying Failure Modes of GFRP Laminate Coupons Using AE Pattern-Recognition Method. J Aerosp Eng 2019;32:1–15. https://doi.org/10.1061/(ASCE)AS.1943-5525.0001015.

[46] Nair A, Cai CS, Kong X. Acoustic emission pattern recognition in CFRP retrofitted RC beams for failure mode identification. Compos Part B Eng 2019. https://doi.org/10.1016/j.compositesb.2018.12.120.

[47] Schillemans L, van Hemelrijck D, De Roey F, Wilde WPD, Cardon AH, Anastassopoulos AA. Defect-identification in composite materials using pattern recognition techniques on ultrasonic data. Adv Compos Mater 1993;3:57–71. https://doi.org/10.1163/156855193X00070.

[48] Su Z, Ye L. Quantitative damage prediction for composite laminates based on wave propagation and artificial neural networks. Struct Heal Monit 2005;4:57–66. https://doi.org/10.1177/1475921705049747.

[49] Shan Q, King G, Savage J. <title>Artificial intelligence for identifying impacts on smart composites</title>. Smart Struct. Mater. 2002 Model. Signal Process. Control, vol. 4693, SPIE; 2002, p. 568–75. https://doi.org/10.1117/12.475254.

[50] Kral ZT. DEVELOPMENT OF A DECENTRALIZED ARTIFICIAL INTELLIGENCE SYSTEM FOR DAMAGE DETECTION IN COMPOSITE LAMINATES FOR AEROSPACE STRUCTURES A Dissertation by. 2009.

[51] Dong Xiaoma, Sun Qingzhen. Research on damage detection of composite materials based on RBFNN. 2010 2nd Int. Conf. Comput. Eng. Technol., IEEE; 2010, p. V1-492-V1-494. https://doi.org/10.1109/ICCET.2010.5486020.

[52] Talaie A, Esmaili N, Lee J-Y, Kosaka T, Oshima N, Osaka K, et al. <title>Pattern recognition application in classification of intelligent composites during smart manufacturing using a C4.5 machine learning program</title>. Smart Struct. Devices, vol. 4235, SPIE; 2001, p. 217–27. https://doi.org/10.1117/12.420861.

[53] Das S, Chattopadhyay A, Srivastava AN. Classifying induced damage in composite plates using one-class support vector machines. AIAA J 2010;48:705–18. https://doi.org/10.2514/1.37282.

[54] Gwon YS, Fekrmandi H. A data-driven approach of load monitoring on laminated composite plates using support vector machine, SPIE-Intl Soc Optical Eng; 2018, p. 32. https://doi.org/10.1117/12.2305840.

[55] Manson G, Pierce SG, Worden K. On the long-term stability of normal condition for damage detection in a composite panel. Key Eng Mater 2001. https://doi.org/10.4028/www.scientific.net/kem.204-205.359.

[56] Tibaduiza D, Torres-Arredondo MÁ, Vitola J, Anaya M, Pozo F. A Damage Classification Approach for Structural Health Monitoring Using Machine Learning. Complexity 2018;2018. https://doi.org/10.1155/2018/5081283.

[57] Tabian I, Fu H, Khodaei ZS. A convolutional neural network for impact detection and characterization of complex composite structures. Sensors (Switzerland) 2019;19:1–25. https://doi.org/10.3390/s19224933.

[58] Miller EJ, Pena F, Jordan A, Hudson L, Lokos W. Evaluation of Wing Load Calibration and Sensing Methods Using Conventional Strain Gages and a Fiber Optic Sensing System Installed on a Straight Tapered Wing n.d. https://doi.org/10.2514/6.2019-0227.

[59] De Oliveira R, Frazão O, Santos JL, Marques AT. Optic fibre sensor for real-time damage

detection in smart composite. Comput. Struct., vol. 82, 2004, p. 1315–21. https://doi.org/10.1016/j.compstruc.2004.03.028.

[60] Rajabzadeh A, Hendriks RC, Heusdens R, Groves RM. Classification of composite damage from FBG load monitoring signals. Sensors Smart Struct. Technol. Civil, Mech. Aerosp. Syst. 2017, vol. 10168, SPIE; 2017, p. 1016831. https://doi.org/10.1117/12.2257660.

[61] Datta A, Augustin MJ, Gupta N, Viswamurthy SR, Gaddikeri KM, Sundaram R. Impact Localization and Severity Estimation on Composite Structure Using Fiber Bragg Grating Sensors by Least Square Support Vector Regression. IEEE Sens J 2019;19:4463–70. https://doi.org/10.1109/JSEN.2019.2901453.

[62] Panopoulou A, Loutas T, Roulias D, Fransen S, Kostopoulos V. Dynamic fiber Bragg gratings based health monitoring system of composite aerospace structures. Acta Astronaut 2011;69:445–57. https://doi.org/10.1016/j.actaastro.2011.05.027.

[63] Loutas TH, Panopoulou A, Roulias D, Kostopoulos V. Intelligent health monitoring of aerospace composite structures based on dynamic strain measurements. Expert Syst Appl 2012;39:8412–22. https://doi.org/10.1016/j.eswa.2012.01.179.

[64] Lu S, Jiang M, Sui Q, Sai Y, Jia L. Damage identification system of CFRP using fiber bragg grating sensors. Compos Struct 2015. https://doi.org/10.1016/j.compstruct.2015.02.038.

[65] Sierra-Pérez J, Güemes A, Mujica LE. Damage detection by using FBGs and strain field pattern recognition techniques. Smart Mater Struct 2013;22. https://doi.org/10.1088/0964-1726/22/2/025011.

[66] Alvarez-Montoya J, Carvajal-Castrillón A, Sierra-Pérez J. In-flight and wireless damage

detection in a UAV composite wing using fiber optic sensors and strain field pattern recognition. Mech Syst Signal Process 2020. https://doi.org/10.1016/j.ymssp.2019.106526.

[67] Alvarez-Montoya J, Sierra-Pérez J. Fuzzy unsupervised-learning techniques for diagnosis in a composite UAV wing by using fiber optic sensors. Proc. 7th Asia-Pacific Work. Struct. Heal. Monit. APWSHM, 2018.

[68] Güemes A, Fernández-López A, Díaz-Maroto PF, Lozano A, Sierra-Perez J. Structural health monitoring in composite structures by fiber-optic sensors. Sensors (Switzerland) 2018;18. https://doi.org/10.3390/s18041094.

[69] Ramu SA, Johnson VT. Damage assessment of composite structures-A fuzzy logic integrated neural network approach. Comput Struct 1995;57:491–502. https://doi.org/10.1016/0045-7949(94)00624-C.

[70] Anderson TA, Lemoine GI, Ambur DR. An artificial neural network based damage detection scheme for electrically conductive composite structures. Collect. Tech. Pap. - AIAA/ASME/ASCE/AHS/ASC Struct. Struct. Dyn. Mater. Conf., vol. 7, 2003, p. 5426–34. https://doi.org/10.2514/6.2003-1997.

[71] Kesavan A, John S, Herszberg I. Structural health monitoring of composite structures using artificial intelligence protocols. J Intell Mater Syst Struct 2008;19:63–72. https://doi.org/10.1177/1045389X06073688.

[72] Nasiri MR, Mahjoob MJ, Aghakasiri A. Damage detection in a composite plate using modal analysis and artificial intelligence. Appl. Compos. Mater., vol. 18, 2011, p. 513–20. https://doi.org/10.1007/s10443-011-9231-x.

[73] Just-Agosto F, Serrano D, Shafiq B, Cecchini A. Neural network based nondestructive

evaluation of sandwich composites. Compos Part B Eng 2008;39:217–25. https://doi.org/10.1016/j.compositesb.2007.02.023.

[74] Gomes GF, de Almeida FA, Junqueira DM, da Cunha SS, Ancelotti AC. Optimized damage identification in CFRP plates by reduced mode shapes and GA-ANN methods. Eng Struct 2019. https://doi.org/10.1016/j.engstruct.2018.11.081.

[75] Teimouri H, Milani AS, Seethaler R, Heidarzadeh A. On the Impact of Manufacturing Uncertainty in Structural Health Monitoring of Composite Structures: A Signal to Noise Weighted Neural Network Process. Open J Compos Mater 2016;06:28–39. https://doi.org/10.4236/ojcm.2016.61004.

[76] Pawar PM, Jung SN. Support vector machine based online composite helicopter rotor blade damage detection system. J Intell Mater Syst Struct 2008;19:1217–28. https://doi.org/10.1177/1045389X07084713.

[77] AM Khatkhate, GM Kamath MR. Sensor failure detection using a combined artificial neural network and finite element analysis approach. ISSS- MEMS Conf. Novemb. 16-17, 2007, 2007.

[78] Gomes GF, Mendéz YAD, da Silva Lopes Alexandrino P, da Cunha SS, Ancelotti AC. The use of intelligent computational tools for damage detection and identification with an emphasis on composites – A review. Compos Struct 2018. https://doi.org/10.1016/j.compstruct.2018.05.002.

[79] Robinson D. A TRIDENT SCHOLAR PROJECT REPORT D UNITED STATES NAVAL ACADEMY ANNAPOLIS, MARYLAND. 1987.

[80] Schulte K, Baron C. Load and failure analyses of CFRP laminates by means of electrical resistivity measurements. Compos Sci Technol 1989;36:63–76.

https://doi.org/10.1016/0266-3538(89)90016-X.

[81] Irving PE, Thiagarajan C. Fatigue damage characterization in carbon fibre composite materials using an electrical potential technique. Smart Mater Struct 1998;7:456–66. https://doi.org/10.1088/0964-1726/7/4/004.

[82] C T, PE I. In Service Damage Monitoring techniques in polymer composites. Proc Aerotech, 1994.

[83] Schueler R, Joshi SP, Schulte K. Damage detection in CFRP by electrical conductivity mapping. Compos Sci Technol 2001;61:921–30. https://doi.org/10.1016/S0266-3538(00)00178-0.

[84] Todoroki A, Tanaka Y. Delamination identification of cross-ply graphite/epoxy composite beams using electric resistance change method. Compos Sci Technol 2002;62:629–39. https://doi.org/10.1016/S0266-3538(02)00013-1.

[85] Wang X, Chung DDL. Sensing delamination in a carbon fiber polymer-matrix composite during fatigue by electrical resistance measurement. Polym Compos 1997;18:692–700. https://doi.org/10.1002/pc.10322.

[86] Wang X, Chung DDL. Continuous carbon fibre epoxy-matrix composite as a sensor of its own strain. Smart Mater Struct 1996;5:799–800. https://doi.org/10.1088/0964-1726/5/6/009.

[87] Prabhakaran R. DAMAGE ASSESSMENT THROUGH ELECTRICAL RESISTANCE MEASUREMENT IN GRAPHITE FIBER-REINFORCED COMPOSITES. Exp Tech 1990;14:16–20. https://doi.org/10.1111/j.1747-1567.1990.tb01059.x.

[88] Louis M, Joshi SP, Brockmann W. An experimental investigation of through-thickness electrical resistivity of CFRP laminates. Compos Sci Technol 2001;61:911–9.

https://doi.org/10.1016/S0266-3538(00)00177-9.

[89] Abry JC, Bochard S, Chateauminois A, Salvia M, Giraud G. In situ detection of damage in CFRP laminates by electrical resistance measurements. Compos Sci Technol 1999;59:925–35. https://doi.org/10.1016/S0266-3538(98)00132-8.

[90] Abry JC, Chateauminois A, Giraud G, Henaff-Gardin C, Lafarie-Frénot MC, Salvia M. DAMAGE MONITORING IN CFRP LAMINATES BY MEANS OF DIELECTRICAL PROPERTIES. n.d.

[91] Glass RC, Taylor SR, Cahen GL, Stoner GE. Electrochemical impedance spectroscopy as a method to nondestructively monitor simulated in-service damage in a carbon fiber reinforced plastic. J Nondestruct Eval 1987;6:181–8. https://doi.org/10.1007/BF00566846.

[92] Bekas DG, Paipetis AS. Damage monitoring in nanoenhanced composites using impedance spectroscopy. Compos Sci Technol 2016;134:96–105. https://doi.org/10.1016/j.compscitech.2016.08.013.

[93] Fazzino PD, Reifsnider KL, Majumdar P. Impedance spectroscopy for progressive damage analysis in woven composites. Compos Sci Technol 2009. https://doi.org/10.1016/j.compscitech.2009.05.007.

[94] Raihan R, Adkins JM, Baker J, Rabbi F, Reifsnider K. Relationship of dielectric property change to composite material state degradation. Compos Sci Technol 2014. https://doi.org/10.1016/j.compscitech.2014.09.017.

[95] Majumdar P, Wilkes C, Katiyar P, Arnold A. Effect of interfacial defects on mechanical and electrical properties of composite materials fatigue. 32nd Tech. Conf. Am. Soc. Compos. 2017, vol. 2, DEStech Publications Inc.; 2017, p. 1137–46. https://doi.org/10.12783/asc2017/15258.

[96] Nandini A, Shute N, Elenchezhian MRP, Vadlamudi V, Raihan R, Reifsnider K. Dielectric property investigation of degraded pre-preg and performance prediction of the final composite part. Int. SAMPE Tech. Conf., vol. 2018- May, 2018.

[97] Elenchezhian MRP, Vadlamudi V, Banerjee PK, Dave C, Mahmood A, Raihan R, et al. Quality assessment of adhesive bond based on dielectric properties. Int. SAMPE Tech. Conf., 2017.

[98] Sri S, Munaganuru N, Elenchezhian RP, Vadlamudi V, Shaik RA, Kishore Adluru H, et al. Effects of Build Parameters on the Mechanical and Di-Electrical Properties of AM parts. n.d.

[99] Seo DC, Lee JJ. Damage detection of CFRP laminates using electrical resistance measurement and neural network. Compos Struct 1999;47:525–30. https://doi.org/10.1016/S0263-8223(00)00016-7.

[100] Grady JE, Tang SS, Chen ILL, Stage F. AI Bases Structural Health Monitoring System 1993:343–52.

[101] Delelegn DT. Non-Destructive Evaluation for Composite Material 2018. https://doi.org/10.25777/vc78-t122.

[102] Marani R, Palumbo D, Galietti U, Stella E, D'Orazio T. Automatic detection of subsurface defects in composite materials using thermography and unsupervised machine learning. 2016. https://doi.org/10.1109/IS.2016.7737471.

[103] Gupta S, Krishnan S, Sundaresan V. Structural health monitoring of composite structures via machine learning of mechanoluminescence. ASME 2019 Conf Smart Mater Adapt Struct Intell Syst SMASIS 2019 2019. https://doi.org/10.1115/SMASIS2019-5697.

[104] Farhangdoust S, Tashakori S, Baghalian A, Mehrabi A, N. Tansel I. Prediction of damage

location in composite plates using artificial neural network modeling 2019:20. https://doi.org/10.1117/12.2517422.

[105] Al-Assaf Y, Kadi H El. Fatigue life prediction of unidirectional glass ®ber/epoxy composite laminae using neural networks. 2001.

[106] Jarrah MA, Al-Assaf Y, Kadi H El. Neuro-Fuzzy Modeling of Fatigue Life Prediction of Unidirectional Glass Fiber/Epoxy Composite Laminates 2001. https://doi.org/10.1106/002199802023176.

[107] Kadi H El, Al-Assaf Y. Prediction of the fatigue life of unidirectional glass ®ber/epoxy composite laminae using di€ erent neural network paradigms. 2002.

[108] Kadi H El, Al-Assaf Y. Energy-based fatigue life prediction of fiberglass/epoxy composites using modular neural networks. 2002.

[109] Al-Assaf Y, Kadi H El. Fatigue life prediction of composite materials using polynomial classifiers and recurrent neural networks. Compos Struct 2007;77:561–9. https://doi.org/10.1016/j.compstruct.2005.08.012.

[110] Al Assadi M. PREDICTING THE FATIGUE FAILURE OF FIBER REINFORCED COMPOSITE MATERIALS USING ARTIFICIAL NEURAL NETWORKS. 2009.

[111] El Kadi H, Deiab IM, Al-Assadi M. Fatigue life prediction of different fiber-reinforced composites using polynomial classifiers. J Eng Mater Technol Trans ASME 2011;133:1–5. https://doi.org/10.1115/1.4003566.

[112] El Kadi H. Modeling the mechanical behavior of fiber-reinforced polymeric composite materials using artificial neural networks - A review. Compos Struct 2006. https://doi.org/10.1016/j.compstruct.2005.01.020.

[113] Vassilopoulos AP, Georgopoulos EF, Dionysopoulos V. Artificial neural networks in

spectrum fatigue life prediction of composite materials. Int J Fatigue 2006;29:20–9. https://doi.org/10.1016/j.ijfatigue.2006.03.004.

[114] Mini MK, Sowmya M. Neural network paradigms for fatigue strength prediction of fiber-reinforced composite materials. Int J Adv Struct Eng 2012;4. https://doi.org/10.1186/2008-6695-4-7.

[115] Abdu_Lateef MS, Abdulrazaq NS, Mohammed AG. Prediction of Fatigue Life of Fiber Glass Reinforced Composite (FGRC) using Artificial Neural Network. vol. 35. 2017.

[116] Vassilopoulos AP, Georgopoulos EF. Computational intelligence methods for the fatigue life modeling of composite materials. Fatigue Life Predict. Compos. Compos. Struct., Elsevier; 2020, p. 349–83. https://doi.org/10.1016/b978-0-08-102575-8.00010-3.

[117] Saxena A, Goebel K, Larrosa CC, Janapati V, Roy S, Chang F-K. Accelerated Aging Experiments for Prognostics of Damage Growth in Composite Materials. 2011.

[118] Chiachio M, J.Chiachio, A.Saxena, G.Rus, K.Goebel. F a t i g u e D a m a g e P r o g n o s i s i n F R P C o m p o s i t e s b y C o m b i n i n g M u l t i - S c a l e D e g r a d a t i o n F a u l t M o d e s i n a n U n c e r t a i n t y B a y e s i a n F r a m e w o r k a n d K . G O E B E L. Int Work Struct Heal Monit 2013. https://doi.org/10.13140/2.1.3968.5123.

[119] Chiachío J, Chiachío M, Saxena A, Rus G, Goebel K. An Energy-Based Prognostic Framework to Predict Fatigue Damage Evolution in Composites. 2013.

[120] Larrosa C, Lonkar K, Chang FK. In situ damage classification for composite laminates using Gaussian discriminant analysis. Struct Heal Monit 2014;13:190–204. https://doi.org/10.1177/1475921713517288.

[121] Peng T, Liu Y, Saxena A, Goebel K. In-situ fatigue life prognosis for composite laminates based on stiffness degradation. Compos Struct 2015;132:155–65.

https://doi.org/10.1016/j.compstruct.2015.05.006.

[122] Corbetta M, Saxena A, Giglio M, Goebel K. An investigation of strain energy release rate models for real-time prognosis of fiber-reinforced laminates. Compos Struct 2017;165:99–114. https://doi.org/10.1016/j.compstruct.2017.01.002.

[123] Corbetta M, Sbarufatti C, Giglio M, Saxena A, Goebel K. A Bayesian framework for fatigue life prediction of composite laminates under co-existing matrix cracks and delamination. Compos Struct 2018;187:58–70. https://doi.org/10.1016/j.compstruct.2017.12.035.

[124] Lahmadi A, Terrissa L, Zerhouni N. A data-driven method for estimating the remaining useful life of a composite drill pipe. 2018 Int. Conf. Adv. Syst. Electr. Technol., IEEE; 2018, p. 192–5. https://doi.org/10.1109/ASET.2018.8379857.

[125] Liu H, Liu S, Liu Z, Mrad N, Dong H. Prognostics of Damage Growth in Composite Materials Using Machine Learning Techniques. 2017.

[126] Liu H, Liu S, Liu Z, Member S. Data-driven Approaches for Characterization of Delamination Damage in Composite Materials 2020;0046:1–11. https://doi.org/10.1109/TIE.2020.2973877.

[127] Eleftheroglou N, Loutas T. A novel approach towards fatigue damage prognostics of composite materials utilizing SHM data and stochastic degradation modeling. 2016.

[128] Loutas T, Eleftheroglou N, Zarouchas D. A data-driven probabilistic framework towards the in-situ prognostics of fatigue life of composites based on acoustic emission data. Compos Struct 2017;161:522–9. https://doi.org/10.1016/j.compstruct.2016.10.109.

[129] Eleftheroglou N, Zarouchas D, Loutas T, Alderliesten R, Benedictus R. Structural health monitoring data fusion for in-situ life prognosis of composite structures. Reliab Eng Syst

Saf 2018;178:40–54. https://doi.org/10.1016/j.ress.2018.04.031.

[130] LOUTAS T, ZAROUCHAS D. Upscaling the Data-driven Prognostic Methodologies Towards a Condition-based Structural Health Management of Composite Structures. Struct. Heal. Monit. 2019, Lancaster, PA: DEStech Publications, Inc.; 2019. https://doi.org/10.12783/shm2019/32282.

[131] Zarouchas D, Eleftheroglou N. In-situ fatigue damage analysis and prognostics of composite structures based on health monitoring data. 2nd ed. Elsevier Ltd.; 2020. https://doi.org/10.1016/b978-0-08-102575-8.00020-6.

[132] Nick Eleftheroglou, Dimitrios Zarouchas RB. An adaptive probabilistic data-driven methodology for prognosis of the fatigue life of composite structures. Compos Struct 2020:112386. https://doi.org/10.1016/j.compstruct.2020.112386.

[133] Teti R and GC. Prediction of composite laminate residual strength based on neural network approach 1994.

[134] Choi SW, Song E-J, Hahn HT. Prediction of fatigue damage growth in notched composite laminates using an artificial neural network. 2002.

[135] Bezerra EM, Ancelotti AC, Pardini LC, Rocco JAFF, Iha K, Ribeiro CHC. Artificial neural networks applied to epoxy composites reinforced with carbon and E-glass fibers: Analysis of the shear mechanical properties. Mater Sci Eng A 2007;464:177–85. https://doi.org/10.1016/j.msea.2007.01.131.

[136] Robinson EI, Marzat J, Raïssi T. Filtering and Uncertainty Propagation Methods for Model-Based Prognosis of Fatigue Crack Growth in Unidirectional Fiber-Reinforced Composites. ASCE-ASME J Risk Uncertain Eng Syst Part A Civ Eng 2018;4. https://doi.org/10.1061/AJRUA6.0000991.

[137] Rabiei E, Droguett EL, Modarres M, Amiri M. Damage precursor based structural health monitoring and damage prognosis framework. Saf. Reliab. Complex Eng. Syst. - Proc. 25th Eur. Saf. Reliab. Conf. ESREL 2015, CRC Press/Balkema; 2015, p. 2441–9. https://doi.org/10.1201/b19094-319.

[138] Liu Y, Mohanty S, Chattopadhyay A. A Gaussian process based prognostics framework for composite structures. Model. Signal Process. Control Smart Struct. 2009, vol. 7286, SPIE; 2009, p. 72860J. https://doi.org/10.1117/12.815889.

[139] Liu Y, Mohanty S, Chattopadhyay A. Condition based structural health monitoring and prognosis of composite structures under uniaxial and biaxial loading. J Nondestruct Eval 2010;29:181–8. https://doi.org/10.1007/s10921-010-0076-2.

[140] Cot LD, Gómez C, Gamboa F, Kopsaftopoulos F, Chang F-K. SHM-based fatigue damage prognostics in composite structures. 2016.

[141] Sankararaman S, Goebel K. Uncertainty in Prognostics and Systems Health Management. Int J Progn Heal Manag 2015.

[142] Fong JT, DeWit R, Marcal P V, Filliben JJ, Heckert NA, Gosselin SR. Design of a PYTHON-Based Plug-In for Benchmarking Probabilistic Fracture Mechanics Computer Codes With Failure Event Data. ASME 2009 Press. Vessel. Pip. Conf. Vol. 6 Mater. Fabr. Parts A B. Prague, Czech Republic. July 26–30, 2009, ASMEDC; 2009, p. 1651–93. https://doi.org/10.1115/PVP2009-77974.

[143] Elenchezhian MRP, Raihan MR, Reifsnider K. The role of uncertainty in machine learning as an element of control for material systems and structures. Am Soc Mech Eng Press Vessel Pip Div PVP 2018;6B-2018:1–8. https://doi.org/10.1115/pvp2018-84930.

[144] Schwabacher M, Goebel K. A Survey of Artificial Intelligence for Prognostics. 2007.

[145] Ruano, Saxena, Carlborg, Goebel. Fatigue Damage Prognosis in FRP Composites by Combining Multi-Scale Degradation Fault Modes in an Uncertainty Bayesian Framework. 2013.

[146] Khawaja T, Vachtsevanos G, Wu B. Reasoning about uncertainty in prognosis: A confidence prediction neural network approach. Annu. Conf. North Am. Fuzzy Inf. Process. Soc. - NAFIPS, vol. 2005, 2005, p. 7–12. https://doi.org/10.1109/NAFIPS.2005.1548498.

[147] Sause MGR, Horn S. Quantification of the uncertainty of pattern recognition approaches applied to acoustic emission signals. J Nondestruct Eval 2013. https://doi.org/10.1007/s10921-013-0177-9.

[148] Miller T. Explanation in artificial intelligence: Insights from the social sciences. Artif Intell 2019. https://doi.org/10.1016/j.artint.2018.07.007.

[149] Kim B, Khanna R, Koyejo O. Examples are not enough, learn to criticize! Criticism for interpretability. Adv. Neural Inf. Process. Syst., 2016.

[150] Molnar C. Interpretable Machine Learning. A Guide for Making Black Box Models Explainable. Book 2019:247.

[151] Abhinav Saxena, Kai Goebel, Cecilia C. Larrosa and F-KC. CFRP Composites Data Set. NASA Ames Progn Data Repos n.d. http://ti.arc.nasa.gov/project/prognostic-data-repository.

[152] Mandell JF, Samborsky DD, Miller DA, Agastra P, Sears AT, Paquette J, et al. SANDIA REPORT Analysis of SNL/MSU/DOE Fatigue Database Trends for Wind Turbine Blade Materials, 2010-2015 2016.

[153] Post NL, Case SW, Lesko JJ, Hyer M, Thangjitham S, Riffle J. Reliability based design

methodology incorporating residual strength prediction of structural fiber reinforced polymer composites under stochastic variable amplitude fatigue loading. 2008.

[154] Siiteri S. SMART POLYMER COMPOSITE STRUCTURES. vol. 25. 1992.

[155] Minakuchi S, Takeda N, Takeda SI, Nagao Y, Franceschetti A, Liu X. Life cycle monitoring of large-scale CFRP VARTM structure by fiber-optic-based distributed sensing. Compos Part A Appl Sci Manuf 2011. https://doi.org/10.1016/j.compositesa.2011.02.006.

[156] Ribeiro MT, Singh S, Guestrin C. "Why should i trust you?" Explaining the predictions of any classifier. Proc. ACM SIGKDD Int. Conf. Knowl. Discov. Data Min., vol. 13-17-August-2016, Association for Computing Machinery; 2016, p. 1135–44. https://doi.org/10.1145/2939672.2939778.

[157] Fisher A, Rudin C, Dominici F. All Models are Wrong, but Many are Useful: Learning a Variable's Importance by Studying an Entire Class of Prediction Models Simultaneously. ArXiv 2018.

[158] 14042-D | 0.011" Thick Unidirectional Fiberglass Prepreg | Rock West Composites n.d. https://www.rockwestcomposites.com/14042-d-group (accessed January 27, 2021).

[159] ASTM International. Standard Test Method for Tension-Tension Fatigue of Polymer Matrix Composite Materials 1. ASTM Int 2019. https://doi.org/10.1520/D3479_D3479M-19.

[160] Vadlamudi V, Elenchezhian MRP, Shaik RA, Nandini A, Raihan R, Reifsnider K, et al. Global prediction of discrete local damage interactions using broadband dielectric spectroscopy. 33rd Tech. Conf. Am. Soc. Compos. 2018, vol. 3, 2018.

[161] Vadlamudi V, Shaik R, Raihan R, Reifsnider K, Iarve E. Identification of current material

state in composites using a dielectric state variable. Compos Part A Appl Sci Manuf 2019. https://doi.org/10.1016/j.compositesa.2019.105494.

[162] Vadlamudi V, Elenchezhian MRP, Das PP, Raihan R, Reifsnider K. Assessment of material state for predicting the durability of composites. Proc. Am. Soc. Compos. - 35th Tech. Conf. ASC 2020, 2020, p. 654–61. https://doi.org/10.12783/asc35/34886.